RECENT ADVANCES IN THE CHEMISTRY OF THE LESS-COMMON OXIDATION STATES OF THE LANTHANIDE ELEMENTS

D. A. JOHNSON

Department of Chemistry, The Open University, Milton Keynes, England

I. Scope of the Article

At one time, a reviewer of the less-common oxidation states of the lanthanide elements would have defined these states as $+2$ and $+4$, and then covered all of their chemistry. A modern article with this brief could hardly be kept to a manageable size so that further restrictions are necessary. In this review, the restrictions are of two kinds.

The first restriction is concerned with species that have an oxidation state of $+2$ as computed from their stoichiometry in the usual way (in this article we shall always use the term "oxidation state" in this sense). Such species can be divided into two distinct groups. Take,

for example, the sulfides EuS and GdS. Now the magnetic and spectroscopic properties of EuS are those appropriate to the [Xe]$4f^7$ configuration of the free Eu^{2+} ion. However, in the case of GdS, the compound is metallic, and the magnetic properties are more appropriate to the [Xe]$4f^7$ configuration of the free tripositive ion, Gd^{3+}, than to the $4f^75d^1$ or $4f^8$ configuration of the Gd^{2+} ion.

It is customary to write GdS as $Gd^{3+}(e^-)S^{2-}$, the odd electron being in a conduction band, and to argue that in such a compound, gadolinium is trivalent because three of its electrons are involved in bonding. However, such a precise assignment of valency is hard to justify in a general sense because, depending on the environment, the involvement of the third electron in the bonding may vary between great, as in GdS, to the other extreme as when Gd^{2+} ions in the $4f^75d^1$ configuration are formed in a fluorite host lattice. To bring more precision to this situation we focus on the configuration of the 4*f* shell and introduce the terms di-*f*, tri-*f*, and tetra-*f*. A di-*f* system is one in which the metal has the same number of 4*f* electrons as the [Xe]$4f^{n+1}$ configuration of the free M^{2+} ion; a tri-*f* system is one in which the metal has the same number of 4*f* electrons as the [Xe]$4f^n$ configuration of the free M^{3+} ion. Thus, EuS is a di-*f* system, and GdS or Gd^{2+} ions in a fluorite host lattice are tri-*f* systems. Correspondingly, PrO_2, in which the metal has the same number of electrons as the [Xe]$4f^1$ configuration of the free Pr^{4+} ion, is a tetra-*f* system.

Using this terminology, we can say that there are some series of lanthanide compounds in oxidation state +2, such as the monosulfides or dihydrides, in which some elements form di-*f* compounds, and others, tri-*f* compounds. In such a case, the properties of the di-*f* compounds are often very different from those of the tri-*f*.

In this article, we concentrate our attention on di-*f* and tetra-*f* species and make no attempt to treat tri-*f* dipositive species comprehensively. In Section V, we discuss the factors that affect the distribution of dipositive species between the di-*f* and tri-*f* states. However, detailed reviews of the chemistry of compounds or ions are confined to di-*f* systems only.

Even when the preceding restriction is implemented, the recent growth of research into di-*f* and tetra-*f* lanthanide compounds makes further restrictions desirable. Coverage of the very extensive chemistry of europium(II) and cerium(IV) is not comprehensive: it is confined to properties that help to establish patterns in the properties of the other +2 and +4 oxidation states across the series or that are of particular research interest in their own right.

In spite of these restrictions, it is hoped that the article follows the spirit of two previous reviews (*21*, *444*) of the less-common oxidation

states of the lanthanides. The article is organized as follows. After a short discussion, in Section II, of the place of the less-common oxidation states in the overall context of lanthanide chemistry, Section III reviews lower oxidation state (less than +3), lanthanide compounds including halides, oxides, chalcogenides, aqueous ions, hydrides, borides, carbides, liquid ammonia systems, and organometallic compounds. Section IV reviews tetrapositive oxide and fluoride systems, and the tetrapositive oxidation states in aqueous solution. In both Section III and Section IV, an attempt is made to extract from the experimental data, the stability pattern of di-*f* and tetra-*f* systems with respect to the common tri-*f* state. Section V discusses the interpretation of these and other patterns in the stabilities of oxidation states, and the principles thus established are then briefly tested further in Section VI against particular problems of redox stability in the actinide and the first-transition series.

II. Introduction

Until relatively recently, the major preoccupation of rare earth chemists was the separation problem, which focused attention upon the complexing and crystallizing processes of the tripositive state. Put in thermodynamic terms, the difficulty was that, with a particular reagent, the standard free-energy change for such reactions usually varies very little from metal to metal. Thus the emphasis on this type of reaction gave rise to the view that the lanthanides were a rather featureless series of elements with very similar properties, which in many cases approached a smooth variation with atomic number.

In about 1920, this view gained force with the publication by Bohr (*72*, *73*) and Bury (*95*) of a structural scheme for the atom that corresponded to the general form of the periodic table. This scheme assigned inner groups of electrons to the transition and lanthanide elements; it foreshadowed the demise of those ideas that placed more than one element in a single space in the periodic table and gave powerful support to the "long form" of the table, which had already been proposed by Alfred Werner (*572*) and others (*51*, *530*). Bohr and Bury's proposals also allowed a rather loosely expressed explanation of the similarities among the rare earth metals: in moving across the lanthanide series, successive electrons are added to the inner shells below the valence electrons and, consequently, chemical properties do not vary much with atomic number (*73*, *95*).

This generalization was widely accepted in spite of important research within the next 10 years by the German chemist Klemm which implicitly challenged it. Klemm's work (*318*, *319*, *320*, *275*) is described

more fully at intervals throughout this review, but it can be briefly summarized by saying that it was concerned chiefly with the preparation of new dipositive and tetrapositive states of different lanthanide elements and with the rationalization of their relative stabilities with respect to the tripositive state. At an early stage it became clear that these stabilities did not vary in a regular way across the entire series. Since Klemm's work, other kinds of reaction of the lanthanides with markedly irregular energy variations have been discovered, but it remains true that the stabilities of dipositive and tetrapositive compounds with respect to the tripositive state provide the most obvious challenge to the view that one lanthanide element behaves chemically very much like the next. Indeed, as we try to show in this review, it is chiefly through the recent study of these stabilities that we can now identify reactions in which the lanthanides behave similarly and distinguish such reactions from others in which the elements behave differently.

III. Compounds in Lower Oxidation States

A. Halides

The widest range of di-*f* lanthanide compounds is found among the halides. Di-*f* dichlorides of neodymium, samarium, europium, dysprosium, thulium, and ytterbium are known, and those of promethium could probably be obtained by standard preparative methods (see Section V,A,3). Di-*f* dibromides are known only for samarium, europium and ytterbium, but $NdBr_2$, $PmBr_2$, $DyBr_2$, and $TmBr_2$ could probably be prepared if desired. Indeed, Spedding and Daane (*505*) reported the melting point of $TmBr_2$ but gave no other information. The situation with regard to di-*f* diiodides is exactly the same as for the chlorides, but there is one important qualification: in addition to di-*f* NdI_2, SmI_2, EuI_2, DyI_2, TmI_2, and YbI_2, *metallic* tri-*f* diiodides of lanthanum, cerium, praseodymium, and gadolinium are known. The exact range of difluorides is uncertain, but it is certainly more restricted than that of the chlorides, bromides, or iodides; for example, the solubility of neodymium in its molten trifluoride is less than 0.5 mole %, suggesting that, unlike $NdCl_2$ and NdI_2, the difluoride is not accessible by reproportionation (*153*). At present, only SmF_2, EuF_2, and YbF_2 have been well-characterized.

The di-*f* saline dihalides are distinguished from the metallic tri-*f* dihalides by their nonmetallic appearances and low electrical conductivity, by crystal structures that are also found among the alkaline earth dihalides, and by their magnetic properties.

In compounds of the first-row transition elements, the orbital angular momentum is wholly or partially quenched, and the spin-only formula for the magnetic moment usually reproduces the experimental values quite well. However, in lanthanide compounds, both spin and orbital angular momenta are active. For ground states arising from the configurations $4f^1$ to $4f^6$, the spin and orbital angular momenta are opposed; for ground states arising from the configurations $4f^8$ to $4f^{13}$, they reinforce each other. This leads to near diamagnetism for the $4f^6$ configuration and to significantly higher magnetic moments in the second half of the series (*454*, *540*).

Early magnetic studies of the dihalides of $SmBr_2$, EuX_2, and $YbCl_2$ have been reviewed by Selwood (*487*, *488*). These allow calculation of molar susceptibilities and effective magnetic moments for ions Sm^{2+}, Eu^{2+}, and Yb^{2+} in these compounds. For Eu^{2+}, the molar susceptibilities at various temperatures are very similar to those of Gd^{3+}, and the effective magnetic moments obtained from the expression

$$\mu_{\text{eff}} = (3\chi_A kT/N)^{1/2} \tag{1}$$

where χ_A is the atomic susceptibility, are close to the theoretical value of 7.94 μ_B for the $^8S_{7/2}$ ground state of the $[Xe]4f^7$ configuration of the free Eu^{2+} ion. The Yb^{2+} is either diamagnetic or has only a small temperature-independent paramagnetism, suggesting the configuration $[Xe]4f^{14}$. Little signs of magnetic ordering have been detected in the europium dihalides, even at low temperatures (*341*, *364*) although some inconclusive evidence for ferromagnetism in EuI_2 exists (*364*).

The results obtained from $SmBr_2$ suggest that the effective magnetic moment of Sm^{2+} at room temperature is about 3.5 μ_B, a theoretical value of zero being implied by the $^7F_0$ ground state of the configuration $[Xe]4f^6$. Furthermore, there is a sizable variation of μ_{eff} with temperature, a result that reveals unusually large deviations from the Curie law according to which $\chi_A T$ in Eq. (1) should be constant. However, the μ_{eff} values at various temperatures agree closely with those obtained for Eu^{3+} in various compounds, and the behavior is theoretically explicable if allowance is made for the population of excited states of the $[Xe]4f^6$ configuration, $^7F_1$ and $^7F_2$, which, unlike in most rare earth ions, are thermally accessible at room temperature (*541*, *542*).

More recent work on $NdCl_2$ and NdI_2 (*480*) has revealed atomic susceptibilities that follow the Curie law reasonably closely at 80–150 K with an effective magnetic moment of about 2.8 μ_B. The theoretical value expected of the $^5I_4$ ground state of the $[Xe]4f^4$ configuration is 2.68 μ_B. However, at higher temperatures of 200 to 600 K, deviations

from the Curie or Curie–Weiss law are observed, but these can be accounted for by allowing for the population of an exited state $^5I_5$ lying above the ground state at an energy given approximately by $\Delta E/k = 1400$ K.

The magnetic properties of dihalides of neodymium, samarium, europium, and ytterbium are thus consistent with the formulation of the saline dihalides as $M^{2+}(X^-)_2$ and with the assignment of electronic configurations of the type [Xe]$4f^n$ to the constituent dipositive ions.

By contrast, the metallic diiodes are usually formulated $M^{3+}(e^-)(I^-)_2$, the odd electron being in a conduction band, because their magnetic properties correspond to those expected of the tripositive ions (*129*). For example, within experimental uncertainties, LaI_2 is diamagnetic at room temperature; its corrected molar susceptibility of 104×10^{-6} emu mol^{-1} is very close to that of lanthanum metal (*129*). The definition given in Section I thus classifies LaI_2, CeI_2, PrI_2, and GdI_2 as tri-*f* compounds.

As indicated earlier in this section, the di-*f* lanthanide dihalides show close structural analogies with the alkaline earth metal dihalides, rather than with the dihalides of the transition elements. This is reflected in the range of coordination numbers (9, 8, 7, and 6) contrasting with the confinement of dihalides of the first-transition series to a coordination number of 6 (*571*) at normal temperatures and pressures. This absence of strong stereochemical preferences in the lanthanide series is also apparent from a survey of the structures of the trihalides (*86*).

Apart from the dihalides, studies of metal–metal trihalide phase diagrams have revealed some chloride, bromide, and iodide phases whose stoichiometries lie between the compositions $MX_{2.00}$ and $MX_{3.00}$, and the compound Gd_2Cl_3, which has an interesting structure. An excellent but selective review of the reduced halides of the rare earth elements has been made by Corbett (*124*).

Finally, although this article contains no detailed consideration of gaseous species, we note that there have been several recent studies of the thermodynamics of vaporization of those di-*f* dihalides that are most stable with respect to disproportionation (*223–225*) and that the gaseous molecules have been investigated both in inert gas matrices (*233*, *136*) and by molecular beam studies (*303*). The gaseous molecules appear to be nonlinear, a property that is shared by some of their alkaline earth metal analogs (*573a*). This is not a result that would be predicted from the valence shell repulsion theory of molecular shape, but it can be accounted for by hybridization schemes that invoke higher orbitals (*130a*).

1. Preparative Methods

a. Hydrogen Reduction or Thermal Decomposition of Trihalides. Hydrogen reduction of trihalides was the preparative method favored by the earliest investigators of lower lanthanide halides. Matignon and Cazes (*381*, *382*) prepared $SmCl_2$ and SmI_2 by this means in 1906, and Urbain and Bourion (*535*) obtained $EuCl_2$ in the same way 5 years later. Later users of the method employed a variety of temperatures, and sometimes introduced ammonia gas into the hydrogen stream. Klemm and Schuth (*324*) used hydrogen reduction to prepare $YbCl_2$ in 1929. Indeed, by 1939, the dichlorides, dibromides, and diiodides of samarium (*381*, *382*, *277*, *464*, *323*, *273*, *278*, *143*), europium (*535*, *143*, *274*, *53*, *308*, *321*), and ytterbium (*324*, *273*, *143*, *281*) and the difluoride of europium (*321*, *57*) had all been prepared in this way, although it now seems that complete reduction is not achieved in the case of samarium compounds (*462*). A more recent modification of the hydrogen reduction method involved the use of lithium borohydride as a source of hydrogen. With this reducing agent, $EuCl_2$ can be obtained by reduction of the trichloride in THF (*475*).

Early workers reported hydrogen reduction to be superior to thermal decomposition of trihalides, except perhaps for the preparation of diiodides (*273*, *281*). This exception is not surprising because the free energy of formation of hydrogen iodide at normal or moderately high temperatures is close to zero, so there is little difference between the equilibrium constants of the two kinds of process. Nevertheless, by purifying the dihalide product by vacuum sublimation, Baernighausen (*35*) has prepared excellent samples of samarium, europium, and ytterbium dihalides by the thermal decomposition of trihalide hydrates.

Both hydrogen reduction and thermal decomposition of trihalides, however, have only a limited range of application. Attempts to extend them to the preparation of the dihalides of metals other than samarium, europium, and ytterbium, including neodymium and thulium, were unsuccessful (*279*, *280*). Indeed, in the case of the fluorides, hydrogen reduction at 1300°C yields a phase of composition MF_2 only for europium. Phases of intermediate composition are obtained for samarium and ytterbium (*22*). Moreover, many of the earlier investigators reported difficulties caused by the corrosion of their containers, even when gold or platinum vessels were used. This corrosion is due to the formation of alloys with the rare earth metals (*84*). More powerful reducing agents and more inert containers were needed to extend the range of lanthanide dihalides beyond samarium, europium, and ytterbium.

TABLE I

REDUCED LANTHANIDE CHLORIDE PHASES

M	Cl/M	Ref.	M	Cl/M	Ref.
La	None	(*314a*)	Gd	1.50	(*387*)
Ce	None	(*388a*)	Tb	Not investigated	
Pr	2.31	(*152*)	Dy	2.00, 2.10	(*127*)
Nd	2.00, 2.27, 2.37	(*151*)	Ho	2.14	(*123, 345*)
Pm	Not investigated		Er	None	(*128*)
Sm	2.0, 2.2	(*459*)	Tm	2.00, 2.04–2.15	(*106*)
Eu	2.00[a]	This work	Yb	2.00[a]	This work

[a] Preparative attempts, but no phase diagram reported.

b. Reproportionation Methods. The preparation of the dihalides of metals other than samarium, europium, and ytterbium was achieved in 1959 with the synthesis of neodymium dihalides (*150*). The trihalide was heated and reduced by the pure rare earth metal, a reducing agent that requires the use of tantalum or molybenum containers. This reaction of the metal with the molten trihalide followed by a rapid quenching reaction has so far yielded new saltlike dichlorides and diiodides of neodymium (*150, 151*), dysprosium (*127, 293*), and thulium (*26, 106*), and it seems unlikely that future attempts to prepare the corresponding dibromides will prove any less successful. The method has also been used to make SmF_2 and YbF_2 (*511, 107*). With these more volatile metals, it is possible to carry out a reaction between the solid trifluoride and metal vapor (*453*).

From a preparative standpoint, the reproportionation method in the form

$$M(s) + 2MX_3(l) \longrightarrow 3MX_2(l) \qquad (2)$$

has been used most successfully by Corbett and his associates who devised techniques for the determination of the M/MX_3 phase diagrams in the temperature range 500°–1200°C. The results of attempts to prepare lower chlorides and iodides by these means are summarized in Tables I and II. As we shall see, they lead to important conclusions concerning the relative stabilities of the dihalides.

c. Reaction of the Metals with Mercuric Halides. Few lanthanide dihalides have been prepared in this way, but to judge by the instances where the method has been successfully applied, it is capable of fairly wide application. Samples of TmI_2 (*26*) and DyI_2 (*44*) have been made by oxidizing the metals with mercuric iodide at 300°–400°C. The working

TABLE II

REDUCED LANTHANIDE IODIDE PHASES

Metal	I/M	Character	Ref.
La	2.00	Metallic	(*125, 129*)
	2.42	Saltlike	(*125, 129*)
Ce	2.00	Metallic	(*125*)
	2.40	Saltlike	(*125*)
Pr	2.00	Metallic	(*125*)
	2.50	Saltlike	(*125*)
Nd	1.95	Saltlike	(*151*)
Pm	Not investigated		
Sm	2.00[a]	Saltlike	This work
Eu	2.00[a]	Saltlike	This work
Gd	2.00	Metallic	(*387*)
Tb	None		(*293*)
Dy	2.00	Saltlike	(*293*)
Ho	None		(*293*)
Er	None		(*128*)
Tm	2.00[a]	Saltlike	(*26*)
Yb	2.00[a]	Saltlike	This work

[a] Preparative attempts, but no phase diagram reported.

temperature is more moderate than that used for reproportionation reactions, and both the mercury metal product and any residual mercuric halide can be removed by distillation, but the formation of rare earth mercury alloys may promote disproportionation of a reduced halide that is formed. The method has recently been used to obtain dihalides of americium (*54, 55*), confirming its ability to synthesize lower halides with powerful reducing properties.

d. Miscellaneous Methods. Preparative methods used in isolated instances for obtaining dihalides of samarium, europium, and ytterbium are listed here. Samarium, europium, and ytterbium dichlorides have been made by reducing the trihalides with zinc and distilling off unwanted products (*135*). Attempts to prepare samarium difluoride by heating the trifluoride with graphite at about 2000°C gave only a 30% yield (*317*). $SmCl_2$ has been made by reducing the trichloride in ethanol with magnesium (*117*).

The liquid ammonia systems for europium and ytterbium have been used to prepare dichlorides, dibromides, and diiodides. Dissolution of the metals in a solution of the appropriate ammonium halide in liquid ammonia gives ammoniated dihalides which lose their ammonia of crystallization on mild warming and evacuation (*257*). Diiodides of

europium and ytterbium can be obtained by reducing the trivalent perchlorates in liquid ammonia with sodium in the presence of iodide ions (*397*).

2. *Stabilities of Dihalides*

Although thermodynamic data on the lanthanide dihalides are sparse, it is possible to construct tentative stability sequences from qualitative observations made, for the most part, in the references cited in the preparative section. In the case of the dihalides, two senses of the word *stability*, both of them thermodynamic, are usefully considered. First, stability with respect to the straightforward oxidation reaction,

$$MX_2(s) + \tfrac{1}{2}X_2 \longrightarrow MX_3(s) \tag{3}$$

and, second, the stability of a dihalide with respect to disproportionation,

$$3MX_2(s) \longrightarrow M(s) + 2MX_3(s) \tag{4}$$

In the case of the first kind of reaction, the following observations are useful: thermal decompositions of samarium dihalides begin at lower temperatures than those of europium dihalides (*273*); hydrogen reduction of samarium trihalides is incomplete (*462*); and hydrogen reduction of trihalides is successful only for samarium, europium, and ytterbium (*279, 280*). This suggests that likely stability sequences with respect to Eq. (3) for a particular halogen, X, are LaX_2—NdX_2 < SmX_2 < EuX_2 ≫ GdX_2 and GdX_2—TmX_2 < YbX_2.

In the case of the disproportionation reaction, information obtained from preparative attempts by reproportionation is particularly important. This is because the stoichiometry of the preparative reaction is the reverse of Eq. (4). As equilibrium seems to be rapidly attained in M/MX_3 melts and as $-\Delta G_T{}^0$ for reaction (2), where $T \sim 500°$–$1200°C$, should not differ greatly from ΔG^0_{298} for reaction (4), a careful investigation of the reproportionation reaction, coupled with phase diagram analyses, gives a strong indication whether a given dihalide is stable or unstable with respect to disproportionation at room temperature, although in borderline cases it may not be completely reliable.

Attempts to prepare lower lanthanide chloride phases by reproportionation are recorded in Table I. The same information for iodides is supplied in Table II. In neither case have di-*f* dihalides been found for lanthanum, cerium, and praseodymium, but successful preparation of both di-*f* dichlorides and diiodides has been achieved for neodymium, samarium, and europium. Neither gadolinium or terbium is known to form di-*f* dihalides, but dysprosium forms a di-*f* dichloride and diiodide. This contrasts with holmium and erbium for which reproportionation

has failed to yield dihalides. At the end of the series, di-*f* dichlorides and diiodides of thulium and ytterbium are readily obtained by reproportionation.

Suppose now we make the assumption that the occurrence or nonoccurrence of a di-*f* dihalide after a reproportionation reaction registers its stability or instability with respect to reaction (4). This assumption might possibly be incorrect when other reduced halides occur in the phase diagram, but with this qualification, it seems reasonable. If one then considers the stability of a di-*f* dihalide with respect to disproportionation as one moves across the series, it seems as if there is an initial region of instability followed by a zone of stability in the neodymium–europium region. A second region of instability occurs at gadolinium and terbium, but a stable point is reached again at dysprosium. A third region of instability occurs at holmium and erbium before we reach the final zone of stability at thulium and ytterbium. These observations are summarized by the following stability sequence for di-*f* dihalides with respect to disproportionation:

$$\text{La, Ce, Pr} < \text{Nd, Sm, Eu} > \text{Gd, Tb} < \text{Dy} > \text{Ho, Er} < \text{Tm, Yb}$$

This sequence can be corroborated and refined by using data on the solubility of the metals in trihalide metals which are also obtainable from the phase diagrams. There is good evidence from freezing point-depression measurements and other data that when the metals dissolve in the trihalide melts, they do so by forming dipositive ions:

$$\text{M(s)} + 2\text{M}^{3+}\text{ (melt)} \longrightarrow 3\text{M}^{2+}\text{ (melt)}$$

This evidence has been reviewed by Corbett (*124*). The solubility of the metal in the trihalide melt at a standard temperature is, therefore, a measure of the stability of the dipositive oxidation state with respect to disproportionation in a halide environment. The solubilities of the metals in the trichloride melts at temperatures in the region of 800°C are plotted in Fig. 1. They suggest the following stability sequence for dichlorides with respect to disproportionation:

$$\text{La} < \text{Ce} < \text{Pr} < \text{Nd} < (\text{Pm}) < \text{Sm, Eu} \gg \text{Gd} < \text{Tb} < \text{Dy} > \text{Ho} > \text{Er} < \text{Tm, Yb}$$

The iodide data also support this sequence, but here allowance must be made for the fact that the melts show some electronic conduction in the cases of lanthanum, cerium, and praseodymium, thus suggesting contributions from a solution process of the type

$$\text{M(s)} \longrightarrow \text{M}^{3+}\text{ (melt)} + 3\text{e}^{-}\text{ (melt)}$$

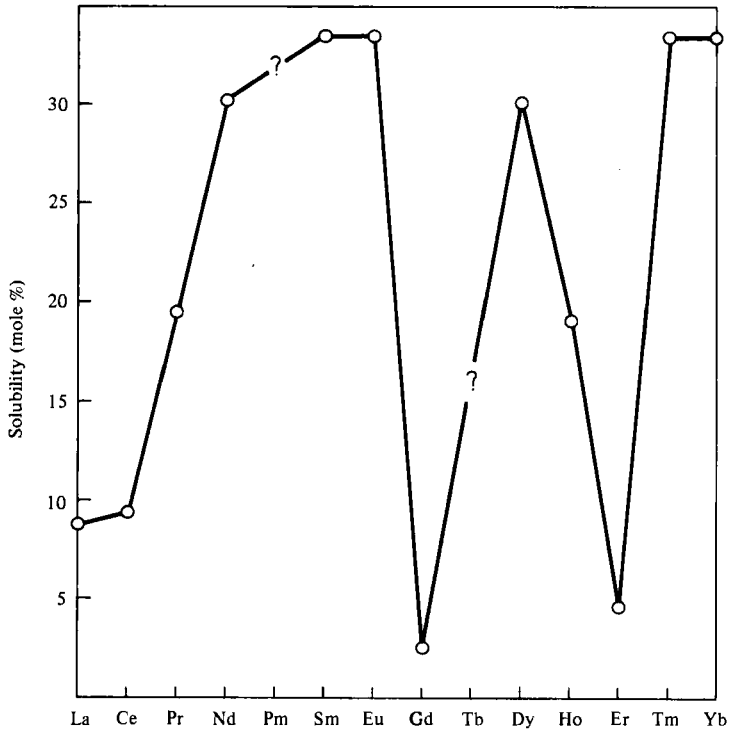

FIG. 1. Solubilities of the lanthanide metals in their trichloride melts at 800° C. [From Corbett (*124*).]

Such a contribution is reasonable in view of the formation of metallic diiodides $M^{3+}(e^-)(I^-)_2$ in the instances cited.

The stability sequence implied by solubility data is quite consistent with the more limited one obtained earlier in this section by considering successful and unsuccessful preparative attempts. Such consistency is to be expected in that high metal solubility correlates with the existence of stable dihalides. There is also a perhaps unexpected consistency between both these sequences and the one obtained by consideration of the straightforward oxidation, reaction (3). If all three are combined, we obtain

$$\text{La} < \text{Ce} < \text{Pr} < \text{Nd} < (\text{Pm}) < \text{Sm} < \text{Eu} \gg \text{Gd} < \text{Tb} < \text{Dy} > \text{Ho} > \text{Er} < \text{Tm} < \text{Yb}$$

From now on, we shall assume that this stability sequence is applicable to both the direct oxidation of di-*f* dihalides and to the disproportionation reaction. It is at present impossible to find conclusive,

TABLE III

STANDARD ENTHALPY DATA FOR REACTIONS (3) AND (4) FOR LANTHANIDE DICHLORIDES[a]

Element	ΔH^0[Eq. (3)] (kcal mole^{-1})	$\frac{1}{3}\Delta H^0$[Eq. (4)] (kcal mole^{-1})
Nd	-80 ± 2	3 ± 2
Sm	-49 ± 5	32 ± 5
Eu	-27 ± 3	48 ± 3
Tm	-66 ± 3	12 ± 3
Yb	-38 ± 4	38 ± 4

[a] Data from Johnson (*291*), Morss and Haug (*407*), and Morss and McCue (*408*).

comprehensive evidence for this assumption, but as shown in this section, it is consistent with Fig. 1, with the distribution of di-*f* dihalides in Tables I and II, and with other information on preparative problems. Further evidence is obtained both from the the rather limited thermodynamic data for chlorides summarized in Table III and from the theoretical reasoning described in Section V,A.

In closing this section we note one important general point: Figure 1 and the scattered distribution of stable dihalides across the series are a striking refutation of the view that the lanthanide elements are chemically very similar.

3. *Properties*

a. Difluorides. The only known difluorides are those of samarium, europium, and ytterbium, although there is some evidence for partial reduction of thulium trifluoride (*107*). Reports of a Mössbauer study of TmF_2 give no preparative details (*534*). Some properties of SmF_2, EuF_2, and YbF_2 suggested by a survey of the cited references are listed in Table IV.

All three fluorides have the fluorite structure in which the metal is coordinated to 8 fluorines at the corners of a cube. However, at a pressure of 114 kbar and a temperature of 400°C, EuF_2 adopts the

TABLE IV

PROPERTIES OF LANTHANIDE DIFLUORIDES

Compound	Color	Structure	a_0 (Å)	Ref.
SmF_2	Purple	Fluorite	5.869	(*107, 453, 511*)
EuF_2	Pale greenish-yellow	Fluorite	5.840	(*22, 107, 341, 452, 453, 524*)
YbF_2	Pale gray	Fluorite	5.599	(*107, 453*)

orthorhombic $PbCl_2$ or $EuCl_2$ structure in which the cation is nine-coordinate. Similar high-pressure transitions are observed in the fluorite phases of CaF_2, SrF_2, and BaF_2, but not in those of CdF_2 or HgF_2 (*486*).

Magnetic studies have been concentrated on the europium compound. Studies of the variation of χ_A with temperature give values of the magnetic moment of the dipositive ion close to the theoretical value of 7.94 μ_B (*321*). Compound EuF_2 obeys the Curie–Weiss law:

$$\chi_A = \frac{C}{T - \theta} \tag{5}$$

but the value of θ is very small (*364*) and, when pure, the compound remains paramagnetic down to 1.6 K (*341*).

The colors of the fluorides given by different workers are somewhat variable, possibly because of the considerable composition range of the fluorite phases on the fluorine-rich side. This has been examined by X-ray studies of the products obtained by heating the metal and the trifluoride in different proportions. In the case of the europium system, the cubic fluorite phase is stable from $EuF_{2.00}$ to about $EuF_{2.17}$ (*524, 451*). From $EuF_{2.17}$ to about $EuF_{2.25}$, the fluorite phase is mixed with various proportions of a tetragonal phase of composition about $EuF_{2.25}$, but from $EuF_{2.25}$ to $EuF_{2.40}$ a new rhombohedral phase can be detected. Above $EuF_{2.40}$, this rhombohedral phase coexists with EuF_3 (*524*). The Mössbauer spectra of the phases between EuF_2 and EuF_3 show two absorptions, one characteristic of Eu(II) and the other of Eu(III), the latter absorption increasing in intensity as the F/Eu ratio increases. Over the range of stability of the fluorite phase, the lattice parameter decreases, whereas there is an increase in the amount by which the bulk density exceeds the density obtained from powder patterns. The data are consistent with the assumption that nonstoichiometry is procured by the incorporation of Eu^{3+} and interstitial fluoride ions into the fluorite lattice (*107*).

Suggestive relationships exist between the cell parameters of the fluorite tetragonal and rhombohedral phases. When allowance is made for the change in cell parameters with increasing fluorine content, then, if the fluorite unit cell side is denoted by x, the tetragonal phase has $c_0 = x$ and $a_0 = x/2^{1/2}$, whereas the rhombohedral phase has $a_0 = (\frac{3}{2})^{1/2}x$. The tetragonal and rhombohedral lattices are interpreted as superlattices of the fluorite structure. Figure 2 shows how unit cells of the appropriate symmetry and cell parameter may be created from the cubic fluorite lattice by ordering of the Eu^{2+} and Eu^{3+} ions. This

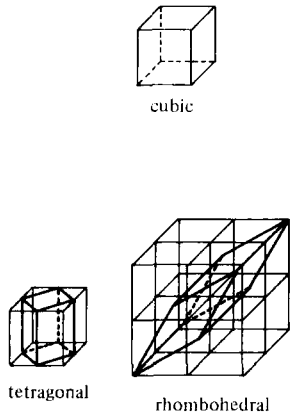

FIG. 2. Superlattices of the fluorite structure in nonstoichiometric phases, EuF_{2+x}. [From Tanguy *et al.* (*524*), Fig. 6.]

elegant interpretation is supported by the absence of superstructures in the SrF_2–EuF_3 system in spite of the very similar cell parameters of the EuF_2 and SrF_2 fluorite structures. This is attributed to the fact that in the EuF_2–EuF_3 system, ordering of the two kinds of cation can occur by electron transfer, but in the SrF_2–EuF_3 system, cation migration is necessary (*524*).

A similar sequence of phases on the fluorine-rich side of MF_2 with similar composition ranges is found in the SmF_2–SmF_3 system. Again, bulk and X-ray density data suggest a model for the nonstoichiometry involving interstitial anions and dipositive and tripositive cations (*107*, *511*).

More recent work disclosed a similar succession of phases for ytterbium and showed that on heating in a vacuum, YbF_2 loses a metal-rich vapor and forms the $YbF_{2.40}$ phase (*66*).

b. Dichlorides. Magnetic investigations on the dichlorides have been reviewed in Section III,A. Other data are shown in Table V.

Neodymium, samarium, and europium dichlorides crystallize in the orthorhombic $PbCl_2$ structure. The metal coordination is hard to define but is probably best described as nine-coordinate and is shown in Fig. 3a. The metal atoms lie at the center of 6 chlorines that form a trigonal prism and are coordinated to 3 other chlorines through the centers of the vertical faces of the prism. Since $SrCl_2$ has the fluorite structure, $EuCl_2$ affords an exception to the almost universal rule that compounds of europium(II) and strontium(II) of the same formula type are isostructural.

TABLE V

PROPERTIES OF LANTHANIDE DICHLORIDES

Compound	Color	Structure	Cell parameters (Å)	Coordination No.	Mp (°C)	Ref.
$NdCl_2$	Dark green	$PbCl_2$	$a_0 = 9.06$ $b_0 = 7.59$ $c_0 = 4.50$	9	841	(*151*)
$SmCl_2$	Red-brown	$PbCl_2$	$a_0 = 8.993$ $b_0 = 7.556$ $c_0 = 4.517$	9	855	(*37*, *144*, *151*, *505*, *582*)
$EuCl_2$	White	$PbCl_2$	$a_0 = 8.965$ $b_0 = 7.538$ $c_0 = 4.511$	9	731	(*37*, *144*, *505*, *582*)
$DyCl_2$	Black	SrI_2	$a_0 = 13.38$ $b_0 = 7.06$ $c_0 = 6.76$	7	721	(*58*, *127*)
$TmCl_2$	Dark green	SrI_2	$a_0 = 13.10$ $b_0 = 6.93$ $c_0 = 6.68$	7	718	(*58*, *106*)
$YbCl_2$	Greenish-yellow	SrI_2	$a_0 = 13.139$ $b_0 = 6.948$ $c_0 = 6.698$	7	702	(*41*, *58*, *176*, *505*)

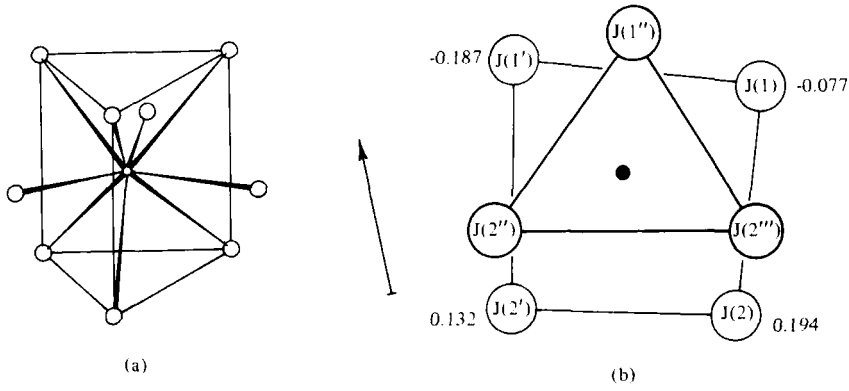

FIG. 3. Coordination of the metal in two lanthanide dihalide structures. (a) Nine-coordinate $PbCl_2$ structure [from F. A. Cotton and G. Wilkinson, "Advanced Inorganic Chemistry," 3rd edition, Wiley (Interscience), New York, 1972, p. 30, Fig. 1-11]. (b) Plan of the seven-coordinate SrI_2 structure [from Rietschel and Baernighausen (*472*), Fig. 3].

Recent single-crystal work on $YbCl_2$ (*58*) has modified structural interpretations of powder data for $DyCl_2$, $TmCl_2$, and $YbCl_2$. These interpretations were based on the work of Döll and Klemm (*144*) on the powder photograph of $YbCl_2$. It is now believed that $DyCl_2$, $TmCl_2$, and $YbCl_2$ have the orthorhombic strontium diiodide structure (*42*, *472*). The cation is seven-coordinate; below the cation, there are 4 halogens lying roughly at the corners of a square, whereas, above, there are 3 at the corners of a roughly equilateral triangle. A projection of the coordination polyhedron is shown in Fig. 3b. Powder patterns of $HoCl_{2.14}$, the only known reduced halide of holmium, bear a close relationship to those of dichlorides with this structure (*123*, *345*).

A gradual decrease in cell parameters occurs in the isostructural series from $BaCl_2$, which also has the $PbCl_2$ structure, through $NdCl_2$ and $SmCl_2$ to $EuCl_2$. Such a decrease is also observable in the three SrI_2-type structures, although $YbCl_2$ cell parameters seem slightly larger than those of $TmCl_2$. However, values for the dichlorides of two adjacent elements differ by such small amounts that the differences cannot confidently be regarded as significant unless both compounds were examined by the same worker. It is probable, therefore, that the cell parameters in Table V support the concept of a general decrease in the sizes of dipositive ions corresponding to the well-established lanthanide contraction in tri-*f* compounds (*525*). The decrease in coordination number from 9 to 7 as the cation decreases in size across the series is a result that one might expect from classic hard-sphere models that relate coordination number to the ratio of cation and anion

radius (*163*). However, the chlorides of samarium and europium can also be viewed as exceptions to such ideas, because the coordination number of 9 for the metal is higher than the value of 8 in the fluorite structures of SmF_2 and EuF_2. In the halides of samarium and europium, therefore, the cation attains the largest coordination number in the chlorides, rather than in the compounds containing the smallest anion. A similar anomaly is observable in the halides of barium (*571*).

The lower stability of the chlorides of neodymium and dysprosium is indicated by the fact that these compounds melt incongruently, forming metal plus melts of approximate composition $MCl_{2.08}$ which, according to the solution model proposed in Section III,A,2, contain some tripositive ions.

All 6 chlorides dissolve in or react with water. Compounds $SmCl_2$, $EuCl_2$, and $YbCl_2$ yield solutions containing dipositive ions that are, then, gradually oxidized as described in Section III,C,1. Oxidation is particularly rapid in solutions of the samarium compound which is also quickly oxidized in moist air. Compounds $NdCl_2$, $DyCl_2$, and $TmCl_2$ react violently with water, evolving hydrogen gas and precipitating the trivalent hydroxides, $M(OH)_3$. A fading red coloration has been observed in the case of the thulium compound (*106*), but, apart from this, there are no signs that the aqueous dipositive ions of neodymium, dysprosium, or thulium can be detected in the course of the dissolution of the dichlorides.

c. Dibromides. It is probable that normal preparations of samarium dibromide crystallize in the tetragonal $SrBr_2$ structure (*144*) which has recently been determined (*499*). This structure, which is definitely adopted by $EuBr_2$ (*228*), is a curious hybrid of the $SrCl_2$ fluorite structure in which the cation is eight-coordinate, and of the SrI_2 structure in which the strontium is seven-coordinate, as shown in Fig. 3b. In the $SrBr_2$ structure, there are both seven- and eight-coordinated cations. The seven coordination is the same as that in SrI_2, but the anions around the eight-coordinated cation lie at the corners of a square antiprism, rather than at the corners of a cube as in $SrCl_2$. However, samarium dibromide crystallizes in the nine-coordinate $PbCl_2$ structure when purified by high-temperature distillation (*37*).

Ytterbium dibromide has the slightly distorted form of the rutile structure, which contains octahedrally coordinated cations and is also adopted by $CaCl_2$ and $CaBr_2$ (*58*). Again, a general decrease in cation coordination number is observed as one moves from samarium to ytterbium. The behavior of the dibromides on addition to water is similar to that of the chlorides.

Data on the dibromides are shown in Table VI.

TABLE VI

PROPERTIES OF LANTHANIDE DIBROMIDES

Compound	Color	Structure	Cell parameters (Å)	Coordination No.	Mp (°C)	Ref.
$SmBr_2$	Red-brown	$SrBr_2$		8/7	669	(*143*, *499*, *505*)
		$PbCl_2$	$a_0 = 9.506$ $b_0 = 7.977$ $c_0 = 4.754$	9		(*37*)
$EuBr_2$	White	$SrBr_2$	$a_0 = 11.574$ $c_0 = 7.098$	8/7	683	(*143*, *228*, *505*)
$YbBr_2$	Yellow	$CaCl_2$	$a_0 = 6.63$ $b_0 = 6.93$ $c_0 = 4.37$	6	673	(*58*, *505*)

d. Diiodides. Neodymium diiodide crystallizes in the strontium dibromide structure which was described in the previous section. Samarium diiodide was shown many years ago (*144*) to be isostructural with one form of EuI_2 which is now known to be monoclinic (*35*), and to contain seven-coordinate europium with a coordination polyhedron very similar to that in the SrI_2 structure (*43*). The actual SrI_2 structure, described in the section on the dichlorides, is adopted by a recently prepared second form of EuI_2 (*43*).

The three remaining diiodides contain octahedrally coordinated cations in layer structures of the $CdCl_2$ and CdI_2 type. It can be seen that again, there is a decrease in coordination number of the cation across the series, and that the iodides of dysprosium, thulium, and ytterbium are the only di-*f* dihalides that form layer structures in which the anions are partly coordinated by other anions, rather than being surrounded entirely by cations. During the development of classical theories of ionic and covalent bonding, the adoption of such structures when the anion becomes large, and the cation small was attributed to polarization effects. Unlike the chlorides, the cell parameters of TmI_2 and YbI_2, which in this case were determined by one set of workers, show the expected order.

Some properties of the di-*f* diiodides are shown in Table VII. All the iodides melt congruently, and when added to air or water, their behavior is very similar to that of the corresponding chlorides. The neodymium, samarium, dysprosium, and thulium compounds are oxidized with great speed in moist air.

The list of known lanthanide diiodides is complete when the diiodides of lanthanum, cerium, praseodymium, and gadolinium (*125*, *387*, *124*) are added to those in Table VII. These compounds were prepared by reproportionation methods but have metallic lusters, significantly higher melting points than the divalent diiodides, and high electrical conductivity. Thus the room temperature resistivity of LaI_2 is $64 \times 10^{-6}\ \Omega$ cm which is very close to that of lanthanum metal. Likewise, the molar susceptibilities of lanthanum and lanthanum diiodide are small and very similar (*129*), a property expected of compounds containing La^{3+} ions. Such observations prompted the formulation $M^{3+}(e^-)I_2$ for the metallic diiodides; the odd electron is in a conduction band composed partly of the 5*d* orbitals of the metal and partly of outer iodine orbitals.

Investigation of the metal–metal triiodide phase diagrams for terbium, holmium, and erbium (*128*, *293*) revealed no lower halides, and this suggested that such compounds are thermodynamically unstable with respect to disproportionation at quite moderate temperatures.

TABLE VII

PROPERTIES OF SALINE LANTHANIDE DIIODIDES

Compound	Color	Structure	Cell parameters (Å)	Coordination No.	Mp (°C)	Ref.
NdI_2	Deep violet	$SrBr_2$		8/7	562	(*151*)
SmI_2	Deep green	EuI_2		7	520	(*143*, *505*)
EuI_2	Brown-green	EuI_2	$a_0 = 7.62$ $b_0 = 8.23$ $c_0 = 7.88$ $\beta = 98°$	7	580	(*35*, *43*, *505*)
		SrI_2	$a_0 = 15.12$ $b_0 = 8.18$ $c_0 = 7.83$	7		(*43*)
DyI_2	Deep purple	$CdCl_2$	$a_0 = 7.445$ $\alpha = 36.1°$	6	659	(*44*, *293*)
TmI_2	Black	CdI_2	$a_0 = 4.520$ $c_0 = 6.967$	6	756	(*26*, *505*)
YbI_2	Black	CdI_2	$a_0 = 4.503$ $c_0 = 6.972$	6	772	(*26*, *143*, *505*)

Thus, of the fourteen elements from lanthanum to ytterbium inclusive, at least ten, and probably eleven form diiodides. The first three form metallic tri-*f* diiodides; the next four, which include promethium, probably form saline di-*f* diiodides; gadolinium diiodide is metallic; terbium forms no diiodide at all; dysprosium yields a saline diiodide; no lower iodides appear to be formed by the next pair of elements; and the series is completed with saline di-*f* diiodides for thulium and ytterbium. The interpretation of this strikingly varied behavior is discussed in Section V,A,4.

e. Other Lower Halides. The lower halides discussed so far have compositions very close to the ideal stoichiometry MX_2. However, phase diagram analysis of M/MX_3 systems has revealed other lower halides, most of which have stoichiometries between the compositions MX_2 and MX_3. These compounds include $LaI_{2.42}$, $CeI_{2.4}$, and $PrI_{2.5}$ (*125*), $PrBr_{2.4}$ (*479*), $PrCl_{2.31}$ (*152*), $NdCl_{2.27}$ and $NdCl_{2.37}$ (*151*), $SmCl_{2.2}$ (*459*), $GdCl_{1.5}$ (*387*), $DyCl_{2.10}$ (*127*), $HoCl_{2.14}$ (*345*), and some ten to fifteen phases between the compositions $TmCl_{2.04}$ and $TmCl_{2.15}$ (*106*). If a melt of approximate composition $TmCl_{2.04}$ is cooled, the initial thermal arrest corresponding to the crystallization of $TmCl_2$ is followed by a remarkable series of other arrests corresponding to the successive crystallization of the phases between $TmCl_{2.04}$ and $TmCl_{2.15}$.

Rough conductivity measurements on the compounds listed in this section suggest that they are either insulators or semiconductors. With the exception of $GdCl_{1.5}$, it is usually assumed that they contain M^{2+} and M^{3+} ions, and, although this is almost certainly true in at least some cases, detailed evidence for it is lacking. Where the assumption is correct, the electronic structure of the dipositive ion is of interest. Compound $LaI_{2.42}$ has been the subject of the most careful studies. Its resistivity is about 10^2–10^3 Ω cm, a figure that is characteristic of a semiconductor, and powder photographs suggest that it is isomorphous with $CeI_{2.4}$ and $PrI_{2.5}$. Magnetic measurements are reasonably consistent with the assumption that the compound contains La^{3+} ions, as well as La^{2+} ions of configuration $[Xe]5d^1$ in an octahedral environment (*129*). The free La^{2+} ion has this configuration (*516*), and configurations of the type $[Xe]4f^n5d^1$ should be further favored in the condensed phase because of the crystal field splitting of the 5*d* orbitals. However, complete determinations of the structure of this compound and others of the same type are badly needed.

The structures of these compounds probably bear little or no relationship to that of Gd_2Cl_3. This interesting compound consists of dark gray needles with a brass reflectance (*387*), and magnetic measurements suggested that $4f^7$ cores are present (*203*). The structure consists

of parallel chains of gadolinium atoms surrounded and separated by chlorines, the Gd—Cl distances being comparable to those found in $GdCl_3$. The structure of the gadolinium chain is shown in Fig. 4 (*347, 348*). It consists of octahedra sharing edges, but at 3.90 Å, the distance between shared edges is rather long for bonding interaction, and the chain is better described as a chain of parallel metal dimers with an internuclear distance of 3.349 Å; each adjacent pair of dimers is linked above and below the chain by gadolinium atoms that are separated from the atoms of the dimers by about 3.75 Å. The internuclear distances in gadolinium metal are about 3.6 Å, so to assume appreciable metal–metal bonding at distances of 3.349 and 3.75 Å is entirely reasonable. If the chlorines separating the chains are assumed to be ionic, the compound can be formulated $(Gd_4^{6+})_n(Cl^-)_{6n}$. The gadolinium chains lie parallel to the long axis of the needlelike crystals and, if electron delocalization occurs within the chains, very possibly constitute a one-dimensional metal. Initial rough and ready attempts to detect appreciable conductivity along the long axis were unsuccessful, but this is now attributed to crystal imperfections that are easily generated at the tips of crystals with this type of habit.

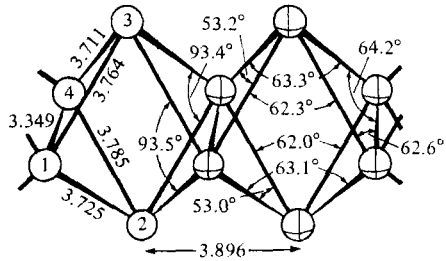

FIG. 4. Portion of the chain formed by gadolinium atoms in Gd_2Cl_3. From Lokken and Corbett (*348*), Fig. 3. Reprinted with permission from the *Inorg. Chem.* **12**, 556 (1973). Copyright by the American Chemical Society.

For a comment on the recently prepared metallic monochlorides, see the Appendix on p. 131.

B. Oxides and Chalcogenides

The number of adequately characterized lower lanthanide oxides has been reduced by recent research. Good grounds for the rejection of earlier claims for NdO, SmO, and YbO have been established (*80, 173*), and work on the Sm—Sm_2O_3 and Yb—Yb_2O_3 phase diagrams has shown that there is no evidence for the existence of lower oxides in samples quenched from temperatures of 1000° to 2000°C (*59, 126*).

Reported preparations of SmO films with the unlikely zinc blende structure (*333*) have been attributed to cubic hydride phases (*194*). It seems, however, that YbO can be prepared at lower temperatures. Its behavior, combined with its absence in the high-temperature regions of the phase diagram, suggest that the compound is of borderline stability with respect to the reaction,

$$3YbO \longrightarrow Yb + Yb_2O_3$$

The existence of EuO is beyond dispute, and its magnetic properties are consistent with the presence of Eu^{2+} ions. It seems, therefore, that the only lanthanide monoxides that are stable with respect to disproportionation at normal temperatures are EuO and YbO, a conclusion that is compatible with the stability sequence for the dipositive oxidation state in di-*f* systems derived in Section III,A,2.

Sulfides, selenides, and tellurides of the formula type MX have been prepared for all the lanthanide elements (*271, 185*). They all have the rock salt structure but there are some distinct differences between SmX, EuX, YbX, TmSe, TmTe, and the others. If the samarium, europium, and ytterbium compounds, TmSe, and TmTe are excluded, then the cell sides lie on smooth curves, the materials have a metallic appearance (*155a, 271*), and the resistivity of about 10^{-4} Ω cm corresponds to semimetallic character and increases slightly with temperature. By contrast, the samarium, europium, and ytterbium compounds are either semiconductors or insulators with resistivities of 10^3–10^4 Ω cm. (*139, 140, 471*) and their cell sides are distinctly larger than those of their neighbors (see Fig. 5). In addition, the magnetic susceptibilities of a number of the compounds and their variations with temperature in the range 100–300 K have been reviewed by McClure (*355*). This information can be used to calculate the effective magnetic moment from Eq. (1) and, thus, to obtain the number of 4*f* electrons. The results correspond closely to the values expected for tripositive ions, in the case of the metallike compounds, and to those expected for dipositive ions, in the case of SmX, EuX, and YbX. The latter are, therefore, classified as di-*f* chalcogenides analogous to the corresponding alkaline earth compounds, whereas the others can be formally written $M^{3+}(e^-)X^{2-}$; the electron giving rise to the metallic properties is delocalized in a conduction band composed perhaps of 6*s* or 5*d* (*355*) orbitals of the metal or of a combination of the two. The transfer of a nonbonding 4*f* electron in the di-*f* compounds to a metallic state in the others accounts for the shorter internuclear distances in the latter.

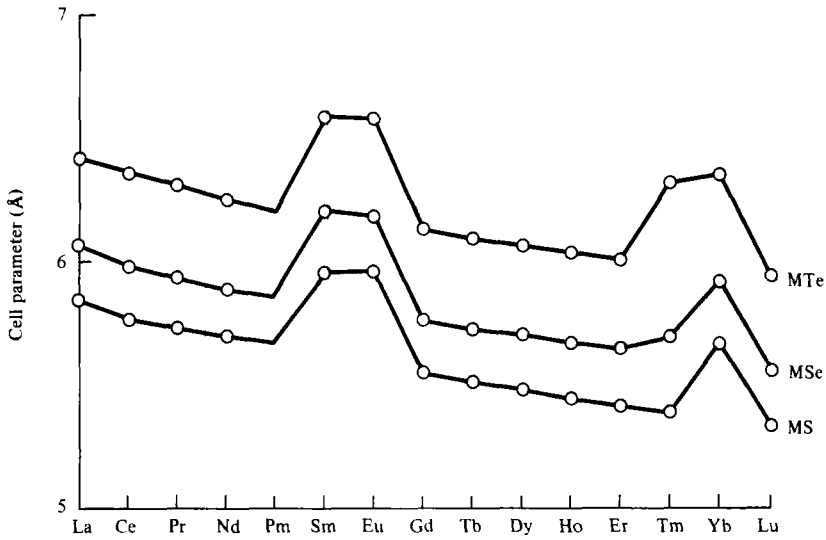

FIG. 5. Cell parameters of the rock salt structure of binary lanthanide sulfides, selenides, and tellurides. Data from Flahaut and Laruelle (*185*), except for SmX (*286*) and TmSe and TmTe (*88*).

The cases of TmSe and TmTe are striking in that the internuclear distances included in Fig. 5, the magnetic moments, and other evidence considered later, all suggest that both M^{2+} and M^{3+} ions are present at normal temperatures. The cell parameters of TmSe and TmTe are critically dependent on chalcogenide concentration, and to judge by the cell parameter, TmSe can be driven from an intermediate state to the tri-*f* state by the presence of a slight excess of selenium (*88*).

1. Preparative Methods

Early attempts to prepare EuO by reducing Eu_2O_3 with hydrogen were unsuccessful (*57*). However, if the reaction is carried out with a mixture of Eu_2O_3 and strontium oxide at 800°–1000°C, a red solid solution of EuO in SrO is obtained (*81*). This solid solution can also be prepared by heating a mixture of the two divalent carbonates. The europium(II) is gradually oxidized at room temperature (*82*). Pure EuO was first made by heating Eu_2O_3 with lanthanum at 1300°–1500°C under a pressure of 10^{-5} mm when the lower oxide sublimed off (*156*).

Other methods have included reduction of the sesquioxide with carbon (*1*), controlled oxidation of the metal (*193*), careful decomposition of the bivalent hydroxide obtained from aqueous media (*485*),

and reduction of the oxyhalides with lithium hydride *in vacuo* at 600°–800°C (*36*). The best method seems to be the reaction of the metal and Eu_2O_3 in tantalum or molybdenum containers at 800°–2000°C. Some workers assert that excess metal should be used, and residual europium distilled off when the reaction is over (*489*); others claim that stoichiometric mixtures are adequate (*306*, *351*). Molybdenum containers are said to be preferable to tantalum (*59*). Large single crystals can be grown from an EuO melt (*211*).

Recent claims to have prepared samples of YbO were rather cautiously phrased. The methods used involved the reaction of oxygen with a solution of ytterbium in liquid ammonia at temperatures of −33°C or less (*177*) and the reaction of oxygen with ytterbium at low pressures and a temperature of 200° to 300°C (*138*). In neither case was it possible to free the sample of Yb_2O_3.

The most widely used method for preparing the sulfides, selenides, and tellurides of samarium, europium, thulium, and ytterbium is the direct combination of the elements (*271*, *539*). The sulfides of samarium and ytterbium have been prepared by the reduction of the trivalent sulfides with aluminum at 1000°–1400°C (*146*, *456*), and samarium selenide by thermal decomposition of Sm_2Se_3 *in vacuo* at 1800°C (*212*). Compounds SmSe and YbSe have also been obtained by heating the sesquiselenides in metal vapor at low pressure and 750°–900°C (*451*).

To make EuS, early investigators of the europium compounds reduced the sulfate or the oxide Eu_2O_3 with H_2S. The first method gave a pure product but the second did not (*57*). This failing of the oxide/H_2S reaction has since been corrected by using higher temperatures (*17*, *145*, *490*). Compounds EuS, EuSe, and EuTe have been prepared by reducing the dichloride with elemental chalcogens at 600°C in hydrogen (*325*). This method is also effective for YbSe and YbTe (*326*). Europium chalcogenides can also be made by heating europium(II) or europium(III) oxalate with H_2S, H_2Se, or H_2Te at 800°C (*458*).

2. *General Properties*

Europium monoxide is a dark red-violet solid with the rock salt structure (a_0 = 5.144 Å). If kept free of water vapor, it does not react noticeably in air (*364*). The phase EuO has only a small composition range, but because the stoichiometric variations have a considerable influence on the magnetic, electrical, and optical properties of the compound, they have been fairly carefully investigated.

Partial determination of the Eu—Eu_2O_3 phase diagram (*491*) showed that the exact composition of the compound depends critically on the

temperature of crystallization and varies from about $EuO_{1.02}$ for the range 1825°–1965°C, where at the highest temperatures it is mixed with a little Eu_3O_4, to about $EuO_{0.99}$ for the range 1300°–1780°C. Intermediate crystallization temperatures of 1780° to 1825°C result in stoichiometric EuO. The melting point of 1965° ± 10°C occurs in the oxygen-rich crystallization region and, therefore, refers to oxygen-rich samples of the oxide. The oxygen-rich samples contain europium vacancies, a charge balance being achieved by the formation of some Eu^{3+} ions. The latter were detected by the Mössbauer spectrum of ^{151}Eu; the isomer shift for the tri-*f* europium is considerably less negative than for the di-*f* state. It was also possible to detect the transitions within the $4f^6(^7F_J)$ multiplet of the Eu^{3+} ion in the infrared spectrum (*491*). The oxygen-deficient samples contain oxygen vacancies and have striking electrical properties (see Section III,B,5). As expected, stoichiometric EuO is an insulator with a room temperature resistivity of about 10^7 Ω cm (*491*).

Pure YbO has not been prepared, but impure samples are grayish-white and have a rock salt structure with $a_0 = 4.87$ Å (*138*, *177*). On heating in oxygen or acid washing, it is converted to Yb_2O_3, and the absence of the compound in the high-temperature Yb—Yb_2O_3 phase diagram (*59*, *126*) suggests that it is unstable with respect to disproportionation at temperatures above about 800°C.

The remaining di-*f* monochalcogenides are the sulfides, selenides, and tellurides of samarium, europium, and ytterbium, TmSe, and TmTe. Most workers state that these compounds are black, although they sometimes have a bluish or violet tinge. The cell parameters of their rock salt structures have been reviewed by Flahaut and Laruelle (*185*), and recent values for the thulium compounds are given by Campagna *et al.* (*100*) and Bucher *et al.* (*88*). As noted earlier, and in Fig. 5, the values lie above the smooth curve obtained when the cell sides of the metallic tri-*f* compounds are plotted against atomic number. Some of the compounds, notably YbS, have a considerable composition range on the sulfur-rich side of the ideal composition, a property associated with the formation of mixed valence compounds, which have recently been reviewed (*183*, *184*, *185*). Thermodynamic data on EuO, EuS, EuSe, and EuTe have been reviewed by McMasters *et al.* (*367*) who also determined high-temperature heat capacity data. Table VIII contains some of their recommended figures except for the value of ΔH_f^0(EuO, s) which is the value of Huber and Holley (*259*, *260*) after recalculation by Morss and Haug (*407*).

Some data on SmSe and SmTe exist (*414*) but the uncertainties are large.

TABLE VIII

THERMODYNAMIC DATA AND CELL PARAMETERS OF EUROPIUM MONOCHALCOGENIDES AT 25°C[a]

Parameter	EuO	EuS	EuSe	EuTe
ΔH_f^0 (kcal mole^{-1})	−141.4	−106.0	−93.8	−93.2
S^0 (cal K^{-1} mole^{-1})	20.0	22.9	25.4[b]	27.2[b]
ΔG_f^0 (kcal mole^{-1})	−134.5	−105.0	−92.8	−92.2
a_0(Å)	5.1435	5.9679	6.1936	6.5984

[a] For sources, see text.
[b] Estimated values of MacMasters *et al.* (*367*).

3. *Magnetic Properties*

An enormous amount of research has been done on the magnetic properties of the europium monochalcogenides, so the magnetism of those compounds is discussed separately from that of other bivalent chalcogenides. We first discuss the samarium, ytterbium, and thulium compounds.

a. Samarium, Ytterbium, and Thulium Monochalcogenides. No magnetic measurements have been made on YbO, but the other ytterbium chalcogenides have very low magnetic susceptibilities consistent with the diamagnetism expected of the [Xe]$4f^{14}$ configuration of the Yb^{2+} ion (*139*, *326*). The samarium chalcogenides SmS, SmSe, and SmTe have room temperature molar susceptibilities in the range 4200–5000 × 10^{-6} cgs units (*90*, *212*, *271*, *455a*) and effective magnetic moments of 4.3 to 4.6 μ_B. These are consistent with the [Xe]$4f^6$ configuration of the Sm^{2+} ion when, as usual for f^6 systems, allowance is made for the population of the excited states $^7F_1$ and $^7F_2$ at normal temperatures. However, the assumption that these compounds contain only di-*f* samarium cannot be sustained under more extreme conditions. At higher temperatures in the range 300–1200 K, studies of the variation of χ_m for SmS with T show that the plot of $1/\chi_m$ against T deviates markedly from the behavior expected of a compound of Sm(II) (*590*). This deviation is associated with unexpectedly low values of χ_m at high temperatures and was attributed to the presence of a thermal equilibrium between Sm^{2+} and Sm^{3+} ions, the ΔE value for conversion of Sm^{2+} to Sm^{3+} being 0.18 eV. Electrical and optical measurements discussed in Section III,B,4 also support the presence of some tri-*f* samarium in SmS, and on p. 36, the conversion of di-*f* SmS to the tri-*f* metallic form at fairly low pressures is examined. Claims that about 3% tri-*f* samarium has been detected in SmX compounds by

low-temperature magnetic measurements have also been made (*90*).

These observations suggest that, unlike the corresponding europium compounds, the samarium monochalcogenides are close to instability with respect to the change

$$M^{2+}X^{2-} \longrightarrow M^{3+}(e^-)X^{2-} \tag{6}$$

at normal temperatures and pressures. This appears to be true also of the compounds TmSe and TmTe. The TmSe follows the Curie–Weiss law [Eq. (5)] with $\theta = -33$ K in the temperature range 50–300 K, and becomes antiferromagnetic below 1.85 K; TmTe obeys the Curie law (*88*). The effective magnetic moments of these compounds in the temperature range 50–300 K are 6.32 μ_B and 4.96 μ_B, respectively, figures that lie between the theoretical values of 4.5 and 7.57 μ_B for Tm^{2+} and Tm^{3+} ions (*100*). These values imply that TmTe is mainly di-*f*, and TmSe is mainly tri-*f* at normal temperatures and pressures, a conclusion that is supported by the cell parameters.

The evidence for the simultaneous existence of two f^n configurations in the monochalcogenides of samarium and thulium, allied with the firm di-*f* characteristics of the corresponding europium and ytterbium compounds, suggest that the stabilities of di-*f* chalcogenides with respect to reaction (6) follow the sequences Nd < (Pm) < Sm < Eu ≫ Gd and Er < Tm < Yb. These sequences are identical with those deduced on p. 12 for the stabilities of di-*f* dihalides with respect to disproportionation or oxidation.

b. Europium Monochalcogenides. Enormous interest in the properties of the europium monochalcogenides sprang from the discovery by Matthias, Bozorth, and Van Vleck in 1961 that EuO was ferromagnetic at low temperatures (*384*). Two important reviews of the properties of these magnetic semiconductors exist (*216*, *396*), and the discussion here is necessarily selective.

Matthias *et al.* found that the magnetic susceptibility of EuO followed the Curie-Weiss formula [Eq. (5), Section III,A,3,a] in the temperature range 90–300 K with $\theta = 77$ K. Another literature value is 76 K (*364*). The magnetic ordering temperature, T_c, is 69.2 K (*207*). The ferromagnetism of EuO at low temperatures was confirmed by neutron diffraction studies at 28 K and at room temperature; very large increases in the intensities of the (111) and (311) reflections are observed at the lower temperature, but there was no sign of any multiplication of the unit cell parameter. The data did not allow determination of the direction of magnetization with respect to the crystallographic axes (*418*).

Apart from possible practical applications touched on in Section III,B,5, the discovery of the ferromagnetism of EuO aroused great theoretical interest. The usual mechanism proposed for the propagation of forces producing long-range magnetic ordering is the Rudermann-Kittel-Kasuya-Yosida interaction: an ion polarizes a nearby conduction electron and the polarization is transmitted outward from the ion in a damped oscillatory way (*311*, *477*, *585*). Neighboring ions interact with the polarized conduction electrons and either align with the polarization wave (ferromagnetic ordering) or against it (antiferromagnetic ordering). Since EuO is an insulator, there are no conduction electrons to propagate the wave, and some modification to the usual explanation or a new mechanism is required. Direct overlap of the $4f$ orbitals on neighboring cations is unlikely because they are thought to be strongly localized, and the cation–cation distances are about 5 Å.

Possible mechanisms have been reviewed (*396*). The preferred mechanism was that based on an early suggestion by Goodenough (*198*) in which cation–cation superexchange occurs via overlap of the $4f^7$ state of one atom with the empty $5d$ state on another.

Like EuO, the remaining three monochalcogenides follow the Curie–Weiss law down to quite low temperatures with effective magnetic moments in the range 7.6–8.2 μ_B (*199*, *361*, *362*, *539*, *577*). The Curie–Weiss temperatures, θ, are shown in Table IX. Table IX also contains the ordering temperatures for the magnetic transitions obtained from peaks in specific heat–temperature plots for EuO (*210*, *330*), EuS (*409*), EuSe (*97*), and EuTe (*97*, *430*). Compound EuS is definitely ferromagnetic, and EuTe is definitely antiferromagnetic. The low-temperature behavior of EuSe is discussed later.

Considerable efforts have been made to identify the orientation and sequence of the sets of opposed spins that give rise to the antiferromagnetism of EuTe. Neutron diffraction studies of EuTe at room temperature and at 4.2 K show important differences (*578*). Below

TABLE IX

MAGNETIC PROPERTIES OF EUROPIUM MONOCHALCOGENIDES AND EXCHANGE INTERACTIONS OBTAINED BY THE MOLECULAR FIELD APPROXIMATION

Compound	Magnetic order (zero field)	Curie-Weiss temp. (K)	Ordering temp. (K)	J_1/k (K)	J_2/k (K)
EuO	Ferromagnetic	76	69.3	0.6	−0.06
EuS	Ferromagnetic	16	16.2	0.2	−0.10
EuSe	See text	6	4.6	0.1	−0.11
EuTe	Antiferromagnetic	−7.5	9.6	0.03	−0.15

the Néel temperature at 4.2 K, the diffraction pattern contains new low-angle reflections, and can be indexed on the basis of a unit cell whose cell parameter is twice the value appropriate at room temperature. This and other features of the pattern show that, below the Néel temperature, the spins of the Eu^{2+} ions lying in the (111) planes of the usual unit cell are ordered so that within any plane the spins are parallel but so that the spins in adjacent planes are opposed (Fig. 6). The new set of equivalent (111) planes, thus, consists of alternate planes drawn from the old set and its members are twice as far apart. The new (111) reflection, therefore, occurs at a lower angle. This type of antiferromagnetic ordering also occurs in the classic case of MnO (*495*). The gradual destruction by applied fields of the antiparallelism of the two sublattices of spins has been studied (*430*).

The behavior of EuSe whose cell parameter falls between that of ferromagnetic EuS and antiferromagnetic EuTe is extremely complex. Early reports of ferromagnetism were based on experiments in applied fields. Studies of the magnetization behavior (*96*, *335*, *363*, *364*) and of the specific heat (*574*) suggest that at zero field, EuSe is antiferromagnetic in the temperature range from 2.8 K to the Néel temperature of 4.6 K.

Neutron diffraction photographs (*178*, *455*) and ^{153}Eu NMR measurements (*328*) suggest that immediately below the Néel temperature, the antiferromagnetic ordering is different from that observed in EuTe. Within each (111) plane, all spins are parallel, but two successive planes whose spins are parallel are followed by two of opposed spin in an arrangement designated NNSS. This contrasts with the NSNS arrangement in EuTe.

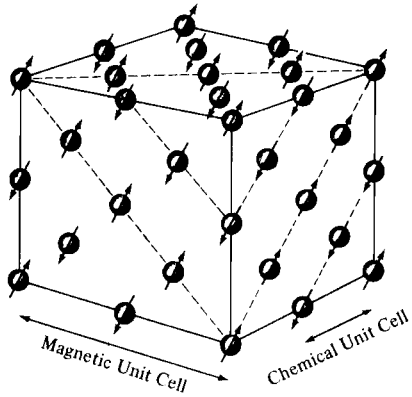

FIG. 6. Positions of europium ions and their relative spin orientations in the antiferromagnetic structure of EuTe below the Néel temperature. (From C. Kittel, "Introduction to Solid State Physics," 3rd edition. Wiley, New York, 1966, p. 481, Fig. 27.

As the temperature is lowered further to the temperature range 2.5–2.8 K, there is some evidence for a change in the magnetic ordering of the antiferromagnetic phase to the NSNS arrangement of EuTe. At all events, in this temperature range, the antiferromagnetic phase or phases coexists with a *ferrimagnetic* phase in which both ferromagnetic and antiferromagnetic ordering is found. The suggested sequence of spins is NNS, two successive planes of parallel spin being followed by one of opposed spin. Below about 2.0 K, the ferrimagnetic phase exists alone.

These data are summarized in the tentative magnetic phase diagram of Fig. 7 (*328*). It can be seen that with increasing applied field, the ferrimagnetic and antiferromagnetic zero-field structures change to an intermediate phase at 2–4 kOe, and finally to the ferromagnetic phase at 4–8 kOe, the exact values depending on the temperature.

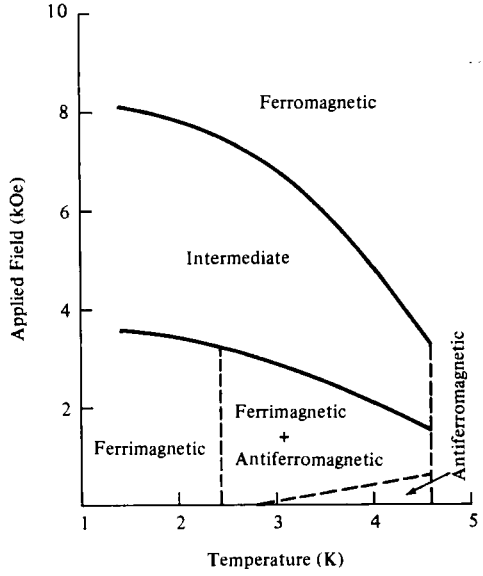

FIG. 7. Magnetic phase diagram for EuSe.

The gradual change from ferromagnetism in EuO to antiferromagnetism in EuTe as the cell parameter increases can be treated by the molecular field approximation. This gives

$$k\theta = \tfrac{2}{3}S(S+1)(Z_1J_1 + Z_2J_2) = 126J_1 + 63J_2$$

$$kT_N = \tfrac{2}{3}S(S+1)(-Z_2J_2) = -63J_2$$

where k is Boltzmann's constant, S is the spin vector, $J = 7/2$ for the $^8S_{7/2}$ ground state of the Eu^{2+} ion, $Z_1 = 12$ is the number of nearest Eu^{2+} neighbors in the rock salt structure, $Z_2 = 6$ is the number of next-nearest neighbors and J_1 and J_2 are the nearest-neighbor and next-nearest-neighbor exchange interactions. The experimental values of the Curie–Weiss temperatures θ for all the europium chalcogenides, and the Néel temperature of EuTe can be used to estimate values of J_1 and J_2 for each compound. Typical results obtained by this and other methods are shown in Table IX (*111*, *364*, *396*). It can be seen that in EuO, there is a strong ferromagnetic nearest-neighbor interaction and a weaker antiferromagnetic next-nearest-neighbor interaction. The former is responsible for the high ordering temperature. As the anion becomes larger and the metal–metal distance increases, ferromagnetic interaction falls off sharply, but the antiferromagnetic interaction is not greatly altered, until with EuTe, J_2 is both negative and predominant so that the compound is antiferromagnetically ordered at low temperatures. With EuSe, the values of J_1 and J_2 are of similar magnitude but opposite sign, indicating that the ferromagnetically and antiferromagnetically ordered states are close in energy as the experimental results show.

It is clear that the dependence of J_1 on internuclear distance is consistent with the coupling mechanisms, already cited, that depend on cation–cation superexchange; conversely, the relatively invariant J_2 values corroborate an antiferromagnetic exchange interaction occurring through anions. More recent work has altered the values of J_1 and J_2 to some extent (*76*, *67*, *379*, *380*, *237*, *430*) but has not changed the general picture. However, there are signs that if improvements on the molecular field approximation are made, particularly allowance for magnetic dipole interactions, then J_2 in EuO is just *positive* and decreases with internuclear distance becoming negative in EuS (*523*). Support for the importance of magnetic dipole interactions comes from an analysis of specific heat data on EuO (*478*).

4. *Electrical Properties, Optical Properties, and Pressure-Induced Transitions*

In the particular case of the europium chalcogenides, reviews of magneto-optical and electrical properties are available (*216*, *396*). The optical properties have been reviewed by Dimmock (*141*). The absorption spectra and reflectance spectra of the europium monochalcogenides show two peaks: a lower energy one at about 2 eV, and a higher at about 4 eV. These are assigned to the transitions between the $4f^7(^8S_{7/2})$ state of the Eu^{2+} ion and the $4f^6(^7F_J)5d$ state that is

split by the ligand field of the octahedral environment into a lower $4f^6(^7F_J)5d(T_{2g})$ component and an upper $4f^6(^7F_J)5d(E_g)$.

Higher-energy peaks are observed in the photoemission spectra corresponding to loss of electrons from the relatively deep-lying valence band (*155*). Such observations corroborated an existing energy level scheme, which is shown in Fig. 8 (*395*, *396*). In an ionic formulation, the valence band is composed exclusively of the outer p orbitals of the anions, and is denoted p^6. The $4f$ level is strongly localized in the cores of the cations and is, therefore, represented by a hairline level between the valence and conduction bands. The $5d$ levels split into two sets, and in the scheme in Fig. 8, the T_{2g} set is placed below a conduction band formed from the 6*s* orbitals of the metal, whereas the E_g set are placed above. The gap ε between the $4f^7$ levels and the base of the T_{2g} set is identified with the absorption *edge* of the low-energy peak mentioned at the beginning of this section. At 300 K, this edge occurs at 1.12, 1.64, 1.8, and 2.0 eV in EuO, EuS, EuSe, and EuTe, respectively.

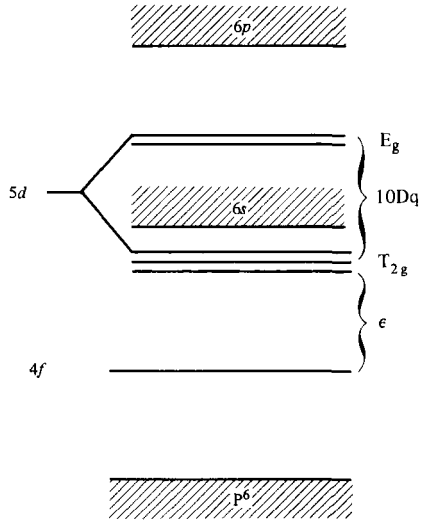

FIG. 8. Proposed energy level scheme for europium chalcogenides and EuO.

However, there is uncertainty as to the width of the two $5d$ sets, and to their position relative to the 6*s* conduction band. In some cases, they may merge with and form part of the conduction band; indeed, as the minimum energy of photons requires to excite conductivity in the europium chalcogenides is almost equal to the absorption edge (*344*), transition $4f^7 \rightarrow 4f^6(^7F_J)5d(T_{2g})$ would appear to be a conduction-

prompting process, and the simplest interpretation of this is to argue that the T_{2g} set overlaps with or forms part of the conduction band (*583*). Recent work on reflectance spectra has revealed the splitting of the ^7F_J multiplet of the $4f^6$ core in the excited state (*213*, *346*); the $4f$ level appears to be about 2.8 eV above the top of the valence band in EuO, and about 1.6 eV in EuSe (*130*).

Similar assignments can be made to the transmission spectra of YbSe and YbTe. In some work, only the lower $4f^{14} \rightarrow 4f^{13}5d(T_{2g})$ peak was clearly resolved; the expected peak corresponding to $4f^{14} \rightarrow 4f^{13}5d(E_g)$ was lost in a region of very heavy absorption above 3 eV (*579*). The absorption edge of the low-energy peak occurs at about 1.5 eV in YbSe, and at about 2 eV in YbTe, values that are very similar to those for the corresponding europium compounds. Again, conduction is excited by photons with energies close to the absorption edges (*267*). In recent work (*521*), the resolution was improved, and new bands in the YbSe and YbTe spectra were assigned to $4f^{14} \rightarrow 4f^{13}5d(E_g)$ transitions. Furthermore, each band corresponding to excitation to a T_{2g} or E_g level occurred twice, a splitting that corresponds to the splitting of the ^2F_J level of the $4f^{13}$ core into $^2F_{7/2}$ and $^2F_{5/2}$ states. Transitions between the valence and conduction bands appeared to begin at about 4 eV. The change of the absorption edge with pressure in Ybs, YbSe, and YbTe has also been measured (*415*).

In the case of the samarium chalcogenides, four peaks are expected from the $4f^6 \rightarrow 4f^5 5d^1$ transition, even when spin orbit coupling is ignored, because the $5d$ electron can be coupled with the ^6H_J ground state of the $4f^5$ core or the excited ^6F_J state. The peaks have all been observed (*247*, *307*) in the absorption and reflectance spectrum of SmS:

$$4f^6(^7F_0) \rightarrow 4f^5(^6H_J)5d(T_{2g}) \qquad \text{at 0.79 eV}$$

$$4f^6(^7F_0) \rightarrow 4f^5(^6F_J)5d(T_{2g}) \qquad \text{at 1.64 eV}$$

$$4f^6(^7F_0) \rightarrow 4f^5(^6H_J)5d(E_g) \qquad \text{at 3 eV}$$

$$4f^6(^7F_0) \rightarrow 4f^5(^6F_J)5d(E_g) \qquad \text{at about 3.5 eV}$$

The lower-energy peak occurs at much smaller energies than in the europium and ytterbium compounds. The exact value of the low-energy absorption edge, which is of great theoretical interest, has been the subject of controversy. In SmSe and SmTe, it lies at 0.46 and 0.63 eV, respectively (*285*), but in SmS, values of 0.4 (*247*), 0.2 (*285*) and, most recently, 0.06 eV (*307*) have been assigned.

The low energies of the absorption edge suggest first that the bivalent samarium chalcogenides might be intrinsic semiconductors,

one of the 4*f* electrons on the Sm^{2+} ion being thermally excited to the conduction band to give an Sm^{3+} ion. In Section III,B,3,a, reference was made to magnetic evidence for this process: in SmS at high temperatures, the magnetic properties correspond to those expected of a compound containing some Sm^{3+} ions, the energy of conversion of the di-*f* to the tri-*f* state being 0.18 eV. This value is in good agreement with the figure of 0.22 eV obtained from a log ρ vs $1/T$ plot for SmS in the range 80–1800 K and both are close to the absorption edge values. The decrease in resistivity, ρ, with temperature is attributed to intrinsic semiconductivity (*590*), and Hall effect measurements show that the conductivity is *n*-type as expected. The phase, however, has a considerable composition range, SmS—$Sm_{1.17}S$, and through most of the samarium-rich region, the conductivity is metallic, possibly because of the formation of an impurity band by interstitial samarium donors (*591*). Further evidence for the existence of two valence states in SmS at room temperature comes from the L_{III} lines in the X-ray absorption spectrum which show two peaks, one of which gets progressively weaker at high temperatures (*68*). A similar phenomenon has been reported in the photoemission spectrum (*188*) although this is a matter for dispute (*101*).

Intrinsic *n*-type semiconductivity has also been observed in SmSe, in contrast to YbSe and YbTe wherein the 4*f* level lies much deeper beneath the conduction band and the conductivity is *p*-type, probably because of lattice defects or impurities (*471*).

Another property of the samarium monochalcogenides associated with the small separation between the 4*f* level and the base of the conduction band is the occurrence of a transition from di-*f* semiconductors to tri-*f* metallic compounds at fairly low pressures. From Fig. 5 it is clear that the process

$$Sm^{2+}S^{2-} \longrightarrow Sm^{3+}(e^-)S^{2-}$$

should occur with a decrease in volume and be favored by increased pressure. When the pressure on a crystal of samarium monosulfide reaches about 6 kbar, points on the black crystal begin to flash. At 6.5 kbar, the resistivity of the sample drops sharply from about 10^{-3} to 10^{-4} Ω cm, there is a sudden decrease in the cell parameter of about 13%, and the crystal becomes bright golden-yellow (*113*, *285*, *316*). The variation of the resistivity of the sample with pressure is shown in Fig. 9. It can be seen that when the pressure on the metallic phase is relaxed, reversion to the di-*f* state occurs at a pressure that is considerably less than 6.5 kbar, and the resistivity–pressure variation follows a hysteresis loop. Gradual substitution of gadolinium for

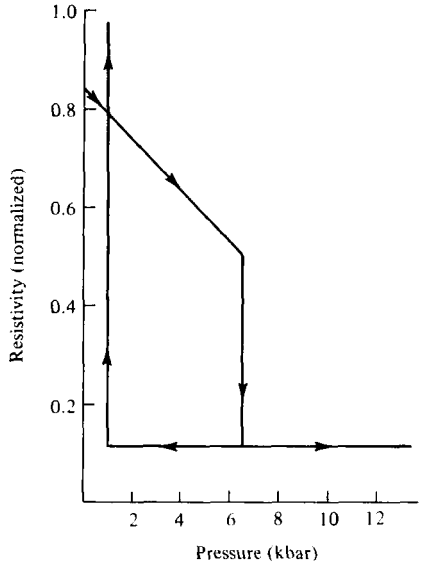

FIG. 9. Variation of the normalized resistivity of SmS with pressure.

samarium in the low-pressure form of SmS lowers the cell parameter and has an effect similar to that of increased pressure. The transition to the metallic phase occurs at 15.5 mole % gadolinium (*283*).

Similar high-pressure insulator–metal transitions are observed in SmSe and SmTe, but they occur gradually over a range of pressures rather than discontinuously as in SmS (*284*, *285*). In SmSe, the range is about 15–40 kbar and in SmTe, 20–50 kbar. In SmS, the resistivity of the sample at zero pressure is already rather low because of intrinsic semiconductivity caused by the very small gap between the 4*f* level and the conduction band. The semiconductivity of SmSe and SmTe is not so marked, and when contributions from crystal defects are excluded, the resistivity of SmTe, for example, appears to drop from about 10^6 to $10^{-4}\ \Omega$ cm between zero pressure and the completion of the insulator–metal transition, a fall of 10^{10}. By assuming that the activation energy ΔE associated with the conduction process is zero when the transition is complete at a pressure P, it is easily shown that

$$\ln \rho/\rho_p = \Delta E/RT$$

where ρ is the resistivity at fixed pressure, and ΔE is the corresponding activation energy. Thus the activation energy at zero pressure is given by

$$\Delta E = kT \ln 10^{10} \sim 0.6 \text{ eV}$$

This figure is close to the spectroscopic absorption edge of 0.63 eV at zero pressure, and a similar agreement is found for SmSe. Furthermore, the absorption edges in the samarium chalcogenides decrease with pressure at a rate suggesting that they become zero in the region of the pressure required for completion of the insulator–metal transition (*90, 307*). Such observations prompt a theoretical model for the transition in which the more exposed outer 5*d* orbitals on the metal are, because of increasing overlap, lowered in energy relative to the localized 4*f* orbitals by increasing pressure, so that the gap between the 4*f* level and the base of the conduction band decreases and has passed through zero when the transition is completed. One 4*f* electron per metal atom has then been transferred to the conduction band.

It seems clear, however, that, even in the case of SmS shown in Fig. 9, the transition from the semiconductor to the metal is not sharp. Thus the cell parameter of the high-pressure form of SmS immediately above 7 kbar is about 0.1 Å larger than the interpolated value for the purely tri-*f* phase obtained from Fig. 5 (*283, 373*), and the magnetic susceptibility in the temperature range 0–400 K is consistent with that of a compound containing a significant proportion of $4f^6$ cores (*373*). Thus the properties of the low-pressure form of SmS, discussed here and in Section III,B,3,a, taken with the properties of the high-pressure form suggest that compounds containing both di-*f* and tri-*f* configurations can exist over an unexpectedly wide range of temperatures and pressures. Likewise, studies of the X-ray photoemission spectra of TmSe and TmTe at normal temperatures and pressures suggest that both di-*f* and tri-*f* states exist together over a range of conditions (*100*). Such systems are said to be in a state of interconfigurational fluctuation in which ions fluctuate between di-*f* and tri-*f* states with 4*f* shells emitting and absorbing conduction electrons.

Attempts to formulate theories that can account for the different degrees of gradualism in the pressure-induced transitions, and for the unexpected coexistence of the two configurations are currently at a formative stage. Two papers by Hirst (*238, 239*) focus particularly on the relatively low density of states in the conduction band as compared with that for the localized 4*f* level. Progressive transfer of electrons from the 4*f* shell to the conduction band progressively raises the Fermi energy and reduces the sharpness of the transition with respect to pressure. Other approaches to the problem exist (*8, 89*).

In addition to those recorded in SmS, SmSe, and SmTe, what are believed to be insulator–metal transitions have also been observed in EuO, TmTe, YbS, YbSe, and YbTe. In the case of EuO and SmTe, this transition, in which the NaCl structure is maintained while the cell pa-

rameter drops, is followed by a transition to a CsCl structure at higher pressure. In the case of EuS, EuSe, and EuTe, no insulator–metal transition has been observed in the pressure range 0–300 kbar (*113*, *282*, *286*), a conclusion that conflicts with earlier work (*474*), but the compounds transform to the CsCl structure at pressures of 215, 145, and 110 kbar, respectively.

In Table X, a list of divalent monochalcogenides in which insulator–metal transitions occur is presented. Values (*286*) are also given for the absorption edge at zero pressure, which is identified with the separation of the 4*f* level and the conduction band, and the rate at which this separation closes with pressure. The colors of the metallic phases are silverish in the case of EuO, deep purple for SmTe and YbTe, copperish for SmSe and YbSe, and golden-yellow for SmS and YbS. In each case, the absorption edge given in Table X and the rate of closure with pressure give a pressure for zero separation of the 4*f* level and the conduction band which is close to the observed pressure for an insulator–metal transition.

TABLE X

PHASE TRANSITIONS IN SOME DIVALENT CHALCOGENIDES[a]

Substance	Absorption edge (E) (eV)	dE/dP (meV kbar^{-1})	New phase	Transition pressure (kbar)
SmS	0.065	−10.0	Metallic	6.5
SmSe	0.50	−11.0	Metallic	0–60
SmTe	0.70	−11.9	Metallic	0–60
			CsCl	110
EuO	1.12	−4.4	Metallic	~300
			CsCl	~400
TmTe	0.22		Metallic	15–30
YbS	1.0	−6	Metallic	150–200
YbSe	1.50	−10	Metallic	150–200
YbTe	1.80	−11	Metallic	150–200

[a] Data are from Jayaraman *et al.* (*286*) and may differ slightly from figures given in the text which are from specific references.

From the transformation pressures for tellurides in particular, it is clear that the stabilities of the di-*f* compounds with respect to processes such as Eq. (6) run in the order La—Nd < Sm < Eu ≫ Gd—Er < Tm < Yb. The same sequence can be obtained from the zero-pressure absorption edge. Thus the relative stabilities of these di-*f* and tri-*f* compounds involved in metal–insulator transitions fit perfectly into the sequences deduced on pp. 12 and 29.

5. *Influence of Nonstoichiometry on Properties and Applications of Monochalcogenides*

This review has concentrated on the properties of stoichiometric compounds, but in this section, we choose from a very wide range of possible references, one to two reports that may convey an impression of the interesting research which has been done on nonstoichiometric europium monochalcogenides. Many useful references to this work may be found in the paper by Shapira and Reed (*493*).

Compound EuO has received most attention. When crystals of EuO are grown in the presence of an excess of europium, the electrical properties are quite different from either the europium-deficient or stoichiometric phases. In particular, the conductivity in the region of 5 K has a high value of about $10^3\ \Omega^{-1}$ cm but drops rapidly with rising temperature and reaches a minimum of about $10^{-11}\ \Omega^{-1}$ cm in the region of the Curie point, $T_c = 69$ K, before increasing gradually to about $10^{-4}\ \Omega^{-1}$ cm at room temperature (*429*, *445*). Hall effect measurements suggest that this metal–insulator transition is due to a change in carrier concentration, the conductivity being *n*-type (*305*, *445*).

Of the models advanced to account for this behavior, the most satisfactory seems to be that of the bound magnetic polaron (*532*, *533*). The europium excess is attributed to oxygen vacancies, and the conductivity to electrons activated from the oxygen vacancies, which can be regarded as donor levels, up into conduction band states. In the paramagnetic region above T_c, two factors tend to localize the potential conduction electrons on to the vacancy sites: the Coulombic attraction of the vacancy, and the magnetic energy gained by an alignment of the spin with a partially ordered ferromagnetic cluster of the spins of those Eu^{2+} ions in its neighborhood. The electron gains magnetic energy by ordering a small number of Eu^{2+} spins, thereby forming a magnetic polaron. However, below T_c, when the Eu^{2+} system becomes fully ferromagnetic, the magnetic binding disappears, the Coulomb energy alone is not enough to bind the electron, and it delocalizes to produce metallic conductivity. Evidence for this mechanism includes the observation that the susceptibility per mole of europium at any temperature increases with the europium excess, and that constant θ in Eq. (5) behaves similarly (*365*, *533*). This is attributed to the contribution from the electrons that arise out of the excess europium, to the exchange interaction within the polaron. A conductivity minimum near the Curie temperature is also found in europium-rich EuS (*493*, *529*).

The magneto-optical properties of the europium chalcogenides have potential applications in advanced memory devices such as beam-

addressable files. This type of device has been described by several authors (*159, 168, 169, 568*). A film of ferromagnetic material below its Curie point is magnetized in a particular direction. In the writing process a pulsed laser beam is used to trigger a change in the magnetic state of the storage material at spots on the film, for example by heating the spots to near or above the Curie point of the material and inducing a reversed state of magnetization by means of a bias magnetic field. With a laser beam, dots of a few microns diameter can be recorded, and the two states of magnetization on the film can be interpreted as elements of a binary code. In the reading process, the reversed magnetization of the written spot is detected by its effect on the polarization state of the laser beam which is then operating at reduced power. This is particularly easy with the europium chalcogenides because their magneto-optical properties, such as the Faraday rotation or Kerr effect, are very large (*204, 519, 520*). A considerable amount of work has been directed at increasing the Curie temperature of EuO into the region of convenient working temperatures for such devices. If the compound is doped with about 7% iron, the Curie temperature rises to about 190 K (*6*), and the addition of both iron and Gd^{3+} results in Curie temperatures in excess of 200 K (*7*).

6. Compounds Containing Mixed Oxidation States

The chemistry of binary and ternary sulfides, selenides, and tellurides of the lanthanide elements, including those containing di-*f* samarium, europium, and ytterbium, has been the subject of recent review articles (*183–185*). This section is, therefore, concerned only with oxides.

The best-known compound of this type is Eu_3O_4. It is a dark red powder made by heating stoichiometric amounts of EuO and Eu_2O_3 in an inert atmosphere at 900°C (*40*). Other methods of preparation include hydrogen reduction of Eu_2O_3 or $Eu(OH)_3$ at 1650°C (*2, 470*). The compound crystallizes in the orthorhombic system, space group *Pnam*, and is isomorphous with Ca_2FeO_4 and with Eu_2SrO_4 which can be made by heating Eu_2O_3 and $SrCO_3$ in air at 1000°C (*40, 470*). The internuclear distances suggest that the compound contains dipositive and tripositive europium. The coordination polyhedron of the Eu^{3+} ion is a distorted octahedron with average Eu—O distances of about 2.34 Å; the Eu^{2+} ions are coordinated to 9 oxygens as in the $PbCl_2$ structure (Fig. 3a) but one of the three Eu—O distances in the equatorial plane is as long as 3.991 Å compared with lengths of 2.64 to 2.96 Å for other Eu(II)—O distances, so it is probably more accurate to describe the coordination number as 8. The average Eu—O distance

for the 8 oxygens is 2.71 Å, considerably longer than the tripositive Eu—O distance. X-Ray data for the mixed valence compound $LiEu_3O_4$ allows a similar distinction to be drawn between dipositive and tripositive europium (*39*).

The magnetic properties of Eu_3O_4 can be related to its structure. The compound is antiferromagnetic with a Néel point, $T_N = 5.0$ K. However, above about 20 K, the Curie–Weiss law as expressed in Eq. (5) (Section III,A,3,a), where $\theta = 5$ K, is obeyed; the sign of θ indicates a predominantly ferromagnetic interaction within the compound. This observation can be related to the fact that, below T_N, Eu_3O_4 is metamagnetic, that is, it becomes ferromagnetic at a critical value of the applied field (*244*, *245*). The magnetic properties are attributed to the Eu^{2+} ions which form chains parallel to the *c* axis of the crystal. Along the chains, the Eu^{2+} ions are separated by 3.5 Å, and strong ferromagnetic coupling is assumed to occur within each chain. However, if weak antiferromagnetic coupling exists between neighboring chains that are separated by 5.6 Å, the total spin vectors for neighboring chains can be opposed, thus producing an antiferromagnetic ground state. The high field metamagnetic state is formed when the spin vectors for half the chains are reversed to bring all spins into alignment with the field. The relationship to the case of EuSe discussed on p. 31 is obvious.

The vaporization thermodynamics of Eu_3O_4 have been investigated in the temperature range 1600–2000 K (*230*); decomposition occurs by the reaction

$$3Eu_3O_4(s) = 4Eu_2O_3(s, \text{monoclinic}) + Eu(g)$$

for which $\Delta H^0_{298} = 93 \pm 3$ kcal mole^{-1}. This allows calculation of an approximate value of $\Delta H_f{}^0(Eu_3O_4, s)$.

The reflectance spectrum of Eu_3O_4 contains a single peak at about 20,000 cm^{-1} (*10*). As this has been assigned to a $4f^7 \rightarrow 4f^6 5d^1$ transition for the Eu^{2+} ion, there are no peaks attributable to intervalence absorptions. This contrasts with the case of Eu_3S_4, and the difference is apparent in the Mössbauer spectrum: whereas the Eu(II) and Eu(III) peaks are clearly resolved in the Mössbauer spectrum of Eu_3O_4 up to 600 K, in Eu_3S_4, they merge above 210 K (*63*, *575*). This merging is attributed to electron transfer between dipositive and tripositive europium in Eu_3S_4. Its absence in Eu_3O_4 has been attributed to the nonequivalence of the two types of europium site in that compound (*575*). In Eu_3S_4, which has the Th_3P_4 structure, all the metal atoms occupy similar, eight-coordinate positions (*183*).

It seems that the compounds Sm_3O_4 and Yb_3O_4 are unknown.

Many mixed oxide compounds of EuO and other oxides have been made by solid state reactions, in part because of interest in the modification produced in the magnetic properties of EuO by compound formation. These compounds include those formed with rare earth oxides, and with oxides of titanium, aluminum, silicon, molybdenum, zirconium, and tungsten. They have been reviewed by McCarthy and Greedan, who emphasize that whether europium(II) or whether europium(III) is present depends on the ease of reduction of the other metal oxide (*202*, *350*).

Mixed oxide compounds usually obtained from aqueous media are reviewed in Section III,C.

C. Aqueous Systems

The only dipositive lanthanide ions that have been adequately characterized in aqueous solution are those of samarium, europium, and ytterbium. However, we note here the claim (*16*) that γ-irradiation of Ho_2O_3 yields a product containing a small proportion of dipositive holmium, which when the oxide is dissolved in dilute acid, persists for surprisingly long times ($t_{1/2} \sim 1$ hr) under anaerobic conditions.

In this section we review the preparation and properties of Sm^{2+}(aq), Eu^{2+}(aq), and Yb^{2+}(aq), and also of certain di-*f* salts such as carbonates and sulfates that are usually made by precipitation or crystallization from aqueous solutions.

1. Preparation

All three ions, Sm^{2+}, Eu^{2+}, and Yb^{2+} can be made by reduction of solutions containing the tripositive ions, either electrolytically (*21*, *47*, *584a*) or with alkali metal amalgams (*242*, *374*, *375*). The greater stability of the Eu^{2+} ion with respect to oxidation is apparent from the fact that it is conveniently prepared by using amalgamated zinc (*122*, *358*). The dipositive ions have also been made by dissolving the dihalides in water (*117*, *274*, *278*, *281*, *324*) and small concentrations have been produced by pulse radiolysis (*172*) and by irradiation of aqueous solutions of the tripositive ions within their charge transfer bands (*232*). However, for some reason, the solutions obtained by pulse radiolysis decay more rapidly than those obtained by more common methods (*115*).

The aqueous Sm^{2+} ion is blood-red, and Yb^{2+}(aq) is green; most authorities state that aqueous solutions containing Eu^{2+}(aq) are pale greenish-yellow, but Asprey and Cunningham (*21*) state that the ion is colorless.

2. Reactions

All three ions are rapidly oxidized by atmospheric oxygen (*357*, *515*). Even in deoxygenated solutions, oxidation of Sm^{2+}, Eu^{2+}, and Yb^{2+} by water or hydrogen ions occurs in daylight (*98*, *115*, *147*, *148*, *515*) and is catalyzed by platinum (*388*), although in the dark, deaerated solutions of Eu^{2+} undergo little or no deterioration over long periods (*147*). The rates of oxidation under similar conditions are in the same sequence as the values (see below) of $-E^0[M^{3+}/M^{2+}]$, namely, Sm > Yb > Eu, a familiar correlation for the oxidation of monatomic aqueous ions (*340*).

In the case of $Eu^{2+}(aq)$, there is evidence (*407*) that oxidation by oxygen yields hydrogen peroxide as a product,

$$\tfrac{1}{2}O_2(g) + H^+(aq) + Eu^{2+}(aq) = Eu^{3+}(aq) + \tfrac{1}{2}H_2O_2(aq)$$

although this presumably occurs only in the presence of excess oxygen, because common oxidizing agents such as chlorine, bromine, nitrate, and bromate attack $Eu^{2+}(aq)$ (*357*).

Determinations of the standard electrode potential $E^0[Eu^{3+}/Eu^{2+}]$ have been reviewed by Morss and Haug (*407*), who also made a measurement of their own. They give $E^0[Eu^{3+}/Eu^{2+}] = -0.35 \pm 0.02$ V and this is close to a recent value of -0.379 ± 0.001 V for the formal potential in *M* $LiClO_4$ (*65*). Only polarographic determinations in chloride media have been made for samarium and ytterbium (*337*, *338*, *531*). If both reduction half-wave potentials are made more positive by 0.08 V, which is the difference between the half-wave potential for europium in a similar medium (*338*) and the E^0 value of 0.35 V, they imply that $E^0[Sm^{3+}/Sm^{2+}] = -1.48$ V and $E^0[Yb^{3+}/Yb^{2+}] = 1.09$ V. It is clear that all three values support the usual stability sequence for the di-*f* state. Other thermodynamic data allow calculation of the thermodynamic properties of the ion, $Eu^{2+}(aq)$. From the data of Morss and Haug (*407*), we take

$$\Delta H_f^0(Eu^{2+}, aq) = -126.1 \pm 2 \text{ kcal mole}^{-1}$$

$$\Delta G_f^0(Eu^{2+}, aq) = -129 \pm 3 \text{ kcal mole}^{-1}$$

$$S^0(Eu^{2+}, aq) = -2 \pm 10 \text{ cal K}^{-1} \text{ mole}^{-1}$$

From the solutions of the dipositive ions, precipitates are obtained by the addition of aqueous anions such as borate, carbonate, phosphate, chromate, hydroxide, sulfate, sulfite, phosphite, citrate, and pyrophosphate (*117*, *122*, *273*, *274*, *277*, *278*, *281*, *324*, *462*). These precipitates mostly have colors similar to those of the solutions of the

dipositive ions with the noticeable exception of that assumed to be a hydroxide of dipositive samarium which is green (*117*). Most of them, particularly the compounds of samarium and ytterbium, are rapidly oxidized in aerated or deaerated water in spite of their initial insolubility, and have been inadequately characterized.

Adequate characterization has, however, been carried out for the sulfates and carbonates that are isomorphous with the corresponding strontium and barium compounds. The carbonates have the orthorhombic aragonite structure and the sulfates, the orthorhombic barytes structure with the exception of greenish-white $YbSO_4$, which is hexagonal and isostructural with $CePO_4$. Cell parameters, colors, and references are given in Table XI. Magnetic studies of sulfates $EuSO_4$ and $YbSO_4$ have been reviewed (*21*, *488*); their behavior is that expected of compounds containing ions with configurations $[Xe]4f^7$ and $[Xe]4f^{14}$.

TABLE XI

DIVALENT SULFATES AND CARBONATES WITH BARYTES AND ARAGONITE STRUCTURES

Compound	Color	Cell parameters (Å)			Ref.
		a_0	b_0	c_0	
$SmSO_4$	Orange-yellow	8.45	5.38	6.91	(*22*)
$EuSO_4$	White	8.32	5.34	6.82	(*21*, *22*, *443*)
$SrSO_4$	White	8.359	5.352	6.866	(*582*)
$BaSO_4$	White	8.8701	5.4534	7.1507	(*582*)
$SmCO_3$	Orange-brown	8.58	5.97	5.09	(*22*)
$EuCO_3$	Yellow	8.45	6.05	5.10	(*22*)
$YbCO_3$	Pale green	8.13	5.87	4.98	(*22*)
$CaCO_3$	White	7.968	5.741	4.959	(*582*)
$SrCO_3$	White	8.414	6.029	5.107	(*582*)
$BaCO_3$	White	8.8345	6.5490	5.2556	(*582*)

The sulfates and carbonates are oxidized in moist air (*47*, *22*), but the deterioration of $EuCO_3$ and $EuSO_4$ is almost negligible in sealed bottles (*357*, *359*, *584a*).

Another europium(II) compound that is said to be air-stable and is, therefore, useful for synthetic purposes is the red-brown oxalate $EuC_2O_4 \cdot H_2O$. This can be made by reacting the sulfate with saturated ammonium oxalate solution (*457*), and it is isostructural with $SrC_2O_4 \cdot H_2O$. Moreover, it is insoluble in hot and cold water but is decomposed by acids.

Other well-characterized compounds of europium(II) include the yellow hydroxide, $Eu(OH)_2 \cdot H_2O$. It may be prepared by heating under vacuum at 100° the hydrated hydroxide obtained by adding NaOH

solution to a solution containing Eu^{2+}(aq) (*193*). The compound is also formed by the corrosion of europium in moist air (*506*), but it is best prepared by the action of 10 *M* NaOH on europium metal (*38*). It gradually deteriorates, even under an inert gas, to form $Eu(OH)_3$. It is orthorhombic, $a = 6.701$, $b = 6.197$, $c = 3.652$ Å and is isostructural with the corresponding strontium and barium compounds. Light green $Eu_3(PO_4)_2$ prepared by dry reproportionation methods is likewise isostructural with strontium phosphate (*386*).

Many studies have been made of the reaction kinetics of the electron-transfer reactions of Eu^{2+} (aq), and one or two papers on samarium(II) and ytterbium(II) solutions have recently been published. Some of the recent work has been reviewed in specialist publications (*91*, *92*). The europium(II)–europium(III) electron-exchange reaction is much faster in chloride than in perchlorate media (*388*), and in the presence of chloride follows the rate law,

$$\text{rate} = k[Eu^{2+}][Eu^{3+}][Cl^-]$$

with little or no hydrogen ion dependence. This suggests the mechanism:

$$Eu^{3+} + Cl^- \rightleftharpoons EuCl^{2+}$$

$$EuCl^{2+} + Eu^{2+} \longrightarrow EuCl^+ + Eu^{3+} \qquad \text{(rate-determining)}$$

$$EuCl^+ \longrightarrow Eu^{2+} + Cl^- \qquad \text{(fast)}$$

As $E^0[Eu^{3+}/Eu^{2+}]$ is very close to $E^0[Cr^{3+}/Cr^{2+}]$, one central concern of research into the reaction kinetics of Eu^{2+}(aq) has been the comparison with Cr^{2+}(aq). Another has been the attempt to establish whether the electron-transfer reactions of Eu^{2+}(aq) occur by inner- or outer-sphere mechanisms, a problem that can only be argued with indirect circumstantial evidence because both Eu^{2+}(aq) and Eu^{3+}(aq) are substitution-labile. The principles underlying such evidence have been critically reviewed by Sutin (*522*), and it seems impossible to come to any straightforward general conclusions.

Early kinetic work suggested that reductions by Cr^{2+}(aq) were faster; thus, the reactions of V^{3+} or $Co(NH_3)_5Cl^{2+}$ with Cr^{2+} are noticeably faster than with Eu^{2+} (*3*). At the same time, it was found that the rate of reaction of Eu^{2+} with $Co(NH_3)_5X^{2+}$ or $Cr(H_2O)_5X^{2+}$ (X = F, Cl, Br, I) was strongly dependent on the nature of X (*4*, *102*), and this was assumed to provide some support for an inner-sphere mechanism. An inner-sphere mechanism had also been suggested for the reaction between Eu^{2+} and iron(III). In perchlorate solution, the rate expression consists of two terms, one of which is strongly depen-

dent on the hydrogen ion concentration (*104*). This implies two parallel reaction paths, one involving participation of Fe^{3+} and the other of $FeOH^{2+}$. The predominant path is that via $FeOH^{2+}$ which reacts more rapidly than $Fe^{3+}(aq)$. In chloride solution the reaction

$$Fe^{3+} + Cl^- \longrightarrow FeCl^{2+}$$

is fairly slow compared with the redox reaction. Both the reactions,

$$Eu^{2+} + Fe^{3+} + Cl^- \longrightarrow Eu^{3+} + Fe^{2+} + Cl^-$$

and

$$Eu^{2+} + FeCl^{2+} \longrightarrow Eu^{3+} + Fe^{2+} + Cl^-$$

could be observed, the reaction of the chloride complex being faster than that of the aquo ion. This sensitivity to a change in the oxidant ligand corresponds fairly closely to that observed in reactions of chromium(II), which is believed to prefer mainly inner-sphere mechanisms, and is quite unlike that of vanadium(II), which is thought to undergo mainly outer-sphere oxidation. Similar anion catalysis by Cl^-, N_3^-, and SCN^- was also observed in the reaction between Eu^{2+} and VO^{2+} (*160*).

The implied preference for inner-sphere mechanisms has, however, been modified by recent work. First, europium(II) reductions of $Co(NH_3)_6^{3+}$ and $Co(en)_3^{3+}$, where the oxidant is substitution-inert and the reaction must be outer-sphere, were found to occur readily with parameters more akin to those for vanadium(II) than for chromium(II) reactions (*149*). This is also true of the reduction of $Co(NH_3)_5X^{3+}$, where X is pyridine or an alkylpyridine (*142*). In these last instances, the europium(II) reductions were found to be faster than the corresponding reactions of chromium(II), in contrast to the reactions mentioned earlier, and the ratios of the rate constants were remarkably constant.

However, if X is altered to an organic group, such as an extended conjugated system favorable to electron transfer by an inner-sphere mechanism, the europium rate constants are virtually unchanged, but those of chromium increase dramatically, and the chromium(II) reactions become faster than those of europium(II). This was taken to be an indication that these europium(II) reactions proceed mainly by outer-sphere mechanisms. Indeed, at present, it seems that where both types of mechanism are conceivable, dipositive lanthanide ions may undergo outer-sphere reactions with some oxidants, and inner-sphere reactions with others. Thus, the reactions of samarium(II), europium(II) and ytterbium(II) with $Co(NH_3)_5X^{2+}$ (X = F, Cl, Br, I, N_3,

SCN) are claimed to be mainly inner-sphere, whereas those with $Ru(NH_3)_5X^{2+}$ are chiefly outer-sphere (*170*). Here, the criteria used to characterize the inner-sphere mechanism were a relatively fast reaction for the case $X = N_3$ compared with the case X = SCN, a kinetic dependence on $[H^+]$, and the absence of chloride ion catalysis. Chloride ion catalysis and rates independent of $[H^+]$ are commonly accepted as indications of outer-sphere reductions for oxidants of this type (*593*). Similar criteria were used to establish that the reactions of ytterbium(II) with $Co(NH_3)_6^{3+}$, $Co(en)_3^{3+}$, and $Co(NH_3)_5H_2O^{3+}$ are outer-sphere, but those with $Cr(H_2O)_5X^{2+}$ are inner-sphere (*115*).

It is clear then that, even in the restricted type of reaction considered here, analogies in reactants and products do not necessarily imply analogies in mechanism, and we conclude this section with one more example: the reductions of uranium(VI) by europium(II) and chromium(II) proceed at similar rates, but a uranium(V)–M(III) complex plays a prominent part in the chromium reaction and not in the europium one (*158*).

3. *Properties*

Magnetic studies of the aqueous tripositive ions have been made only for the case of europium. The molar susceptibility of 26.25×10^3 cgs units at room temperature is very close to the theoretical value of 26.1×10^3 cgs units expected for the configuration $[Xe]4f^7$ (*147*).

The spectrum of the aqueous Sm^{2+} ion has been recorded by Butement (*98*). The main features are a series of five or six broad bands between 10,000 and 50,000 cm^{-1}. They tend to obscure the narrow bands that are usually associated with lanthanide spectra and assigned to transitions within the 4*f* shell. The broad bands are assigned to $4f \rightarrow 5d$ transitions. Similar spectra are obtained from solutions of Sm^{2+} in acetonitrile (*154*) and in alkali metal halide melts (*294*). Assignment of the bands is difficult because of a lack of information on coordination numbers in solution, but similar spectra are obtained from di-*f* dipositive samarium in alkali and alkaline earth metal halide crystals where the coordination number is fairly certain and more confident assignments can be made. Data on the spectra of dipositive rare earth ions in crystals can be found in Refs. *154*, *186*, *295*, *354*, and *562*.

Two sets of typical energies for the band peaks of Sm^{2+} in host lattices are shown in Table XII. In KCl, the coordination should be octahedral, and in CaF_2 eightfold cubic. One plausible assignment is essentially the same as that described earlier for the samarium chalcogenides. The $4f^5$ core of the $4f^55d^1$ configuration is (*LS*) coupled and

TABLE XII

ABSORPTION BANDS FOR Sm^{2+} IN HOST LATTICES

Host crystal	Energies of band peaks (kilokayser): 1	2	3	4	5
KCl	17.5	23.5	29.8	36.0	40.2
CaF_2	15.9	23.2	32.0	39.5	—

gives rise to ^6H and ^6F states; the $5d$ levels are split by the crystal field into T_{2g} and E_g sets. In an octahedral field, the T_{2g} level lies below E_g, but in the eightfold cubic field the reverse is true. A T_{2g} or E_g state for the $5d$ electron can then be coupled with either a ^6H or ^6F state of the core to give four excited states with the same spin multiplicity as the ground state; the octahedral field case is shown in Fig. 10.

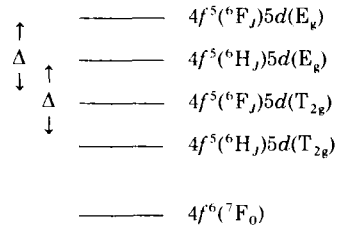

FIG. 10. Energy level scheme for Sm^{2+} in an octahedral field.

Transitions from the ^7F ground state to the four levels just discussed then give four spin-allowed transitions that account for four of the bands in the spectrum, and they are usually allocated to the four bands of lowest energy (*296*). It can be seen that for each spectrum the difference between bands 1 and 3 should be roughly equal to that between bands 2 and 4 because according to Fig. 10, both differences are equal to the crystal field splitting Δ. This is true of the figures in Table XII.

The spectra of Eu^{2+} and Yb^{2+} in aqueous solution (*98, 172, 192, 294*) show only two broad bands, and this can be explained by the assignment given above because in (*LS*) coupling, the $4f^6$ and $4f^{13}$ cores of the excited configurations $4f^65d^1$ and $4f^{13}5d^1$ give a single ^7F state for europium and a single ^2F state for ytterbium. This is coupled to either a $5d(T_{2g})$ or $5d(E_g)$ state of the $5d$ electron to give *two* excited states with the ground-state multiplicity. The two spin-allowed bands

occur at about 31 and 41 kK for Eu^{2+}(aq) and at about 28 and 39 kK for Yb^{2+}(aq). The references listed earlier for samarium show that similar spectra are obtained from the dipositive ions in host lattices.

D. Hydrides

Excellent recent reviews of the rare earth hydrides already exist (*342*, *343*, *560*).

All the lanthanide elements form dihydrides, MH_2, but only those of europium and ytterbium are di-*f*. At room temperature, the stable forms of EuH_2 and YbH_2 are isostructural with the alkaline earth metal hydrides (*331*), whereas the other dihydrides have the fluorite structure (*410*). With the exception of the europium and ytterbium compounds, the effective magnetic moments of the dihydrides are close to the theoretical values for the M^{3+} ions (*560*). Furthermore, they are good electrical conductors, in at least some cases better than the pure metals (*342*). These facts prompt the formulation $M^{3+}(e^-)(H^-)_2$ for the metallic dihydrides. This hydride formulation, which implies that hydrogenation removes electrons from the conduction band of the metal, is favored by recent investigation of Mössbauer spectra, X-ray emission spectra, magnetic susceptibilities, and specific heats at the expense of a protonic model in which the hydrogen electrons are donated to the metal conduction band (*75*, *342*, *343*, *509*, *560*).

Stoichiometric deviations can occur on either side of the ideal composition, $MH_{2.00}$, for a metallic dihydride. In particular, for the lighter lanthanides from lanthanum to neodymium inclusive, further hydrogenation can occur by incorporation of hydrogen into the octahedral holes of the fluorite structure up to a composition MH_3; for the remaining metallic dihydrides of the heavier lanthanides a structural change to a hexagonal phase occurs before the composition MH_3 is reached. The anionic formulation implies that the electrons in the conduction band in $M^{3+}(e^-)(H^-)_2$ are absorbed by the additional hydrogen atoms; in agreement with this, there is a sharp increase in resistivity and the hydrides become semiconductors even before the composition $MH_{3.00}$ is reached (*342*, *343*, *410*). The properties of the dihydrides thus fit into a familiar pattern: the two elements that form di-*f* dihydrides are those whose di-*f* dihalides, according to the sequence on p. 12, are the most stable with respect to oxidation. The other lanthanide metals form dihydrides best described as tri-*f* because their magnetic and electrical properties can be understood in terms of a formulation containing M^{3+} ions. The situation resembles the di-iodides, but the range of di-*f* compounds is much more restricted.

Preparation and Properties

Both europium and ytterbium combine with hydrogen at atmospheric pressure to form hydrides with compositions close to $MH_{2.0}$ (*331*). A reaction temperature of 350°C is convenient (*222*). The stable forms of the two dihydrides at normal temperatures are orthorhombic and isostructural with the alkaline earth metal hydrides that have a distorted form of the nine-coordinate $PbCl_2$ structure (*62*). Cell parameters have been reported for both dihydrides and dideuterides (Table XIII).

TABLE XIII

CELL PARAMETERS FOR THE ORTHORHOMBIC STRUCTURES OF EUROPIUM AND YTTERBIUM DIHYDRIDES AND DIDEUTERIDES

Compound	*a* (Å)	*b* (Å)	*c* (Å)	Ref.
EuD_2	6.21	3.77	7.16	(*331*)
EuH_2	6.26	3.80	7.21	(*393*)
YbD_2	5.861	3.554	6.758	(*331*, *564*)
YbH_2	5.904	3.57	6.792	(*331*, *332*)

The maximum hydrogen content for these phases appears to be about $MH_{1.95}$ (*222*, *331*, *564*), although some workers state that it is somewhat lower (*589*). Both hydrides are black; YbH_2 is attacked fairly slowly by air and water, but EuH_2 reacts much more quickly. They react rapidly with acids, but unlike the metals are insoluble in liquid ammonia (*332*).

Magnetic measurements have been made on a europium hydride sample of composition $EuH_{1.86}$ (*589*). The substance becomes ferromagnetic at low temperatures with a Curie temperature of 24 K. Above 30 K, the Curie–Weiss law is obeyed, and the variation of susceptibility with temperature suggests an effective magnetic moment of 7.0 μ_B. This is fairly close to the theoretical value of 7.94 μ_B for the Eu^{2+} ion. A somewhat lower value of T_c (16.2 K) is suggested by Mössbauer studies that confirm the di-*f* quality of the compound (*412*). The problem of explaining the ferromagnetic ordering is similar to the case of EuO. Samples of ytterbium dihydride close to the composition YbH_2 are almost diamagnetic as expected for a compound containing Yb^{2+} ions with the configuration $[Xe]4f^{14}$; the weak paramagnetism may be due to contamination by ytterbium(III) (*561*, *564*). The electronic properties of a sample with composition $YbH_{1.90}$ were those of a high-resistivity semiconductor (*236*), although the rapid wetting and dispersion of the substance by mercury (*567*) suggests that it may well be only just stable with respect to the metallic state.

At temperatures above about 800°C, YbH_2 and EuH_2 decompose to give hydrogen and the metal vapor. Studies of the equilibrium involving gaseous ytterbium have been made in the temperature range 720–930 K (*226*), and results are also available for the high-temperature equilibrium involving solid ytterbium (*390*). Haschke and Clark (*226*) used estimated heat capacities for the dihydride to obtain both second- and third-law values of $\Delta H_f^0(YbH_2, s)$ at 298.15 K and give -42 ± 1 kcal mole^{-1}. This figure agrees closely with the second-law value of Messer *et al.* (*390*).

If EuH_2 is heated under pressures of hydrogen up to 60 atm, no further uptake of hydrogen is observed. Under the same conditions, YbH_2 absorbs hydrogen to give a new phase with a maximum observed H/Yb ratio of 2.55 (*565*). The new phase is black, air-stable, and has a wide composition range. It has a face-centered cubic unit cell, and the phase of composition $YbH_{2.55}$ has a cell constant of 5.19 Å which is close to the value that would be expected for a hydrogen-deficient YbH_3 phase with the face-centered cubic structure of the heavier lanthanide trihydrides. The molar susceptibility of $YbH_{2.55}$ is 4140×10^{-6} cgs units, a value intermediate between those expected for Yb(II) and Yb(III) compounds (*564*). It, therefore, seems reasonable to describe the compound as an assembly of Yb^{2+} and Yb^{3+} ions arranged in a face-centered cubic lattice with hydride ions in nearly all the tetrahedral holes and in about 55% of the octahedral holes. The equivalence of the two types of cation is accounted for by electron exchange. If $YbH_{2.55}$ is heated to 350°–400°C and then quenched, a very weakly paramagnetic fluorite phase of cell constant $a_0 = 5.253$ Å and composition $YbH_{2.04}$ is obtained. This reverts slowly to the orthorhombic form of the dihydride on standing at room temperature. Reversion is rapid if the compound is annealed from a temperature of 400°C (*392*, *564*).

Considerable interest has been shown in compound $LiEuH_3$, which can be made either by hydrogenation of a mixture of lithium and europium metals at 550°–750°C (*393*) or by crystallization from a molten mixture of EuH_2 and excess LiH (*200*). Ytterbium or ytterbium hydride does not yield such a compound under similar preparative conditions (*393*), and in this respect, europium behaves like strontium and barium, which form $LiSrH_3$ and $LiBaH_3$, whereas ytterbium behaves like calcium and yields only the hydride MH_2 (*391*). However, the LiH—EuH_2 and LiH—YbH_2 phase diagrams are similar at the lithium hydride-rich end; the melting point of lithium hydride, 691°C, is depressed to a eutectic of 664°C by 6.8 mole % EuH_2, and of 669°C by 6.8 mole % YbH_2 (*394*).

Compound $LiEuH_3$ is reddish-orange and melts incongruently at about 780°C (*200*). It has a cubic perovskite structure for which $a_0 = 3.796$ Å and, in the absence of neutron diffraction data, is assumed to be of the inverse type (*393*). In such a structure, the lithium ions would be octahedrally coordinated, whereas the Eu^{2+} ions would be twelve-coordinate. This high coordination number supplies a possible reason for the failure to observe such phases incorporating the smaller Ca^{2+} and Yb^{2+} ions. The $LiEuH_3$ is a ferromagnetic semiconductor like EuO with a Curie temperature of about 38 K (*201*). The nearest-neighbor exchange constant, J_1, has been estimated to be over 10 times the second-nearest-neighbor constant, J_2, suggesting that the compound is a nearly ideal ferromagnet (*114*).

E. Liquid Ammonia Systems

Europium and ytterbium metals dissolve in liquid ammonia to give blue solutions containing the ammoniated electron (*566*). So far as is known, they are the only lanthanide metals to do so; samarium and gadolinium, for example, do not undergo this reaction (*498, 566*). Some writers imply that the divalency of metallic europium and ytterbium is responsible for the liquid ammonia reaction, but as the unknown trivalent forms of the two metals are unstable with respect to the divalent allotropes (see p. 92), it is clear that the trivalent forms of europium and ytterbium would be even less stable with respect to the reaction,

$$M(s) = M^{2+}(amm) + 2e^{-}(amm)$$

The ESR spectrum of the Eu^{2+} ion in liquid ammonia, which can be obtained from an ammoniacal solution of EuI_2, is visible in the spectrum of the solution of the metal and indicates that in dilute solution the metal ions and solvated electrons are well separated (*108, 526*). The electronic absorption spectra of the europium and ytterbium solutions each contain two bands with positions similar to those in the spectrum of aqueous Eu^{2+} and Yb^{2+} ions (*108, 527*). They invite an assignment similar to that on p. 49.

In their reduction of organic compounds, the solutions behave like those of the alkaline earth metals (*498*). Various organic acids precipitate yellow or white salts, but the dialaninate is said to be soluble and may prove to have synthetic possibilities (*504*). Phosphine precipitates ammoniated hydrogen phosphides of approximate composition $M(PH_2)_2 \cdot 7NH_3$. These substances decompose when removed from an ammonia atmosphere. If heated, the final products are the tri-*f*

phosphides, and the ytterbium compound decomposes more easily than the europium one (*256*). The use of the ammoniacal solutions of the metals to prepare dihalides was mentioned on p. 9.

The possibility of attaining a higher oxidation state leads to some interesting differences from the alkaline earth metal system. In water, higher oxidation states are often stabilized in alkaline media, in many cases because of the lower solubilities of higher oxides or hydroxides. In neutral ammonia, Yb^{2+}(amm) does *not* dissociate thus:

$$M^{2+}(amm) = M^{3+}(amm) + e^{-}(amm)$$

but the addition of potassium amide solution to a solution of the diiodide, YbI_2, in liquid ammonia causes the appearance of the ammoniated electron and precipitation of the insoluble M(III) amide:

$$Yb^{2+}(amm) + 3NH_2^{-}(amm) = Yb(NH_2)_3(s) + e^{-}(amm)$$

Europium is said to behave similarly (*481*).

The solutions of europium and ytterbium metals in liquid ammonia decompose on standing with the formation of precipitates (*108*, *566*). The europium precipitate is orange and consists of the amide, $Eu(NH_2)_2$ (*258*). It can be made by carrying out the reaction between europium and liquid ammonia at 20°–50°C in a sealed bomb. The compound crystallizes with the tetragonal anastase structure and is isostructural with the calcium and strontium amides (*218*, *302*). It hydrolyzes very rapidly to the yellow hydroxide, $Eu(OH)_2 \cdot H_2O$, which reverts slowly to $Eu(OH)_3$. Some workers state that thermal decomposition of the amide yields the tripositive compound EuN (*218*), but others report EuNH (*258*); it is probable that the imide of the +2 state is an intermediate in tripositive nitride formation. The molar susceptibility of $Eu(NH_2)_2$ in the range 90–270 K followed the Curie–Weiss law in the form $C/T - \theta$, with $\theta = 12$ K, and gave an effective moment of 7.80 μ_B, close to the theoretical value of 7.94 μ_B for the Eu^{2+} ion (*218*). Like the value of θ, the line width of the ESR signal indicates some ferromagnetic interaction (*327*), and the Curie temperature is, in fact, 5.4 K (*264*).

The synthetic methods described for $Eu(NH_2)_2$ failed to produce a pure specimen of $Yb(NH_2)_2$ free of $Yb(NH_2)_3$. The best sample contained only about 75% $Yb(NH_2)_2$ (*218*, *219*), but the diamide was clearly isostructural with the corresponding europium, clacium, and strontium compounds.

Synthetic methods that avoid the liquid phase altogether are said to yield good samples of $Yb(NH_2)_2$. The reaction of the metal with dry

ammonia at 4 atm pressure is recommended, and the product is a rust-brown pyrophoric solid (*563*). However, magnetic measurements show that some Yb(III) is still present. As expected from the reaction of Yb^{2+}(amm) and NH_2^-(amm), compound $Yb(NH_2)_2$ reacts with potassium amide solution to give the ammoniated electron and a precipitate of $Yb(NH_2)_3$:

$$Yb(NH_2)_2 + NH_2^-(amm) = Yb(NH_2)_3(s) + e^-(amm)$$

The equilibrium constant for this reaction appears to be about 200. If it is that small, data on the corresponding europium reaction would be interesting.

By evaporation of the solvent from the solutions of europium and ytterbium in liquid ammonia, bronze-colored solids of a metallic appearance with compositions close to $Eu(NH_3)_6$ and $Yb(NH_3)_6$ are obtained (*528*, *566*). Both compounds are isostructural with the calcium, strontium, and barium hexammines, and they have body-centered cubic structures in which the metals are octahedrally coordinated by 6 ammonia molecules (*428*). The ytterbium compound is slightly less stable with respect to the metal and ammonia than is the europium compound. The variation of the ammonia pressure in the temperature range 230–265 K has been used to obtain thermodynamic data for the reaction

$$M(NH_3)_6(s) = M(s) + 6NH_3(g) \qquad (7)$$

at 0°C (*191*). This is shown in Table XIV. When the data for the alkaline earth metal hexammines are included, it is found that the five values of ΔH^0 or of ΔG^0 differ by only 1 kcal $mole^{-1}$.

The bonding in the europium and ytterbium hexammines is of interest. One solution (*428*) is to promote the two 6*s* electrons in the metal atoms to higher levels such as 7*s* and 7*p*; the vacant 6*s*, 6*p*, and 5*d* metal orbitals can then be used to form d^2sp^3 hybrids that accommodate the

TABLE XIV

THERMODYNAMIC DATA FOR REACTION (7) AT TEMPERATURES OF ABOUT 273.15 K

Compound	ΔH^0 (kcal $mole^{-1}$)	ΔG^0 (kcal $mole^{-1}$)	S^0 (cal K^{-1} $mole^{-1}$)
$Eu(NH_3)_6$	9.5	1.1	30.6
$Yb(NH_3)_6$	8.9	0.6	30.4

12 electrons from the 6 surrounding ammonia molecules. The metallic properties can then be explained by the formation of a conduction band by 7*s* and 7*p* orbitals. There are also vacant 5*d* orbitals that could serve this purpose.

Magnetic susceptibility studies are consistent with such formulations in the temperature range 50–200 K, indicating diamagnetism for the ytterbium compound and a Curie–Weiss law dependence with an effective moment close to the theoretical value for the europium compounds (*428*). However, the same workers report marked increases in magnetic moment below 31 K for $Yb(NH_3)_6$ and below 47 K for $Eu(NH_3)_6$; at the same time they found $Eu(NH_3)_6$ to be ferromagnetic with a Curie temperature of 5.5 K. These claims are contradicted by measurements of the Mössbauer effect in $Eu(NH_3)_6$ that reveal a nearly constant ^{151}Eu isomer shift in the temperature range 2–80 K (*87*, *439*, *441*), suggest that there is no magnetic ordering above 1.2 K, and lead to attribution of contradictory reports to impurities (*439*, *441*). The constancy of the isomer shift implies that no important electronic transition occurs at 47 K, and its value of -12.5 mm sec^{-1} with respect to Eu_2O_3 is very similar to that for EuO and EuS. Formulation as a compound of di-*f* europium with 2 electrons in a conduction band thus seems justified. The only phase transition detected by Mössbauer measurements occurs at 69.5 K and was attributed to the quenching of the ammonia rotation (*440*).

Solutions of europium and ytterbium in liquid ammonia have been used to synthesize organometallic compounds, which are reviewed in Section III,F,3. We mention in this context only compound $Yb(o\text{-phen})_4$, $Yb(bipy)_4$, and $Eu(bipy)_4$ that are made by adding the appropriate ligand to the ammonia solutions (*172a*). The magnetic moments of the ytterbium compounds are very similar to that of $Ba(bipy)_4$ and are close to those that would be obtained from a compound in which there were diamagnetic Yb^{2+} ions and 2 free unpaired electrons per formula unit delocalized on the adjacent ligands. However, the room temperature magnetic moment of $Eu(bipy)_4$ is about 5.7 μ_B, considerably less than that expected from the $4f^7$ core of the Eu^{2+} ion plus the ligand electrons. To account for this, and to maintain the analogy with the bivalent ytterbium and barium compounds, antiferromagnetic coupling has been postulated between the two ligand electrons of the $bipy_4^{2-}$ system ($J = 1$) and the Eu^{2+} ion ($J = 7/2$). This gives a ground level with $J = 5/2$ and a moment of $g[J(J+1)]^{1/2} = 5.92\ \mu_B$ which is close to the observed value. Such behavior becomes particularly interesting if the electrons on the ligands are regarded as partly localized conduction electrons. The need to take account of magnetic interaction

between genuine conduction electrons and the localized moments of rare earth ions is noted elsewhere in connection with SmS (p. 38) and SmB_6 (p. 59).

F. Miscellaneous Dipositive Lanthanide Compounds

In this section, references are given to dipositive compounds other than those considered in Sections III,A–E. The list is not intended to be complete, and the chief purpose of the section is to emphasize further that di-*f* properties are largely confined to samarium, europium, and ytterbium, and that where this is the case, the chemical behavior of compounds suggests that stability with respect to the tri-*f* state follows the sequence Sm < Yb < Eu.

1. Borides

The rare earth elements form a series of hexaborides, MB_6 (*9*, *15*), which are usually made by direct combination of the elements or by strongly heating the metals with B_2O_3 and removing lower oxides of boron *in vacuo*. These compounds have been reviewed by Post (*463*). They are all isostructural and have the cubic CaB_6 structure described by Stackelberg and Neumann (*555*) in which the metal cation lies at the center of a cube, and octahedra of boron atoms bound by boron–boron bonds lie at the eight corners. The lattice parameters (*69*, *157*, *405*, *463*) are plotted in Fig. 11; with the exception of samarium, europium,

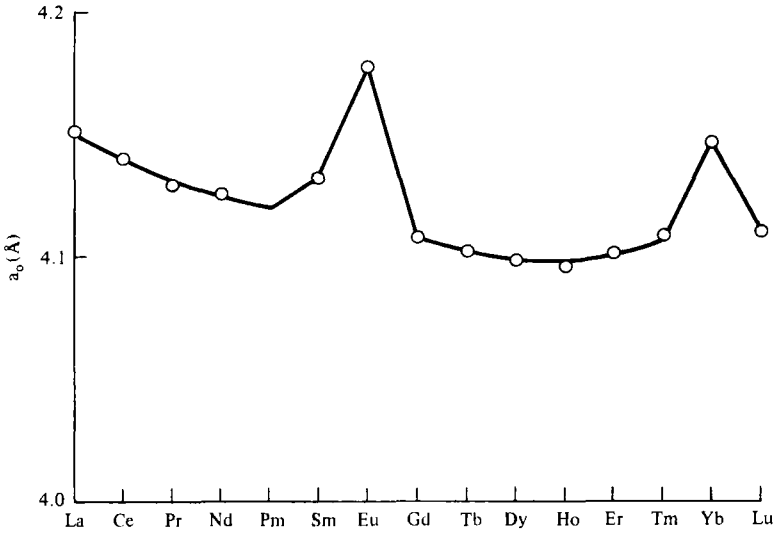

Fig. 11. Cell parameters of cubic hexaborides.

ytterbium and, possibly, thulium, the values vary almost smoothly with atomic number. The lattice parameters of the exceptions are anomalously large, but the displacement from the curve for SmB_6 is much less than that for EuB_6 and YbB_6.

Measurements that are especially sensitive to the stoichiometry of the compounds are hampered by considerable composition ranges for the boride phases, but investigations of the electrical properties (*432*, *482*) suggest that except for SmB_6, EuB_6, and YbB_6 the hexaborides have low electrical resistances in the 15–45 $\mu\Omega$ cm range and small negative Hall coefficients, indicating high concentrations of conduction electrons. Hexaborides EuB_6 and YbB_6 have appreciably higher resistivities and much more negative Hall coefficients indicating very low numbers of conduction electrons; in this they resemble the alkaline earth metal hexaborides.

Longuet-Higgins and Roberts (*349*) have pointed out that the bonding molecular orbitals in the B_6 octahedron can be filled if 2 electrons are acquired from a metal atom. Coupled with the experimental details quoted above, this prompts the formulation $M^{3+}(e^-)B_6{}^{2-}$ for most of the rare earth hexaborides, but reserves $M^{2+}(B_6)^{2-}$ for the europium, ytterbium, and alkaline earth metal compounds, which therefore should be semiconductors when pure. The magnetic properties in the temperature range 80–300 K (*217*, *431*) and ESR spectra (*482*) support these formulations, indicating di-*f* formulations for EuB_6 and YbB_6 and tri-*f* formulations for other hexaborides apart from SmB_6. Various investigations have shown that EuB_6 is a ferromagnetic semiconductor with a Curie temperature of about 8.8 K, although there is some small disagreement on the nature of the $1/\chi_m$ vs T variation at very low temperatures (*33a*, *195*, *217*, *492*). This contrasts with the behavior of the metallic tri-*f* hexaborides that order antiferromagnetically at low temperatures (*385*). As in the case of the europium chalcogenides, controversy over the mechanism of ferromagnetic interaction has flourished (*181*, *383*, *492*, *580*).

Compound YbB_6 shows only a weak temperature-dependent paramagnetism, which is probably due to impurities, and it resembles CaB_6 and SrB_6 rather than LaB_6 or ThB_6 in that its specific heat at low temperatures displays no electronic contribution and is characteristic of a semiconductor (*161*).

The most interesting hexaboride is SmB_6. This has a temperature-dependent magnetic moment that falls between the theoretical values for the Sm^{2+} and Sm^{3+} ions (*431*). The X-ray *L*-absorbtion spectra of EuB_6 and YbB_6 are shifted to lower energies by about 8 eV as compared with Eu_2O_3 and Yb_2O_3, respectively, but in the SmB_6 spectrum, this

absorption appears as a shoulder on a peak whose energy is close to the peak energy in the oxide spectrum (*538*). Other studies by X-ray photoelectron spectroscopy reveal splitting of the spectra of several core levels (*15a*). These observations were interpreted as a sign that in SmB_6, at room temperature, di-*f* and tri-*f* samarium in the ratio 2:3 are statistically distributed in equivalent positions through the lattice. The implications that such an idea carries for the variation of the properties of the compound with temperature has aroused considerable debate.

At room temperature, SmB_6 is a metal, although it is a poorer conductor than the other metallic hexaborides. It changes from a metal to a semiconductor with decreasing temperature, and shows no sign of magnetic ordering at temperatures as low as 0.35 K (*389*). The $4f^6$ configuration of the Sm^{2+} ion is nonmagnetic at low temperatures, but the strong magnetism of the $4f^5$ configuration of Sm^{3+} should generate magnetic ordering on cooling. These results were, therefore, interpreted as a sign that SmB_6 contained only Sm^{2+} at low temperatures and that the Sm^{3+} ions present at room temperature took up the conduction electrons as the temperature was lowered. This interpretation proved inconsistent with the Mössbaeur spectrum (*120*). At room temperature, the difference in isomer shift for the two valencies was too small to resolve two resonances, but the single-resonance line lay between the values expected for di-*f* and tri-*f* samarium and was consistent with the existence of 40% samarium(II) and 60% samarium(III). However, the isomer shift did not change with temperature, thus giving no support to the belief that there is a change in the proportion of the two configurations on cooling. Furthermore, the variation in molar susceptibility with temperature can be closely reproduced with a model assuming that the susceptibility is due solely to the 40% samarium present as $Sm^{2+}(4f^6)$, there being no magnetic contribution from the remaining samarium sites (*119*).

One solution to this problem (*373*) assumes the possibility of interconfigurational fluctuations of the type discussed for SmS on p. 38. The absence of any increase in the susceptibility of the $4f^5$ cores at low temperature, and their failure to order magnetically, are attributed to the speed of fluctuation at any samarium site.

An even more radical proposal (*419*) is that between the completely delocalized and decoupled $M^{3+}(e^-)B_6$ situation in, say, LaB_6 and the completely localized and coupled situation in, say, EuB_6, there can be an intermediately localized and coupled form. For example, if one assumes that the conduction electrons occupy a band composed of 6*s* orbitals and describes the system as $4f^5 6s^1$, then if the ground state has

all spins parallel, its quantum numbers are $S = 3$, $L = 5$, and $J = L - S = 2$. With the Landé formula, this gives $g = 0$, and the magnetic moment of these samarium sites vanishes.

It is clear that in both these proposals, there is an implication that SmB_6 lies in some sense between the purely di-*f* phase, $Sm^{2+}(4f^6)B_6^{2-}$, and the purely tri-*f* phase, $Sm^{3+}(4f^5)(e^-)B_6^-$. On this basis, it is possible to construct band models that can account for the electrical properties (*419*). The intermediate characteristics of SmB_6, taken in conjunction with the di-*f* qualities of EuB_6 and YbB_6, are consistent with the familiar sequence Sm < Yb < Eu for the stability of the di-*f* with respect to the tri-*f* state.

It is worth noting that in spite of its curious properties, the composition range of the SmB_6 phase extends on the boron-rich side in a way similar to that of the tri-*f* metallic borides. It covers a range from $Sm_{0.68}B_6$ to SmB_6 and is caused by samarium deficiencies (*420*). The charge balance is maintained as samarium is removed by the elimination of conduction electrons that accompany tri-*f* samarium already present or by conversion of Sm^{2+} to Sm^{3+}, so the theoretical boron-rich phase limit is that corresponding to 100% Sm^{3+} and no conduction electrons. This limit is $Sm_{0.67}B_6$ and is close to the observed value. As expected, the conductivity falls as the samarium content drops (*420*).

2. *Carbides*

The lanthanide elements form a series of carbides, MC_2, with many resemblances to the borides. They can be made by direct combination of the elements in the correct stoichiometric proportions (*507*), although the preparation of EuC_2 by this method has only been achieved relatively recently (*196*). The compounds are all isostructural and have the tetragonal CaC_2 structure. This can be indexed on the basis of either a body-centered or face-centered unit cell (*549*). In the latter instance, Wells (*571*) has pointed out that the structure may be regarded as a rock salt structure in which a tetragonal distortion has been introduced by the replacement of chloride by C_2^{2-}. The lattice parameters (*196*, *507*, *554*) show the familiar decrease across the series except for YbC_2 and EuC_2 which have somewhat larger values. The displacement of the YbC_2 point from the curve is small, however, being only 10–20% of that of the EuC_2 point.

Compound CaC_2 is an insulator, and the C—C distance in the carbide grouping is 1.191 Å, close to the value in acetylene, whereas LaC_2 has a conductivity close to that of lanthanum metal and a C—C distance of 1.303 Å (*27*, *31*). The formulation $M^{3+}(e^-)(C_2^{2-})$ for the tri-*f* carbides is consistent with the implication that the conduction electrons occupy

a band to which the π^* antibonding orbitals of the C_2^{2-} ion contribute. In agreement with this idea, the C—C distance in metallic tetravalent carbides, such as UC_2, is even longer than in LaC_2 (*32*). Participation of π^* C_2^{2-} orbitals in the conduction band requires definite participation of 5*d*, as opposed to 6*s*, orbitals as well.

It appears that of the lanthanide dicarbides, only EuC_2 can definitely be regarded as di-*f*. The abnormal cell parameter was mentioned above, and the isomer shift in the EuC_2 Mössbauer spectrum lies in the region expected for a compound containing Eu^{2+} ions (*121*). Like many other di-*f* europium compounds, it is ferromagnetic at low temperatures; the Curie temperature is 40 K (*246*). The C—C distances in the trivalent carbides lie in the range 1.276–1.303 Å (*27–30*), the value for YbC_2 at 1.291 Å giving no sign of the undue shortening that would be expected in an alkaline earth metal-type carbide (*30*). The variation in the molar susceptibility of YbC_2 with temperature gave an effective magnetic moment of 4.14 μ_B (*476*), not too distant from the theoretical value of 4.6 μ_B for Yb^{3+}, and was attributed to the presence of about 80% Yb^{3+} and 20% Yb^{2+} (*27*). It should be mentioned that this magnetic study of YbC_2 challenged earlier work that also claimed to have detected some di-*f* samarium in SmC_2 (*550, 551*). If this claim were correct, however, the position of the SmC_2 value on the smooth curve through the cell parameters of the tri-*f* dicarbides would seem unexpected, as would the fact (*287*) that the conductivity of SmC_2 is close to that of samarium metal.

Dicarbide EuC_2 is black (*196*), and YbC_2 golden (*227*). Both are hydrolyzed in moist air, and acetylene forms the bulk of the gaseous products (*13, 196*). Above about 1000 K, the compounds begin to decompose into graphite and metal vapor. Studies of the variation in the vapor pressure of the metal with temperature have been used (*166, 197, 229*) to obtain values for the enthalpy change of the reaction.

$$MC_2(s) = M(g) + 2C(s)$$

and, thus, for $\Delta H_f^0(MC_2, s)$ at 298.15 K. The values quoted by Eick and his co-workers are -9 ± 2 kcal mole^{-1} for EuC_2 and -18 ± 1 kcal mole^{-1} for YbC_2, although the figure for EuC_2 differs considerably from that quoted by Faircloth *et al.* (*166*). The thermochemistry of some tri-*f* rare earth carbides has recently been reviewed (*12*).

3. *Organometallic Compounds*

Some organometallic compounds of di-*f* europium and ytterbium have been prepared, the solutions of the metals in liquid ammonia

having proved a particularly useful starting material. Treatment of these solutions with cyclopentadiene gave residues that, when heated under vacuum at 200°C, were claimed to yield yellow $Eu(C_5H_5)_2$ and red $Yb(C_5H_5)_2$ (*179*, *180*). The europium compound is strongly paramagnetic with an effective magnetic moment of 7.6 μ_B, and its ^{151}Eu Mössbauer spectrum (*261*) shows an isomer shift close to that of $EuCl_2$ and strongly negative with respect to Eu_2O_3 and EuF_3; the ytterbium compound is diamagnetic. Both substances were rapidly oxidized in air and hydrolyzed by traces of moisture; they sublimed at about 400°C and appeared to have ferrocene-like structures. Surprisingly, in view of the diamagnetism of the compound, it has been subsequently claimed (*99*) that the red ytterbium compound contained tri-*f* ytterbium and that it may be $Yb(C_5H_5)_2H$. The same workers state that $Yb(C_5H_5)_2$ is the emerald green diamagnetic product obtained by reduction of tri-*f* ytterbium cyclopentadiene compounds with sodium or ytterbium metals in THF. Reduction in THF also gives the purple pyrophoric di-*f* samarium compound, $Sm(C_5H_5)_2 \cdot THF$ (*569*). The molar susceptibility is about that expected for a di-*f* samarium compound, being drastically reduced on exposure to air when the color changes to yellow-gray. Unfortunately, attempts to desolvate the compound caused decomposition.

Addition of cycloctatetrene to the metal–ammonia solutions followed by desolvation at 200°C gives orange Eu(COT), whose EPS spectrum supports the presence of di-*f* europium, and pink diamagnetic Yb(COT) (*235*). Propyne reacts with europium in liquid ammonia to give the brown propynide, $Eu(CH_3C{\equiv}C)_2$, which is hydrolyzed by water to $Eu(OH)_2$ and propyne (*411*). The same reaction with ytterbium gives a product heavily contaminated with amides. Acetylene forms $Eu(HC{\equiv}C)_2$. This is said to yield the dicarbide when heated at 90°C under vacuum and could form the basis of a useful preparative route to EuC_2.

Finally, europium and ytterbium react readily with alkyl or aryl iodides in THF at 230–300 K to give brown solutions containing compounds analogous to the Grignard reagents (*162*). The effective magnetic moment of the europium solutions is 7.5 μ_B, suggesting the presence of nearly 99% europium(II); in the ytterbium case, the proportion of the di-*f* state was about 90%. With samarium, the reaction was much slower, the solutions were an intense blue-green and only about 50% of the metal was present as samarium(II). These observations suggest that the stability of the di-*f* state varies in the usual sequence, Sm < Yb < Eu, although in the absence of thermodynamic data it is difficult to separate kinetic and thermodynamic standpoints.

IV. Tetrapositive Oxidation States

Tetrapositive lanthanide compounds have been clearly established only for the elements cerium, praseodymium, neodymium, terbium and dysprosium. The chemistry of cerium(IV) is very extensive, and is not reviewed here in detail, but some cerium(IV) compounds and their properties are discussed so that comparisons can be made with analogous tetrapositive compounds of other lanthanide elements.

The widest range of tetrapositive states is found in fluorine compounds; tetra-*f* oxides and oxyanion salts are at present known only for cerium, praseodymium and terbium. If cerium is ignored, this almost completes the survey of tetrapositive species, but there exist claims that solutions of praseodymium(IV) and, to a lesser extent, terbium(IV) can be prepared in strongly acidified aqueous media, and used to prepare certain compounds. This work is reviewed in Section IV,C.

A. Fluorine Compounds

Tetrafluorides of cerium, praseodymium, and terbium have been prepared. Cerium tetrafluoride was first made by fluorination of $CeCl_3$ (*332*), but subsequent methods have included the action of fluorine on CeO_2 at 350°–500°C, on anhydrous CeF_3 at 300–350°C, or on the hydrated trifluoride, $CeF_3 \cdot \frac{1}{2}H_2O$ at 350°C (*18, 556*). Attempts to dehydrate the compound $CeF_4 \cdot H_2O$, made by precipitation of cerium(IV) solutions with HF, yield mainly CeF_3 (*18*). Fluorination of the trifluoride at 320°C was the route used for the first preparation of TbF_4 (*131*). In these preparations, fluorine can be replaced by fluorinating agents such as ClF_3 and XeF_2. The XeF_2 oxidizes TbF_3 to TbF_4 at 300°–350°C (*508*), and ClF_3 at 300°–450°C converts the trifluorides of cerium and terbium to the tetrafluorides (*52*).

Attempts to make tetrafluorides of praseodymium, neodymium, samarium, and dysprosium by fluorination of the trifluorides or trichlorides have been unsuccessful (*131, 322, 448, 461*) even at fluorine pressures of over 300 atm (*304*). The failure to prepare PrF_4 in this way attracted particular attention, in that higher *oxides* of praseodymium have been known for very many years. Attempts to assess the stability of PrF_4 (*447*) led to the conclusion that the compound should be extremely stable with respect to the reaction

$$PrF_4(s) = PrF_3(s) + \tfrac{1}{2}F_2(g)$$

but these attempts were based on dubious analogies with uranium

compounds, and subsequent research suggests that the conclusion is highly optimistic. Impure PrF_4 was first made (*502*) by leeching out NaF from the compound Na_2PrF_6 with liquid hydrogen fluoride:

$$Na_2PrF_6(s) + 2HF(l) = 2NaHF_2(solv) + PrF_4(s)$$

The product was only 40% pure. Other workers (*20*) improved the method by carrying out the leeching process in a fluorine atmosphere. They obtained a much purer sample, showing that PrF_4 was isostructural with CeF_4 and TbF_4, and identifying the $^2F_{5/2} \rightarrow {}^2F_{7/2}$ transition within the ground state multiplet of the $[Xe]4f^1$ configuration of Pr^{4+}. Other reports of the preparative method exist (*52*).

All three lanthanide tetrafluorides are white and have the monoclinic UF_4 structure in which the metal atoms are coordinated by 8 fluorines arranged at the corners of a slightly distorted square antiprism (*587*). References and lattice parameters are given in Table XV.

TABLE XV

CELL PARAMETERS OF SOME TETRAFLUORIDES

Compound	a_0 (Å)	b_0 (Å)	c_0 (Å)	β (°)	Ref.
CeF_4[a]	12.58	10.58	8.28	126	(*587*)
PrF_4	12.47	10.54	8.18	126.4	(*20*)
TbF_4	12.10	10.30	7.90	126	(*131*)
HfF_4[a]	11.66	9.82	7.60	126.1	(*587*)

[a] Cell sides calculated from the data in Zachariasen (*587*) by using the conversion factor 1 kX = 1.00206 Å.

Neither CeF_4 or TbF_4 seems affected by 10-min exposure to hot or cold water, but both dissolve slowly in dilute nitric acid, dissolution being accelerated by the addition of aluminum nitrate. The resulting solutions probably contain tripositive cerium and terbium, because a gaseous product, presumed to be oxygen, is evolved (*131*).

Information on other properties is largely confined to CeF_4. Klemm and Henkel (*322*) noted the virtual diamagnetism of CeF_4, a property expected of compounds containing the ion Ce^{4+}. The compound is reduced to the trifluoride by heating with hydrogen, ammonia, or water vapor at 350°C. At higher temperatures, water vapor gives a quantitative yield of CeO_2. However, CeF_3 and oxygen, are the products when CeF_4 is heated with CeO_2 at 400°C (*18*).

The dissociation pressure of fluorine over the tetrafluoride is of interest in connection with the stability of the compound with respect

to the tripositive state. It is reported by Asker and Wylie (*18*) to be less than 0.5 mm Hg at 500°C, and the same workers state that in dry oxygen, CeF_4 is virtually unaffected up to 700°C. This suggests much greater stability than reported in earlier work (*131*, *322*), but the latter may have been affected by impurities. Mass spectrometric studies show that CeF_4 sublimes in high vacuum with little decomposition in the temperature range 800°–950°C, whereas TbF_4 and PrF_4 lose fluorine at much lower temperatures (*304*). Perceptible decomposition of TbF_4 is observed in a high vacuum at room temperature (*234*).

In spite of the lack of systematic or quantitative investigation, there can be little doubt that CeF_4 is more stable with respect to the trifluoride than is PrF_4, which cannot be made by fluorination of PrF_3. Likewise, TbF_4 is more stable with respect to the trifluoride than is the unknown DyF_4.

The range of known tetrapositive lanthanide elements is extended in the alkali metal fluorometalate(IV) compounds. Many compounds of this kind containing Ce(IV), Pr(IV), and Tb(IV) have been prepared. They have been reviewed by Brown (*86*) and are treated fairly briefly here. They are made by the fluorination of stoichiometric mixtures of alkali metal chlorides with oxides CeO_2, Pr_6O_{11}, or Tb_4O_7 (*86*, *251–253*, *473*) or with trichlorides (*25*) at temperatures in the range 200°–500°C.

With the exception of K_3CeF_7, all possible compounds of the formula type A_3MF_7 have been prepared, where M = Ce, Pr, or Tb and A = Na, K, Rb, or Cs. No details of terbium compounds of the formula type A_2MF_6 have appeared, but such compounds are known for cerium and praseodymium, where A = Na, K, Rb, or Cs.

The cerium compounds (*253*) are colorless and diamagnetic; they decompose slowly in moist air and water, liberate iodine from potassium iodide solution, and give a yellow precipitate of hydrated ceric oxide with a solution of caustic soda.

The praseodymium compounds (*20*, *25*, *251*) are also colorless but appear yellow under hot fluorine. Decomposition occurs in moist air, and they liberate oxygen from water forming solutions of praseodymium(III). They obey the Curie–Weiss law in the temperature range 90–300 K with rather large negative values of θ (-40 to -130 K) and have magnetic moments of 2.1 to 2.4 μ_B, which compare favorably with the theoretical value of 2.56 μ_B for the $[Xe]4f^1$ configuration of the Pr^{4+} ion (*251*). Spectroscopic studies are also consistent with the presence of this configuration (*20*) and the Mössbauer effect of the 145-keV line in ^{141}Pr reveals that the isomer shift of Cs_2PrF_6 is positive with respect to PrO_2, whereas those of tri-*f* praseodymium compounds are strongly negative (*309*). The same Mössbauer study reports that Cs_2PrF_6 reveals no magnetic ordering down to 2.45 K.

The terbium compounds (*86*, *252*, *473*) are colorless. Compound Cs_3TbF_7 is stable in moist air and is said to undergo no perceptible change in water (*252*). It follows the Curie law in the temperature range 90–300 K, and the effective magnetic moment is 7.4 μ_B compared with theoretical values of 7.9 μ_B for Tb^{4+} and 9.7 μ_B for Tb^{3+}.

Among the scattered details of other stoichiometries (*86*), compound $Na_7Pr_6F_{31}$ (*20*), originally reported to be $NaPrF_5$ (*25*) is notable. It is hexagonal, space group $C_{3i}{}^2$–$R\bar{3}$ with a_0 = 14.48 Å and c_0 = 9.677 Å. The compound is isostructural with $Na_7Zr_6F_{31}$ in which the tetravalent metal is coordinated by 8 fluorines at the corners of a square antiprism as in the tetrafluoride.

Crystallographic details of other compositions have been reviewed by Brown (*86*). Compounds K_3TbF_7, Rb_3CeF_7, Rb_3PrF_7, Rb_3TbF_7, Cs_3CeF_7, Cs_3PrF_7, and Cs_3TbF_7 are cubic and probably have the $(NH_4)_3ZrF_7$ structure reported by Hampson and Pauling many years ago (*221*). If so, the lanthanide is seven-coordinated, and more recent structural investigations favor a dynamically disordered, pentagonal bipyramid for the coordination polyhedron of the tetravalent metal (*103*, *265*, *266*, *588*). Particularly interesting is the fact that, in at least some cases, the positions of the metal atoms in the structure are the same as those in the structures of the corresponding A_3MF_6 compounds (*70*, *221*), where the lanthanide is octahedrally coordinated; corresponding A_3MF_6 and A_3MF_7 compounds then have similar powder patterns and only slightly different cell parameters. In these instances, the net result of fluorination of A_3MF_6 is merely the insertion of a single fluorine into the octahedral coordination sphere of the metal, and a slight expansion of the cell parameter. Seven-coordination is also found in Na_3CeF_7, Na_3PrF_7, and Na_3TbF_7 which have the tetragonal Na_3UF_7 structure (*586*). Nine-coordination is prominent in A_2MF_6 compounds.

Perhaps the most interesting fluorometalates(IV) are those containing tetravalent neodymium and dysprosium for which tetrafluorides are unknown. They are deep orange solids obtained by fluorination at 150°–350°C of trivalent compounds of the formula type Cs_3MF_6, Cs_3MCl_6, and $Cs_3M(SO_4)_3$ in which the caesium–lanthanide atomic ratio is 3:1 (*19*, *546*, *547*). Up to 95% conversion to the composition Cs_3MF_7 has been claimed (*19*, *546*), but spectroscopic investigations show that the tripositive oxidation state is present in the products. In the case of dysprosium, where the effective moment is sensitive to oxidation state, the values obtained lie midway between the theoretical values of 9.7 μ_B and 10.6 μ_B for Dy^{3+} and Dy^{4+}, respectively.

The deep color of the compounds is steadily bleached in moist air, and rapid evolution of oxygen occurs in water—so rapid that the

iodometric determination of the oxidation number is hampered by the competing oxidation of water. The X-ray powder patterns of Cs_3NdF_7 and Cs_3DyF_7 are little different from those of the cubic Cs_3MF_6 compounds, so it would seem that the tetravalent complexes have the $(NH_4)_3ZrF_7$ structure like Cs_3CeF_7, Cs_3PrF_7, and Cs_3TbF_7.

The absorption spectra confirm the presence of the tetrapositive oxidation state. The orange colors are caused by broad absorption bands at about 25,000 cm^{-1}, which Jørgensen (*301*) has assigned to ligand-to-metal charge-transfer transitions. At lower energies, the spectrum of Cs_3NdF_7 contained two absorptions that could be assigned to transitions from the $^3H_4$ ground state of Nd^{4+} to the remaining $^3H_5$ and $^3H_6$ levels of the ^3H multiplet (*547*). It was also possible to identify the three transitions to all three levels, $^3F_2$, $^3F_3$, and $^3F_4$, of the first excited multiplet. In Cs_3DyF_7, a progression of six absorptions in the rnage 2570–7460 cm^{-1} was assigned to transitions from the $^7F_6$ ground state of Dy^{4+} to the six remaining levels of the ^7F multiplet (*546*).

Inability to obtain these compounds in the pure state suggests that they are less stable with respect to the tripositive state than Cs_3PrF_7 or Cs_3TbF_7. When this fact is combined with the observations already made on the stability of the tetrafluorides, with the range and behavior of other fluorometalate(IV) compounds, and with the observation (*19*, *546*) that fluorination of Cs_3HoCl_6 yields no evidence for the formation of Ho(IV), it is clear that the likely stability sequences for the tetra-*f* state in fluorine compounds are Ce > Pr > Nd in the first half of the series and Tb > Dy > Ho in the second.

B. Oxygen Compounds

Dioxides MO_2 are known only for cerium, praseodymium, and terbium. Early claims to have prepared higher oxides of neodymium have been reviewed by Pearce (*444*) and by Asprey and Cunningham (*210*). Subsequent investigations (*376*, *433*, *460*) have failed to substantiate these claims; in particular, Pagel and Brinton (*433*) heated the tripositive oxides of neodymium, lanthanum, samarium, gadolinium, erbium, and ytterbium to various temperatures in pure oxygen at pressures up to 27 and found no evidence of oxidation. Atomic oxygen does not perceptibly oxidize Nd_2O_3 (*208*). Oxyanion salts of cerium(IV), praseodymium(IV), and terbium(IV) are formed with alkali and alkaline earth metals, but the preparation of this type of compound has not yet resulted in an extension of the range of tetrapositive states that occur in the dioxides.

The formation of dark brown or black higher oxides by praseodymium and terbium was recognized in the latter half of the nineteenth

century. Such compounds are formed when the trivalent oxide, oxalate, carbonate, or nitrate are ignited in air, and at an early stage it was realized that their oxygen content was less than that corresponding to the formulas MO_2.

Thus, during his discovery of praseodymium, von Welsbach (*557*) noted that decomposition of $Pr(NO_3)_3$ in air yielded a dark brown oxide that dissolved in dilute sulfuric acid with evolution of oxygen and which, to judge by iodometric analyses, had the formula Pr_4O_7. A similar formula was reported for the terbium compound by Urbain and Jantsch (*536*), who also showed that higher oxides of dysprosium were not formed under the same conditions. The exact formulas of the higher oxides aroused much controversy in the past (*444*), but it is now clear that when the tripositive oxides, nitrates, or oxalates are heated and cooled in air, the praseodymium oxide obtained has the formula Pr_6O_{11} (*85*, *174*, *270*). In the case of terbium, the composition is somewhat more variable, but it is close to Tb_4O_7 (*34*, *465*, *497*). However, if the temperature and oxygen pressure are more widely varied, it becomes clear that a large number of intermediate oxide phases occur between the compositions $MO_{1.5}$ and MO_2. For praseodymium and terbium, the existence of these phases has been established mainly through the careful work of Eyring and his associates; for cerium, mainly by Bevan and Brauer. This work on intermediate oxide phases has been reviewed by Brauer (*77–79*) and others (*164*, *269*, *484*) and is considered rather briefly in this article which concentrates mainly on the dioxides and their oxyanion derivatives.

Oxygen pressure vs composition isotherms (*175*, *214*, *268*, *269*), X-ray and differential thermal analysis (*93*, *94*, *214*, *215*, *269*, *484*), and conductivity studies (*576*) suggest that the oxide systems MO_x, where M = Ce, Pr, and Tb and $1.5 < x < 2.0$, consist of a sequence of single phases with narrow composition ranges separated by two-phase regions. The formulas of the single phases appear to constitute a homologous series with the general formula M_nO_{2n-2} (*269*, *484*). Thus, for praseodymium, phases with $n = 4, 7, 9, 10, 11, 12$, and ∞ have been recorded; the especially prominent Pr_6O_{11} is $Pr_{12}O_{22}$ ($n = 12$), and Pr_2O_3 and PrO_2 are the initial and final members with $n = 4$ and $n = \infty$, respectively. For terbium, recorded values of n are 4, 7, 8 (possibly), 11, 12, and ∞. Insufficient structural information is available to establish the relationship between the different series members with complete confidence but some promising speculations have been made. It seems clear from powder photographs that for $n \geqslant 7$, the positions of the metal atoms in the different phases are very similar to those in the fluorite structure of the oxides MO_2 and that formulas of the intermediate oxides are established by ordered omission of oxide anions.

Thus, McCullough (*360*) showed that the intensities of the lines in the powder photograph of Pr_6O_{11} were best explained in terms of a anion vacancy model, and Martin (*378*) obtained a negative Seebeck coefficient for the compound below 780°C, which indicates conduction by electrons and the presence of anion vacancies. Negative Seebeck coefficients for other phases in the oxygen-rich region were obtained by others (*248*). The existence of these vacancies implies that the intermediate oxides contain M^{3+} and M^{4+} ions, an implication supported by the intermediate values of the effective magnetic moments (*315*, *336*, *353*, *468*, *548*).

Plausible structural relationships between the different phases have been described in different ways by Eyring *et al.* (*484*), by Caro (*105*), and by Martin (*377*). The most elegant description of the generation of the nonstoichiometric phases is probably that of Martin, but here most attention is given to the work of Eyring because this focuses attention on the coordination of the metal.

We begin by comparing the structures of the M_2O_3 and MO_2 terminal members of the series. Compounds CeO_2, PrO_2, and TbO_2 have the fluorite structure, which may be pictured as a series of cubes of oxygen atoms linked only by edges and each possessing an eight-coordinated metal atom at its center (Fig. 12). If a series of strings are laid along the four $\langle 111 \rangle$ directions and suitably spaced, as in Fig. 13, then on elimination of the oxygen atoms through which they pass, a structure in which there are two types of metal coordination is generated. In both cases the coordination is sixfold, but one-quarter of the metal atoms lie at the center of a cube that lacks the 2 oxygens on the body diagonal, whereas the remaining three-quarters lack the 2 oxygens on a face diagonal. In the first case, the metal coordination is nearly regular octahedral; in the second, the octahedron is highly distorted. This structure is the cubic *C*-type M_2O_3 structure that occurs for both praseodymium and terbium.

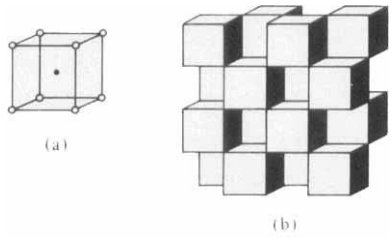

FIG. 12. Fluorite structure showing (a) coordination of the metal atom and (b) construction of the total structure from the unit in figure a. [From Sawyer *et al.* (*484*), Fig. 4.]

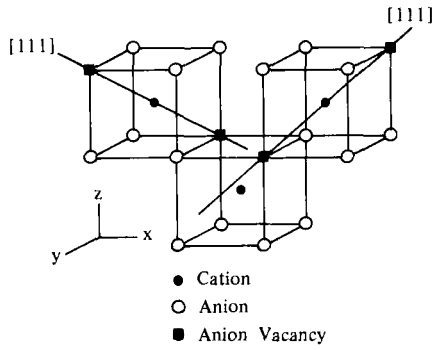

FIG. 13. Suitably spaced ⟨111⟩ strings through oxygen vacancies in the fluorite structure of PrO_2. [From Sawyer *et al.* (*484*), Fig. 5.]

It has been suggested that this kind of ordered omission of oxide anions, which can be pictured and described by the concept of sets of ⟨111⟩ strings, generates the intermediate oxide phases from the fluorite parent. It is clear from Fig. 13 that a particular string eliminates 2 oxygens for every metal through which it passes. If we write the formula of MO_2 as M_xO_{2x}, where x is the total number of atoms in the crystal, and consider the case where the strings pass through y of the x metal atoms ($y < x$), then $2y$ oxygen atoms are eliminated. The formula then becomes Pr_xO_{2x-2y} or Pr_nO_{2n-2}, where $n = x/y$. This accounts neatly for the formula of the homologous series, but it will be noted that there is an additional unsatisfied condition, namely that x/y should be integral. This is one way of stating the incompletely solved problem: What concentration and geometrical arrangement of strings will generate the necessary values of n for each observed phase in the series M_nO_{2n-2}?

The concentration of the strings determines the value of n, and the geometrical arrangement in one, two, three, or four ⟨111⟩ directions in the fluorite lattice determines the crystal symmetry. Sufficient structural information has been obtained to answer the question for the M_7O_{12} phase that is isostructural for cerium, praseodymium, and terbium. The strings are all parallel to only one of the ⟨111⟩ directions and evenly spaced, and the structure, therefore, has rhombohedral symmetry (*50*, *484*, *552*). This results in a structure in which one-seventh of all the cations are in the strings and are in trigonally compressed, octahedral coordination whereas the remaining six-sevenths are seven-coordinated. They lie at the center of cubes of oxygen atoms in which one oxygen is missing. Figure 14 shows how one of the parallel strings generates 6 seven-coordinated cations for every six-coordinated cation through which it passes. The Pr–O distance at the six-coordinated sites

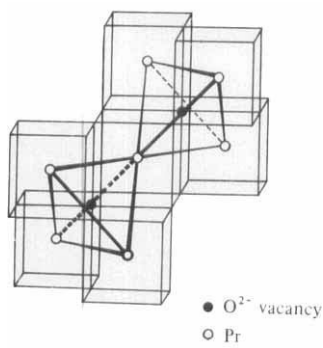

FIG. 14. A ⟨111⟩ string in the fluorite structure and its position in relation to the six- and seven-coordinate metal atoms in Pr_7O_{12}. [From Sawyer *et al.* (*484*), Fig. 7.]

is 2.22 Å, significantly shorter than at the seven-coordinated sites and close to the value in the tetravalent perovskite, $BaPrO_3$. This suggests that the octahedral sites are occupied mainly or exclusively by tetravalent praseodymium, and the seven-coordinate sites by a random mixture of Pr^{3+} and Pr^{4+} ions in a ratio close to 2:1 (*269*, *552*). Because conductivity occurs by an electron-hopping mechanism, it should be a maximum when the numbers of randomly distributed Pr^{3+} and Pr^{4+} ions are equal. With either exclusive occupation of the one-seventh six-coordinated sites by Pr^{4+} or with complete randomization of Pr^{3+} and Pr^{4+}, this would be so at about $PrO_{1.75}$ or Pr_8O_{14}. The conductivity is rather variable (*110*, *248*) but it does reach a maximum in the $PrO_{1.70-1.83}$ region.

In this description of the intermediate oxide phases, attention has been focused on metal coordination, which brings out one distinctive feature. Homologous series, such as Ti_nO_{2n-1} and Mo_nO_{3n-1}, occur among the transition metals (*14*, *558*), but here the octahedral coordination of the metal atoms is often preserved and the difference in formula is caused by a different linking of the octahedra—a change in the coordination number of the oxygen (*368*). In the case of the CeO_x, TbO_x, and PrO_x systems, it is the metal coordination number that changes, there being, for example, two kinds of six-coordination in C—M_2O_3 structures, six- and seven-coordination in M_7O_{12}, and eight-coordination in MO_2. Thus one distinctive feature of the lanthanide compounds may be attributed to the lack of a strong stereochemical preference that we have already noted when the structures of di-*f*-dihalides were examined.

Other descriptions of the generation of the nonstoichiometric phases focus on the packing of anions (*105*) or on anion vacancies. In the fluorite structure, the anion is tetrahedrally coordinated and lies at

the center of a cube, four of whose corners are occupied by cations (Fig. 15a). Martin (*377*) introduced the concept of a *coordination defect*, composed of a cube of this type with the anion missing and with the six intact surrounding cubes attached to the faces of the central cube (Fig. 15b). Such a unit has the composition $M_{7/2}O_6$ and the stoichiometry M_7O_{12}, which corresponds to the lowest known intermediate oxide of the Pr_nO_{2n-2} series with $n = 7$. The structure of this phase can be described as closest-packed array of the coordination defects shown in Fig. 15 and this is achieved by placing the defects wholly in the {213} planes of a cube of side $7a/2$, where a is the cell parameter of the fluorite unit cell. The intact cube shown in Fig. 15a has the composition $Pr_{1/2}O$, and addition of y such cubes per coordination defect gives the composition $Pr_{(7/2)+(1/2)y}O_{6+y}$ or Pr_nO_{2n-2}, where $n = y + 7$, thus offering the possibility of generating phases with $7 < n < \infty$, in which the defect {213} planes are increasingly separated by oxide-intact {213} planes. *Removal* of the oxide-intact {213} planes from M_7O_{12} brings about first corner- and then edge-sharing of coordination defects and generates structures with $4 \leqslant n < 7$. However, the only ordered binary structure currently known in this region is the sesquioxide (*255*).

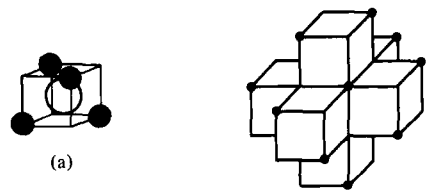

(a) (b)

FIG. 15. Portions of the fluorite structure: (a) coordination of the anion; (b) portion of formula $Pr_{7/2}O_6$ formed from units in figure a (the oxygen of the central cube is absent). [From Martin (*377*), Figs. 2a and 3b.]

We now consider the preparation and properties of the dioxides, MO_2. It does not appear possible to obtain a pure sample of PrO_2 by heating lower oxides in air (*433*), and carefully controlled conditions are needed to achieve complete conversion to the tetrapositive state by heating in pure oxygen at 1 atm pressure. Some of the earliest samples were obtained by heating lower oxides with oxygen at pressures of up to 300 atm and at temperatures in the range 300°–400°C (*360*, *433*, *497*) or by the action of atomic oxygen on the lower oxides at 250°–400°C (*208*).

It now appears that PrO_2 can be made by heating Pr_6O_{11} in pure oxygen at 1 atm pressure for 2 days at temperatures just below 320°C

(*270*); under these conditions, the oxidation of Pr_2O_3 to Pr_6O_{11} is rapid, but subsequent conversion of Pr_6O_{11} to PrO_2 is comparatively slow. Compound TbO_2 has not been obtained by heating lower oxides in oxygen, even though pressures of up to 4000 atm were used (*34*, *353*); the highest oxide obtained had a composition of about $TbO_{1.83}$. The first sample of TbO_2 was made by treatment of Tb_4O_7 with atomic oxygen at 350°C (*208*).

Rather surprisingly, it later proved possible to obtain both PrO_2 and TbO_2 by disproportionation of intermediate oxides in aqueous media. This work has been reviewed by Clifford (*116*) and Brauer (*78*, *79*). If Pr_6O_{11} is boiled in water, it disproportionates into $Pr(OH)_3$ and PrO_2, and the hydroxide can be dissolved in hot concentrated acetic acid leaving pure PrO_2 (*83*). The direct action of hot or cold concentrated acetic acid is equally effective. In the case of terbium, disproportionation of Tb_4O_7 to TbO_2 is induced by a hot mixture of hydrochloric and acetic acids, by prolonged standing in 0.1 *M* HCl (*483*), or by methanolic ammonium acetate (*401*). These reactions seem less remarkable in the context of the familiar disproportionation of red lead in nitric acid when PbO_2 and aqueous lead(II) nitrate are formed. Nevertheless, in view of the expectation that aqueous Pb^{4+}, Pr^{4+}, and Tb^{4+} ions should be very strong oxidizing agents (see below), the precipitation of the dioxides in acid solutions must be an indication of extreme insolubility with respect to the reaction

$$MO_2(s) + 2H_2O(l) = M^{4+}(aq) + 4OH^-(aq)$$

Formation of the dioxides in hydrothermal reactions also involves disproportionation. Compound Pr_6O_{11} or Pr_2O_3 with a suitable oxidizing agent yields $Pr(OH)_3$ and PrO_2 in the presence of 1000 atm of water vapor above 700°C, but TbO_2 is not formed in the analogous terbium reaction (*231*); however, lower oxides form TbO_2 when heated with $HClO_4 \cdot H_2O$ at 300 atm (*353*).

By comparison with the preparation of the praseodymium and terbium compounds, that of CeO_2 is straightforward. It is readily prepared by heating cerous oxalate in air, and lower oxides are pyrophoric at 400°–500°C (*64*, *112*).

Compound CeO_2 is pale yellow (*112*), PrO_2 is dark brown (*116*), and TbO_2 is dark red (*353*). The cell parameters of the three fluorite structures are 5.410 (*112*, *360*), 5.393 (*116*, *352*, *360*, *484*, *497*), and 5.220 Å (*116*, *353*), respectively. Somewhat lower values were reported in preparations involving atomic oxygen (*208*). Diffuse reflectance spectra of the tetrapositive ions have been obtained in a ZrO_2 fluorite matrix (*543*); broad absorption bands at 36,000 (Ce^{4+}), 31,200 (Pr^{4+}), and

28,600 cm^{-1} (Tb^{4+}) are assigned to oxide to metal ion charge-transfer transitions, and this assignment is confirmed by observations on a wider range of host lattices (*240*).

The magnetic properties of PrO_2 have been studied by several groups of workers (*315, 352, 468, 548*). The Curie–Weiss law is obeyed in the temperature range 100–300 K, with a value of θ of about 105 K. The effective magnetic moments obtained from the plots all agree closely and fall in the range 2.47–2.51 μ_B; this compares favorably with the theoretical value of 2.54 μ_B for the Pr^{4+} ion, and the isomer shift of the ^{141}Pr Mössbauer spectrum is distinctly different from the values for tri-*f* praseodymium compounds (*60, 309*). Deviations from linear Curie–Weiss plots were observed above 300 K (*548*) and below 100 K (*315*). Kern (*315*) accounted successfully for the low-temperature deviations by assuming a distortion along the ⟨111⟩ axis of the fluorite unit cell, which gives rise to D_{3d} symmetry, and carrying out a crystal field calculation. He attributed the high-temperature deviations to the involvement of excited states and observed no magnetic ordering down to liquid helium temperatures. This last observation was challenged by MacChesney *et al.* (*352*) who state that PrO_2 is antiferromagnetic with a Néel temperature of 14 K, a conclusion supported by the splitting of the Mössbauer spectrum by internal fields below 16 K (*60*).

In the temperature range 80–300 K, TbO_2 also follows the Curie–Weiss law with $\theta = 15$ K and a magnetic moment of 7.90 μ_B for Tb^{4+} (*353*). In the range 77–500 K, the compound gives a single temperature-independent ESR signal with $g = 2.0147 \pm 0.0002$ (*33*). Like PrO_2 it is antiferromagnetic but with a Néel temperature of only 3 K (*353*). New lines with odd indices appear in the neutron diffraction powder photographs at 1.5 K and imply a doubling of the cell parameters (*467*). This suggests that alternate (111) planes of ferromagnetically aligned spins are opposed as in the cases of MnO and EuTe (Section III,B,3,b).

Thermal decomposition of PrO_2 and TbO_2 proceeds at much lower temperatures than that of CeO_2. The CeO_2 can be annealed in oxygen at 800°C without decomposition and loses only a little oxygen under vacuum at 980°C (*112*), but PrO_2 and TbO_2 lose oxygen rapidly when heated in *air* at about 350°C to form Pr_6O_{11} and a phase with the approximate composition $TbO_{1.8}$ (*483*). At 314°C, Pr_6O_{11} is slowly oxidized to PrO_2 in a stream of oxygen at 1 atm pressure, but subsequent replacement of the oxygen by argon results in the regeneration of Pr_6O_{11} (*270*). As noted earlier, TbO_2 has not yet been made by the action of molecular oxygen on lower oxides, even at high pressures,

and this, combined with the general observation that under comparable conditions of temperature and oxygen pressure, the praseodymium system attains a higher level of oxidation than the terbium one (*497*), suggest that in oxide systems, tetra-*f* praseodymium is more stable with respect to the tri-*f* state than is tetra-*f* terbium. Such a conclusion is certainly valid for the reaction

$$\tfrac{1}{2}M_2O_3(s) + \tfrac{1}{4}O_2(g) = MO_2(s) \qquad (8)$$

at 298.15 K, as shown by the values of ΔH^0 in Table XVI.

TABLE XVI

THERMODYNAMIC DATA FOR LANTHANIDE OXIDES INCLUDING STANDARD ENTHALPIES FOR REACTION (8)

M	$\frac{1}{2}\Delta H_f^0(M_2O_3, s)$[a] (kcal mole^{-1})	$\Delta H_f^0(MO_2, s)$ (kcal mole^{-1})	ΔH^0[Eq. (8)] (kcal mole^{-1})	Ref.
Ce	−215.1	−260.6	−45.5	(*45, 46*)
Pr	−218.4	−232.9	−14.5	(*165, 514*)
Tb	−222.9	−232.2	−9.3	(*182*)

[a] Hexagonal form of Ce_2O_3, cubic forms of Pr_2O_3 and Tb_2O_3.

These figures, combined with the nonexistence of NdO_2 and DyO_2, suggest that the stability of the tetravalent state with respect to reduction varies as Ce > Pr > Nd in the first half of the series, and as Tb > Dy in the second.

By using the data in column 3 of Table XVI, the entropies of the metals (*243*), the entropy of CeO_2 (*573*), estimated entropies of 16 and 20 cal K^{-1} mole^{-1} for PrO_2 and TbO_2, respectively, and the standard free energies of formation of the aqueous tripositive ions (*292*), we calculate:

$$CeO_2(s) + 4H^+ + e = Ce^{3+} + 2H_2O \qquad E^0 = 1.26\ V$$

$$PrO_2(s) + 4H^+ + e = Pr^{3+} + 2H_2O \qquad E^0 = 2.5\ V$$

$$TbO_2(s) + 4H^+ + e = Tb^{3+} + 2H_2O \qquad E^0 = 2.3\ V$$

The figure for the couple,

$$PbO_2(s) + 4H^+ + 2e = Pb^{2+} + 2H_2O$$

calculated from data of Wagman *et al.* (*559*), is $E^0 = 1.46$ V.

These figures suggest that in acid media, PrO_2 and TbO_2 are very powerful oxidizing agents. As already noted, the higher oxides show some resistance to very dilute mineral acids, but if the acid concentration is sufficient, oxygen is liberated and the trivalent ions are formed (*165*, *557*). They oxidize moderately concentrated hydrochloric acid to chlorine, and manganous salts to permanganate in acid solution (*553*). These reactions require standard redox potentials in excess of 1.6 V.

It can be seen that the redox potentials have a very strong hydrogen ion dependence and fall rapidly with increasing pH. This effect is eventually moderated by the precipitation of $Pr(OH)_3$, but the dioxides are, nevertheless, much less powerful oxidizing agents in alkaline media. Using the solubility product of $Pr(OH)_3$ (*404*), we calculate

$$PrO_2(s) + 2H_2O + e = Pr(OH)_3(s) + OH^- \qquad E^0 = 0.5\ V$$

in basic solution, and persulfate or H_2O_2 in alkaline media converts $Pr(OH)_3$ to a mixture of hydrated PrO_2 and $Pr(OH)_3$. This mixture is said to yield pure, yellow hydrated PrO_2 when heated in 20–50 atm of oxygen at 200°C (*434*). Electrochemical oxidation of terbium(III) to terbium(IV) is also possible in basic solution (*466*).

Mixed oxide compounds of the formula type M_2CeO_3, M_2PrO_3, and M_2TbO_3 have been prepared by heating CeO_2, Pr_6O_{11}, and Tb_4O_7 with peroxidized forms of alkali metal oxides, usually in a stream of oxygen (*249*, *250*, *254*, *339*, *438*, *592*). Most of these have either the NaCl structure, probably with a statistical distribution of the singly and quadruply charged ions throughout the lattice, or the orthorhombic Li_2SnO_3 structure which has an hexagonal pseudocell. For some compounds, such as Na_2PrO_3 and K_2TbO_3, both structural forms are known (*249*, *438*). In both structure types, the lanthanide is octahedrally coordinated. The praseodymium and terbium compounds follow Curie–Weiss laws and have the expected magnetic moments (*438*); their colors are yellow or reddish-brown.

Octahedral coordination of the tetravalent lanthanides is also found in the mixed oxide compounds $BaCeO_3$, $BaPrO_3$, and $BaTbO_3$, which are white, yellow, and yellow, respectively. They can be made by heating $BaCO_3$ with an oxide of the appropriate lanthanide in oxygen at about 900°C (*48*, *272*, *438*) and have distorted forms of the perovskite structure. Compounds $BaCeO_3$ and $BaPrO_3$ are orthorhombic, and $BaTbO_3$ is rhombohedral, but, nevertheless, the oxygen octahedra around the lanthanide are almost regular, with average M—O distances of 2.24, 2.22, and 2.15 Å, respectively, the most marked

distortion being a $1\frac{1}{2}°$ twist about a trigonal axis of the octahedron in $BaTbO_3$ (*272*). Extra reflections appear in the neutron diffraction powder pattern of $BaTbO_3$ at low temperature and show that the compound is antiferromagnetic with a Néel temperature of 36 K (*48, 272*). The magnetic moment has a value close to that expected for the $^8S_{7/2}$ ground state of the free Tb^{4+} ion (*48, 438*). The $BaPrO_3$ is not ordered down to 4.2 K (*272*).

Although the whole of this section has so far been concerned with condensed phases, it has proved possible to vaporize higher oxides of cerium, praseodymium, and terbium and to trap discrete molecules in rare gas matrices at 4 K. The infrared spectra suggest that the molecules are slightly bent (*137*), and, in the case of CeO_2, this conclusion is supported by molecular beam studies (*313*).

C. Aqueous Systems

Orange aqueous solutions of tetravalent cerium can be used as an oxidant in redox titrations, but the exact value of the standard electrode potential, $E^0[Ce^{4+}/Ce^{3+}]$ is unknown. In any case, if known, the value would be of limited use, because the formal potential for equal concentration of cerium(IV) and cerium(III) varies very considerably with the nature and concentration of the acidic medium. In *M* H_2SO_4, the formal potential is 1.44 V; in *M* HNO_3, 1.61 V; in *M* $HClO_4$, 1.70 V; and in 8*M* $HClO_4$, 1.87 V (*334, 421, 494, 501*). This unusually large variation is attributed mainly to hydrolysis of $Ce^{4+}(aq)$, which is reduced at high acidity, and to strong complexing of $Ce^{4+}(aq)$ by anions such as SO_4^{2-} and NO_3^- which are normally regarded as weak complexing agents (*494*). The variation has detectable chemical consequences; for example, a very dilute solution of manganese(II) perchlorate is oxidized to permanganate by cerium(IV) in dilute perchloric acid, but permanganate is reduced to Mn^{2+} by cerium(III) in dilute H_2SO_4 (*288*).

By using the formal potentials for the Ce(IV)/Ce(III) potential in the different media, it is possible to estimate the formal potentials of the couples Pr(IV)/Pr(III) and Tb(IV)/Tb(III) under the same conditions. Thus, if one assumed that ΔG^0 for the reaction,

$$MO_2(s) + 4H^+(aq) = M^{4+}(aq) + 2H_2O$$

is similar for cerium, praseodymium, and terbium and that complexing by acid anions occurs to equivalent extents, the formal potentials in

any medium are obtained by adding $E^0[MO_2/M^{3+}] - E^0[CeO_2/Ce^{3+}]$ to the formal potential of the Ce(IV)/Ce(III) couple. From data cited in the preceding section, the increments are 1.2 V for praseodymium and 1.0 V for terbium, giving, for example, 2.9 V and 2.7 V, respectively, for the M(IV)/M(III) formal potentials in *M* $HClO_4$. The assumption of a smooth but slight variation in the ΔG^0 values for oxide dissolution and for anion complexing is reasonable because in these reactions the 4*f* electrons are conserved (see p. 103), but the estimate should be more reliable for praseodymium, the element *adjacent to* cerium, than for terbium. An essentially similar method of estimation was used by Eyring *et al.* (*165*) who assumed that ΔG^0 for the oxide dissolution was identical for praseodymium and plutonium, added the oxide free-energy increment to the Pu(IV)/Pu(III) formal potential, and obtained 2.9 V for the Pr(IV)/Pr(III) electrode in *M* $HClO_4$.

Such large values are perfectly compatible with the rapid oxidation of water that is observed when aqueous praseodymium(IV), with an absorption band at 290 nm, is prepared in dilute acid solution by pulse radiolysis (*171*). They mean, however, that claims to have prepared long-lived tetravalent praseodymium in aqueous solution are somewhat startling, but the preparative conditions do maintain a very high concentration of anions that would ensure strong complexing of the tetravalent state. Solutions of PrO_2 in concentrated HNO_3, HCl, or H_2SO_4 are said to contain yellow praseodymium(IV), oxidation of water occurring on dilution with formation of hydrogen peroxide (*434*). Solutions in nitric acid are said to be formed by electrolysis (*5*).

Existence of praseodymium(IV) in the HCl solutions has been disputed on the grounds that the absorption bands attributed to it are caused by other species (*71*), and an unsuccessful attempt to repeat the electrolytic experiments in nitric acid attributed previous reports of oxidation of praseodymium(III) to cerium contamination (*413*). Even in an as strongly complexing medium as 15*M* H_3PO_4, attempted anodic oxidation was unsuccessful. The claim (*434*) that yellow or yellow-brown compounds of formula M_2PrCl_6 were obtained by adding alkali metal chlorides to PrO_2 suspended in ice-cold, chlorine-saturated concentrated HCl has been rejected by Nugent *et al.* (*425*) on the grounds that the reported color is incompatible with their estimate (see p. 107) of the spectrum of the $PrCl_6^{2-}$ ion.

Such disagreements would be resolved by crystallographic and magnetic measurements which are badly needed. In part, these exist for concentrated sulfuric acid solutions, from which the compound $Pr(SO_4)_2 \cdot 2H_2SO_4$ was crystallized. This had an effective magnetic moment of 2.88 μ_B, suggesting that nine-tenths of the praseodymium

is in the tetravalent state. The compound decomposed at 115°C to give green praseodymium(III) (*434*). Well-characterized compounds could not be obtained from the nitrate solutions, but if we turn to nonaqueous media, ozonized N_2O_5 reacts with a suspension of PrO_2 in dry nitromethane to give a white solid that corresponds analytically to 50% $Pr(NO_3)_3$ and 50% $Pr(NO_3)_4$. Water produces the expected volume of oxygen after catalytic decomposition of the hydrogen peroxide that is formed (*503*).

Other supposed praseodymium(IV) compounds obtained from aqueous media include pale yellow hydrated oxalates $(NH_4)_2Pr(C_2O_4)_3 \cdot nH_2O$, where $n = 4$ or 6, prepared by the reaction of hydrated PrO_2 with concentrated ammonium oxalate at pH 8.0–8.5. They have effective moments of 2.6–2.7 μ_B (*435*). On the other hand, the attempt to establish the formation of tetravalent carbonates and oxalates during the thermal decomposition of praseodymium(III) carbonate and oxalate noticeably lacks magnetic as well as crystallographic support (*436*, *437*). The possibility of preparing terbium compounds analogous to the praseodymium(IV) compounds discussed in this section has not been investigated, although one claim to have oxidized terbium(III) to terbium(IV) in aqueous nitrate has been made (*537*). In view of the refutation (*413*) of corresponding work on praseodymium, this requires reinvestigation.

In conclusion, the existence of praseodymium(IV) in aqueous media is far from certain; in some cases, the solid compounds obtained lack crystallographic and magnetic characterization. In particular, proof of isomorphism with corresponding cerium compounds and attempts to prepare terbium analogs should clarify the situation.

V. Interpretation of Redox Stability

In Sections III and IV, observations relevant to the problems of redox stability were found to be consistent with three tentative generalizations about the stabilities of lanthanide compounds.

1. With any particular ligand, the thermodynamic stability of the di-*f*, dipositive oxidation state of the lanthanides with respect to the tripositive oxidation state varies in the order,

$$\text{La} < \text{Ce} < \text{Pr} < \text{Nd} < \text{Sm} < \text{Eu} \gg \text{Gd} < \text{Tb} < \text{Dy} > \text{Ho} > \text{Er} < \text{Tm} < \text{Yb}$$

The same sequence describes the thermodynamic stability of the di-*f* dipositive oxidation state with respect to disproportionation into the metal and the tripositive oxidation state.

2. Where a particular ligand can form both saltlike di-*f* insulators and metallic tri-*f* compounds of the same formula type, the stability of the saltlike state with respect to the metallic state follows the sequence given in the first assumption.

3. With any particular ligand, the thermodynamic stability of the tetrapositive oxidation state varies in the order, Ce > Pr > Nd > Sm and Gd ≪ Tb > Dy > Ho.

Before discussing these assumptions further, it is important to emphasize their generality. This generality is apparent in that it is possible to make statements about the change in stability of an oxidation state from metal to metal without specifying the particular ligand that must be chosen for the purpose of comparison. Thus, so far as is known, the sequence given in the first assumption applies to di-*f* dihalides, dipositive aqueous ions, and, judging from rather scant data (*356*), to dicyanides. Statements of such generality are not possible for the outer-transition series. For example, whereas the stabilities of the divalent chlorides or aqueous ions of the first-transition series with respect to the trivalent state follow the sequence Cr < Mn > Fe < Co, those of the cyanides run in the order Cr < Mn < Fe > Co (*288*, *109*, *417*). One of the chief uses of the concept of oxidation state is that, when compounds of an element are classified in this way, it is possible to make generalizations about them, sometimes without paying too much attention to the nature of the ligand. From this standpoint, it is in the lanthanide series that the concept of oxidation number attains its greatest power and usefulness (this point is considered further on p. 89).

An early and very productive interpretation of assumptions 1 and 3 above was suggested by Klemm in about 1930 (*318–320*, *276*). At that time, di-*f* compounds were known only for samarium and europium. Klemm noticed that the europium compounds were the most stable with respect to oxidation and that, on an ionic formulation, they contained the Eu^{2+} ion with the half-filled shell configuration $[Xe]4f^7$. The association of *filled* shells with stability was, however, a more familiar concept, and, obviously, the dipositive ion with the configuration $[Xe]4f^{14}$ would be Yb^{2+}. Klemm, therefore, heated ytterbium trichloride in hydrogen and thus obtained the first compound of ytterbium(II) (*324*). The same preparative method failed to yield dihalides of the elements from gadolinium to thulium inclusive (*279*, *280*). On the strength of such experiments, Klemm suggested that compounds containing ions with the empty, half-filled, or filled shell configurations had a special stability with respect to oxidation or reduction and, to account for the stability of dipositive samarium,

that the stability of the di-*f* state increased as the configuration approached the filled or half-filled shell configuration from *below*. In the case of the tetrapositive oxidation states, he suggested that stability increased as the empty or half-filled shell configuration was approached from *above*.

Klemm's rationalizations have been largely substantiated by subsequent research. They are still perfectly consistent with current knowledge of the stability of the tetrapositive state, which is summarized by assumption 3 in the foregoing. They proved capable of accommodating the work done on the preparation and properties of neodymium and thulium dihalides in the early 1960s (*26*, *150*, *151*), and it was only when dysprosium(II) halides were obtained under conditions that failed to produce dihalides of holmium or erbium (*127*, *128*, *293*, *345*) that their inadequacies became apparent. A second failing is their qualitative nature.

More recently, two related approaches to the problem of redox stabilities have been tried. In one, the thermodynamics of the oxidation–reduction reaction are analyzed by means of thermodynamic cycles, and the terms in the cycles are interpreted by current theories, in particular, by the theory of many-electron attoms. In the other, correlations are established between known thermodynamic data for the oxidation–reduction reaction and the energies of certain spectroscopic transitions in lanthanide atoms or compounds; the transition energies can be interpreted by the theory of many-electron atoms and used to enlarge the volume of thermodynamic data. Both kinds of approach can be used to make quantitative predictions about the redox stabilities of lanthanide compounds.

Before going further, it must be stressed that we shall be dealing with processes whose energy varies both irregularly and substantially as we move from metal to metal across the lanthanide series. In the past, there has been much interest in irregularities in the energies of complexing of tripositive lanthanide ions with a particular ligand (*403*, *454*). These irregularities have been attributed to the influence of one or more effects drawn from phenomena such as steric repulsion, ligand field stabilization energies, changes in coordination number (*403*, *454*, *510*), and the change in interelectronic repulsion of the 4*f* electrons on complexing (*298*, *423*, *446*). A typical example of this type of variation is plotted as the bottom curve in Fig. 23 (see Section V,A,6).

Irregularities of this kind are interesting in their own right, but as Fig. 23 shows it is important to note that they usually involve departures of no more than 3 kcal $mole^{-1}$ from a smooth variation. The energies of redox reactions, which are the main concern of this article,

may involve irregularities of more than 50 kcal mole^{-1}. It is because such irregularities are so large that the distribution of the less-common oxidation states in the lanthanide series is so uneven.

A. Interpretation by Thermodynamic Cycles

1. Oxidation of the Dipositive State

This mode of interpretation can be demonstrated by examining the thermodynamic stability of the dichlorides with respect to the straightforward oxidation reaction,

$$MCl_2(s) + \tfrac{1}{2}Cl_2(g) \longrightarrow MCl_3(s) \qquad (9)$$

The evidence cited in Section III,A,2 suggests that, as one moves across the lanthanide series, the standard Gibbs energy change, ΔG^0, for this reaction at 298.15 K varies in the sequence

$$La < Ce < Pr < Nd < Sm < Eu \gg Gd < Tb < Dy > Ho > Er < Tm < Yb$$

In Fig. 16, a thermodynamic cycle has been drawn around reaction (9), and a standard enthalpy change assigned to each step. All known

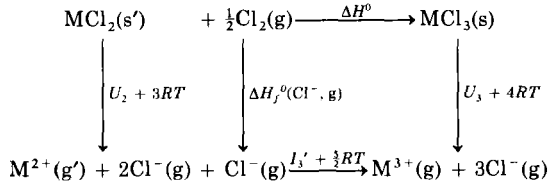

FIG. 16. Thermodynamic cycle for the oxidation of a divalent lanthanide dichloride.

dichlorides are di-*f* compounds; that is, they have the properties that would be expected of compounds containing M^{2+} ions with electronic configurations of the type [Xe]$4f^{n+1}$, n being the number of $4f$ electrons carried by the *tripositive* ion in its ground state. Thus, in the cycle, U_2 is the lattice energy of the solid dichloride or internal energy change when 1 mole of the compound containing ions of this type at 1 atm pressure is converted, at 298.15 K, into the gaseous ions M^{2+} and Cl^- which are infinitely removed from one another, the gaseous M^{2+} ion also having the configuration [Xe]$4f^{n+1}$. In the cycle, the prime against the physical state of the dichloride emphasizes that

the compound contains $[Xe]4f^{n+1}$ ions. Likewise, I_3' is a third ionization energy of the metal where the prime indicates that the electron is lost from a dipositive ion of configuration $[Xe]4f^{n+1}$. Unusually careful specification of the configurations of the ions is necessary because in one or two cases which are considered in more detail later, the ground-state configurations of M^{2+} ions are not of the type $[Xe]4f^{n+1}$.

From the cycle,

$$\Delta H^0 = U_2 - U_3 + I_3' + \Delta H_f^0[(Cl^-, g)] + \tfrac{3}{2}RT \quad (10)$$

$$\Delta G^0 = U_2 - U_3 + I_3' + \Delta H_f^0[(Cl^-, g)] + \tfrac{3}{2}RT - T\Delta S^0 \quad (11)$$

As one moves across the lanthanide series, terms $\Delta H_f^0[(Cl^-, g)]$ and $\frac{3}{2}RT$ remain fixed, and, if small irregularities caused by magnetic entropy are ignored, the entropy change for such a series of analogous reactions should be virtually constant. Thus the *variations* in ΔG^0 can be obtained from

$$\Delta G^0 = U_2 - U_3 + I_3' + \text{constant} \quad (12)$$

Data on the molar volumes of di-*f* dihalides in Section III,A,3 and on the well-known lanthanide contraction in tripositive compounds (*525*) suggest that the ionic radii of dipositive and tripositive lanthanide ions with configurations of the type $[Xe]4f^{n+1}$ should decrease nearly smoothly across the series. The familiar dependence of lattice energies on the inverse of the sum of the ionic radii (*310*), combined with the small size of ligand field effects in lanthanide compounds (*300*) then implies that U_2 and U_3 should increase nearly smoothly from lanthanum to ytterbium. Thus, any marked irregularities in ΔG^0 should be caused by those in I_3'.

Unfortunately, the atomic spectra of the lanthanides are very complex, and it has not yet been possible to obtain a comprehensive set of I_3 values by the usual method of extrapolating long series in the spectra to the series limit. Spectroscopic values have been obtained very recently by using an assumed parallelism between the variations in certain transitions in lanthanide spectra and the variations in I_3 (*517*, *544*), but virtually complete sets of third ionization potentials were first obtained from thermodynamic cycles (*167*, *289*). This method is worth considering further because, as we shall see when we come to consider stability with respect to disproportionation, it concentrates attention on the distinctive features of lanthanide redox reactions.

If we use the Born-Haber cycle in the case of the formation of a trivalent rare earth oxide from its elements, we obtain

$$\Delta H_f^0(MO_{1.5}, s) = \Delta H_{atm}^0(M, s) + I_1 + I_2 + I_3 - U(MO_{1.5}) + \tfrac{3}{2}\Delta H_f^0(O^{2-}, g) + 5RT \quad (13)$$

where $\Delta H_f^0(O^{2-}, g)$ is the standard enthalpy change for the reaction,

$$\tfrac{1}{2}O_2(g) + 2e^-(g) \longrightarrow O^{2-}(g)$$

which has been obtained from lattice energy calculations, and other symbols have their usual meanings. If Eq. (13) is rearranged, then

$$I_3 = -\Delta H_{atm}^0(M, s) - I_1 - I_2 + U(MO_{1.5}) + \Delta H_f^0(MO_{1.5}, s) - \tfrac{3}{2}\Delta H_f^0(O^{2-}, g) - 5RT \quad (14)$$

Apart from the lattice energies of the oxides, values for the terms on the right-hand side of this equation have been obtained for all the lanthanide elements save promethium. [Sources for these data can be found in Johnson (*289*, *292*).] When this method of calculating third ionization energies was first used, I_3 values for lanthanum, cerium, praseodymium, and ytterbium had already been obtained by the estimation of series limits in the third spectra of the elements. These four values were substituted into Eq. (14) to obtain lattice energies for $LaO_{1.5}$, $CeO_{1.5}$, $PrO_{1.5}$, and $YbO_{1.5}$. The four values lay very nearly on a smooth curve when they were plotted against atomic number, thus corroborating the assumption made earlier in this section about the variation in the lattice energies of tripositive compounds. The curve can be fitted to a Kapustinskii-type lattice energy function (*310*) of the form

$$U = \frac{A}{r_+ + r_-}\left(1 - \frac{\rho}{r_+ + r_-}\right) \qquad \rho = 0.345 \text{ Å}$$

where r_+ and r_- are the radii of the cation and anion, respectively, and A is a constant within experimental uncertainty. From this function the unknown lattice energies could be obtained, and then substituted back into Eq. (14) to obtain the third ionization energies for all the remaining elements save promethium.* Obviously not only

* Although the argument is developed through an ionic model, the estimated I_3 values are almost unaffected by any deviation of the oxides from ionic behavior because they are very insensitive to the chosen value of $\Delta H_f^0(O^{2-}, g)$.

TABLE XVII

THIRD IONIZATION POTENTIALS OF THE LANTHANIDES AS CALCULATED BY VARIOUS WORKERS

Element	Thermodynamic cycles[a] (eV)			Spectroscopic interpolation (eV)	
	Ref. (*167*)	Ref. (*289*)[b]	Ref. (*406*)	Ref. (*517*)	Ref. (*544*)
La	19.18	19.18	19.18	19.1774	19.1774
Ce	20.0	20.08	20.11	20.20	20.20
Pr	21.6	21.64	21.66	21.62	21.62
Nd	22.2	22.07	22.06	22.14	21.85
Pm	—	—	—	22.32	22.04
Sm	23.7	23.70	23.68	23.43	23.20
Eu	24.9	24.93	25.13	24.70	24.66
Gd	20.6	20.77	20.72	20.63	20.48
Tb	21.9	21.64	21.99	21.91	21.71
Dy	22.9	22.94	23.11	22.79	22.80
Ho	23.1	22.81	23.02	22.84	22.80
Er	22.6	22.72	22.87	22.74	22.74
Tm	23.8	23.76	23.89	23.68	23.68
Yb	25.3	25.02	24.96	25.03	25.03

[a] Different workers used slightly different auxiliary data and slightly different interpolation procedures, but the latter are basically as described in the text.

[b] Uncertainties in estimated figures have been lowered from the original values because of now diminished uncertainties in the spectroscopic value for ytterbium. Values have also been adjusted to the values of ΔH^0_{atm} in Johnson (*292*).

the oxides, but any set of tripositive lanthanide compounds can be used in the calculation provided that their standard enthalpies of formation, and the standard enthalpy of formation of their gaseous anion are known.* Factor and Hanks (*167*) used the arsenides and oxides; we (*289*) use the oxides alone, and Morss (*406*) used the complex chlorides, Cs_2NaMCl_6. The I_3 values from each study are listed in Table XVII and compared with the spectroscopic estimates from Sugar and Reader (*517*) and Vander Sluis and Nugent (*544*). The agreement between the thermodynamic and spectroscopic values confirms the assumptions implicit in each method; the spectroscopic values support the assumption of a nearly smooth variation in the lattice energies, and the thermodynamic values validate the interpretation procedure used in the spectroscopic determinations.

* As the previous footnote implies, the latter quantity does not need to be accurately known. Indeed, the use of a particular value could be avoided by interpolating, for example, $U(MO_{1.5}) - \frac{3}{2}\Delta H_f^0(O^{2-}, g)$, instead of $U(MO_{1.5})$, thus freeing the method from apparent dependence on the ionic model.

The variation in I_3 across the lanthanide series is plotted in Fig. 17. The I_3 values in Table XVII refer to ionizations in which the ions are in their ground-state configurations. In almost all cases, it turns out that this ionization is of the type

$$M^{2+}([Xe]4f^{n+1}) \longrightarrow M^{3+}([Xe]4f^{n}) + e^{-}$$

but in two cases, those of lanthanum and gadolinium, the gaseous dipositive ions have the configurations $[Xe]5d^1$ and $[Xe]4f^75d^1$, respectively. However, it is easy to allow for this because spectroscopic investigations (*517, 518*) show that the lowest level derived from the

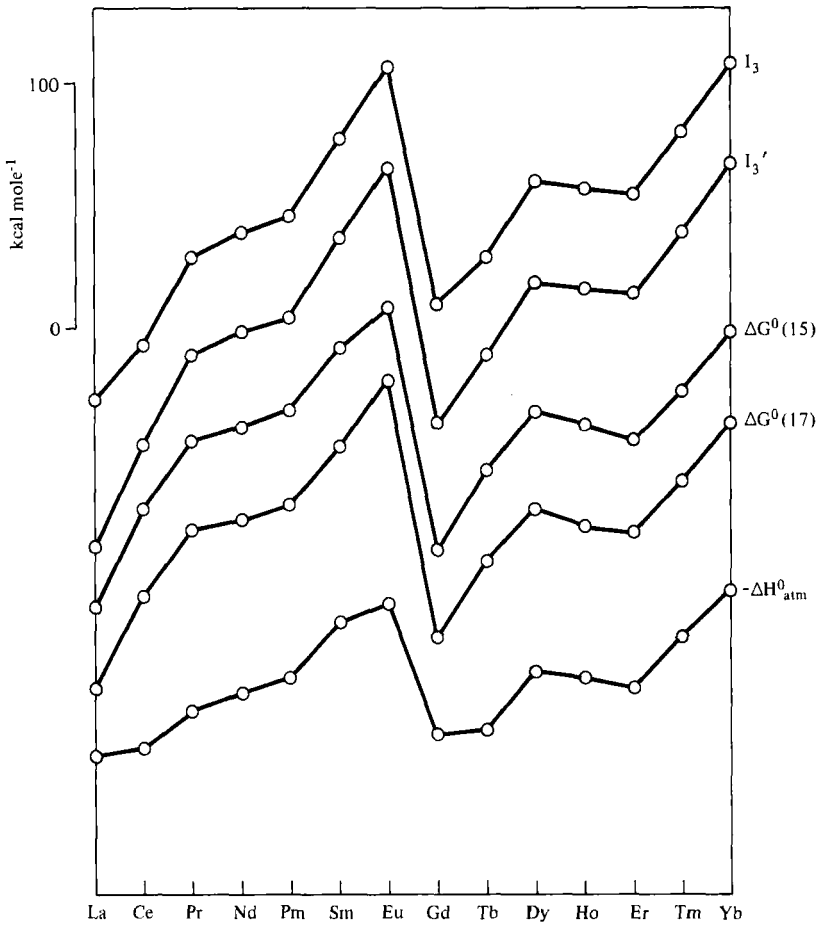

FIG. 17. Variations in the energies of various lanthanide processes.

$[Xe]4f^1$ configuration of the La^{2+} ion lies 0.8881 eV above the ground state, whereas the lowest level derived from the $[Xe]4f^8$ configuration of the Gd^{2+} ion lies only 0.295 eV above the ground state. Thus, for these two ions, I_3' is not equal to, but slightly less than I_3. As the similarity of the I_3 and I_3' plots in Fig. 17 shows, however, the correction makes little difference to the overall variation.

As expected from the earlier discussion of Eq. (12), the values of I_3' correlate extremely well with the irregular variation in the stability of the di-f dipositive state. There are two overall increases, from lanthanum to europium and from gadolinium to ytterbium, separated by a sharp drop from europium to gadolinium; these general changes give thermodynamic expression to Klemm's generalization. However, the I_3' variation also displays a decrease from dysprosium to erbium which accounts for the relative stability of dysprosium dihalides and instability of erbium dihalides together with the consequent failure of Klemm's generalization in this region of the series. The general variations in ΔG^0 in Eq. (12) are thus determined to a very large extent by those in I_3'.

The problem of explaining the variations in ΔG^0 can thus be restated as the problem of explaining the variations in I_3'. However, this restatement is useful because I_3' is the energy of a simple atomic process, whereas ΔG^0 is the energy of a complicated molecular change. One consequence of this is that the variation in I_3' can be interpreted theoretically. Indeed, one of the most satisfactory features of the I_3' variation as calculated by the thermodynamic method is that, qualitatively speaking, it is precisely what the Slater-Condon theory of many-electron atoms predicts for an $f^n \rightarrow f^{n-1}$ ionization.

In this theory, the ionization energies of an f^n configuration can be written down as the sum of a term U, the Coulombic energy of an f electron in the field of the positively charged noble gas core, and a series of terms representing the change in the repulsion energy between the f electrons that is attendant upon ionization. The ionization energies take a particularly simple form if the change in repulsion energy is written as a linear combination of the Racah parameters (*469*) E^0, E^1, and E^3 (*289*). This is done in Table XVIII. The term $U - (n-1)E^0$ is responsible for the overall increase across the series because U increases much more rapidly with the core charge than $(n-1)E^0$ increases with the number of electrons. In other words, unlike the Racah parameters, U changes drastically across the series. The drop at the half-filled shell is caused by the sudden appearance of the term $-9E^1$ once n has become equal to 8, and the terms in E^3 are responsible for the three-quarter-shell effect. Formulas in Table XVIII suggest that there should be a quarter-shell effect as well; this is visible

TABLE XVIII

THEORETICAL IONIZATION POTENTIALS FOR f^n IONS

n	$E(f^{n-1}) - E(f^n)$	n	$E(f^{n-1}) - E(f^n)$
1	U	8	$U - 7E^0 - 9E^1$
2	$U - E^0 + 9E^3$	9	$U - 8E^0 - 9E^1 + 9E^2$
3	$U - 2E^0 + 12E^3$	10	$U - 9E^0 - 9E^1 + 12E^3$
4	$U - 3E^0$	11	$U - 10E^0 - 9E^1$
5	$U - 4E^0 - 12E^3$	12	$U - 11E^0 - 9E^1 - 12E^3$
6	$U - 5E^0 - 9E^3$	13	$U - 12E^0 - 9E^1 - 9E^3$
7	$U - 6E^0$	14	$U - 13E^0 - 9E^1$

in the variation in Fig. 17, but it is smaller and does not succeed in reversing the general increase in I_3'. Spectroscopic measurements confirm that E^3 values are appreciably larger in the second half of the series (*300*).

Unfortunately it has not yet proved possible to give adequate *physical* expression to the formulas in Table XVIII. The overall increase in I_3' may be attributed to the increasing nuclear charge as one moves across the series, and the steep drop at the half-filled shell can be understood through the concept of exchange energy (*206*, *288*, *416*). The exchange energy stabilizes a particular configuration and is roughly proportional to the number of parallel spin interactions, so that, on ionization, the exchange energy loss is proportional to the number of parallel spin interactions that are destroyed. For configurations f^1 to f^7, this number increases in steps of one from 0 to 6, but the eighth electron has its spin opposed to the other seven, so that no parallel spin interactions between f electrons are destroyed when an f^8 configuration ionizes. The 0–6 pattern is thus repeated from f^8 to f^{14}, and this accounts for the break at the half-filled shell. The general sawtooth shape of the I_3' variation can, thus, be understood in terms of increasing nuclear charge and exchange energy losses, but it has not yet proved possible to give a physical, as opposed to a mathematical interpretation of the quarter and three-quarter-shell effects.

The argument at this point can be summarized by saying that when the standard Gibbs energy changes, ΔG^0, for the reaction

$$MCl_2(s') + \tfrac{1}{2}Cl_2(g) = MCl_3(s)$$

for a di-f lanthanide dichloride are analyzed by Eq. (12), it is found that the variations in ΔG^0 are determined almost entirely by those in I_3', and these can be explained by the theory of many-electron atoms.

The treatment can easily be extended to other oxidation processes such as

$$M^{2+}(aq) + H^{+}(aq) = M^{3+}(aq) + \tfrac{1}{2}H_2(g)$$

Here the lattice energy terms in Eq. (12) are merely replaced by hydration energies of ions. Ionic models suggest that these should vary smoothly with ionic radius like the lattice energies. In fact, there is evidence that the hydration energies of the tripositive ions do not vary smoothly across the series because of changes in hydration number (*402*, *510*). Even when this is allowed for, there are further irregularities probably attributable to the tetrad effect (*298*, *423*, *446*) rather than to ligand field effects as initially supposed (*510*). These irregularities are discussed further on p. 105. Here we merely note that they seem to be only about 1–2 kcal mole^{-1}, so that the hydration energies probably do vary nearly smoothly across the series and the variations in ΔG^0 are again very similar to those in I_3'. This suggests why general statements can be made about the redox stability of lanthanide compounds and why the concept of oxidation number is so powerful in the lanthanide series: the variation in terms such as lattice or solvation energies across the series are nearly smooth so that the variations in the energies of the redox processes are determined almost entirely by I_3' which is independent of the ligand. The smooth variation, in turn, is owing to the fact that in compounds the 4*f* orbitals are part of the core and suffer little exposure to the ligands. The situation is different with the outer-transition series where ligand field stabilization energies cause irregularities in lattice or complexing energies; redox stability variations are then strongly dependent on the ligand.

2. *Disproportionation Reactions*

A further problem that requires examination is why the stability sequence for the di-*f* state on p. 79 serves as well for disproportion reactions as for straightforward oxidation. This is conveniently approached via Eq. (14). If one examines the variations across the series of the terms on the right-hand side of this equation, one finds that any irregularities in all but one of them are for the most part small and attributable to the occasional intrusion of unusual electronic configurations (*289*). The striking exception is the variation in $-\Delta H^0_{atm}$, and the extent to which this is true can be seen by showing how closely the irregularities in I_3 on the left-hand side of the equation parallel those in ΔH^0_{atm} on the right. The values of ΔH^0_{atm} are recorded

TABLE XIX

STANDARD ENTHALPIES OF ATOMIZATION OF LANTHANIDE ELEMENTS AT 25°C

Element	ΔH^0_{atm} (kcal mole^{-1})[a]	Element	ΔH^0_{atm} (kcal mole^{-1})[a]
La	103.0 ± 2	Gd	95.0 ± 1
Ce	100.2 ± 1	Tb	92.9 ± 1
Pr	85.0 ± 1	Dy	69.4 ± 1
Nd	78.3 ± 2	Ho	71.9 ± 0.6
Pm	72 ± 8	Er	75.8 ± 2
Sm	49.4 ± 1	Tm	55.5 ± 2
Eu	42.4 ± 0.4	Yb	36.4 ± 0.6

[a] Sources of data are given in Johnson (*292*).

in Table XIX, and the variation in $-\Delta H^0_{atm}$ in Fig. 17. The parallelism between $-\Delta H^0_{atm}$ and I_3 or I_3' is very marked.

Now, when the standard Gibbs energy change for a disproportionation reaction such as

$$MCl_2(s') = \tfrac{1}{3}M(s) + \tfrac{2}{3}MCl_3(s) \quad (15)$$

is analyzed by the thermodynamic cycle of Fig. 18, the equation,

$$\Delta G^0 = U_2 - \tfrac{2}{3}U_3 + \tfrac{2}{3}I_3' - \tfrac{1}{3}(\Delta H^0_{atm} + I_1 + I_2') + \tfrac{1}{3}RT - T\Delta S^0 \quad (16)$$

is obtained, where I_2' refers to the second ionization in which the gaseous M^{2+} ions have the configuration $[Xe]4f^{n+1}$, which is the ground-state configuration except for La^{2+} and Gd^{2+}. Except for ΔH^0_{atm} and I_3', all terms on the right-hand side vary nearly smoothly with atomic number, so that the variations in ΔG^0 are determined almost entirely by those in the combination $(\frac{2}{3}I_3' - \frac{1}{3}\Delta H^0_{atm})$. Because

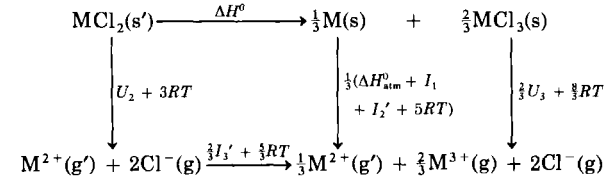

FIG. 18. Thermodynamic cycle for the disproportionation of a dihalide.

the parallelism between I_3' and $-\Delta H^0_{atm}$ is so close, changes in this combination are very similar to those in I_3'. Consequently, the variations in ΔG^0 for the disproportionation reaction, like those for oxidations, strongly reflect the variations in I_3'. The reason why the stability sequence for the di-*f* state serves equally well for disproportionation and oxidation must, therefore, be sought in the similarity between the variations in I_3 and $-\Delta H^0_{atm}$ which is the standard enthalpy of condensation of the gaseous metal:

$$M(g) = M(s) \qquad \Delta H^0 = -\Delta H^0_{atm}$$

This can be understood once it is realized that the ground-state configurations of the gaseous metal atoms are nearly all of the type $[Xe]4f^{n+1}6s^2$ (*187*), except for lanthanum, cerium, and gadolinium where the ground-state configurations are $[Xe]4f^n5d^16s^2$. On the other hand, the configurations in the *solid* metals are usually written $[Xe]4f^n5d^16s^2$ except for europium and ytterbium where they are thought to be $[Xe]4f^{n+1}6s^2$ (*209*).* Thus for most metals the condensation process involves a transition of the type $4f^{n+1}6s^2 \rightarrow 4f^n5d^16s^2$ in which the number of 4*f* electrons decreases by 1, so the energy variation is similar to that for a $4f^{n+1} \rightarrow 4f^n$ ionization. The analogy with a $4f^{n+1} \rightarrow 4f^n$ process depends on the fact (*581*) that the coupling between the outer 5*d* or 6*s* electrons and the $[Xe]4f^{n+1}$ or $[Xe]4f^n$ core is relatively weak. Such coupling is strong enough to cause the peculiar properties of SmS and SmB_6 mentioned on pp. 38 and 59, but it is only of the order of $kT(T \sim 300\ K)$ or less and is particularly weak in comparison with the very strong interactions of the 4*f* electrons with one another. Consequently, the energy of an outer 5*d* or 6*s* electron in the field of the core varies nearly smoothly with *n* and with increasing atomic number.

Griffith's interpretation (*205*) of the variation in $-\Delta H^0_{atm}$ for the outer transition elements can then be applied in a simplied form. The condensation process is split up into three steps; the first involves promotion of an electron by the process $4f^{n+1}6s^2 \rightarrow 4f^n5d^16s^2$, the second the elimination of the coupling between the three outer electrons and between these electrons and those in the 4*f* shell, and the third, the condensation of this "valence state" to form a lattice in which all except the three outer electrons of the tri-*f* metals are virtually nonbonding. The energy of step 3 varies smoothly because

* The number of 4*f* electrons is obtained magnetically. The assignment of the conduction band is somewhat arbitrary but immaterial to the argument used here.

the number of bonding electrons is fixed, and the coupling conditions already described lead to a nearly smooth variation in the energy of step 2 and a variation for step 1 that closely parallels that in I_3'. Consequently $-\Delta H^0_{atm}$ parallels I_3'.

Although the parallelism between $-\Delta H^0_{atm}$ and I_3' in Fig. 17 is close, it is less than perfect. For the most part this is because, in the cases of lanthanum, cerium, europium, gadolinium, and ytterbium, the change in configuration during condensation is not $4f^{n+1}6s^2 \rightarrow 4f^n5d^16s^2$. The parallelism is greatly enhanced by the appropriate adjustments. For example, as europium and ytterbium are di-*f* metals, they must be stable with respect to the tri-*f* allotropes. The stabilizations can, in fact, be estimated from the displacement of the europium and ytterbium points in plots of $\Delta H_f^0(MCl_3, s)$ or $\Delta H_f^0(M_2O_3, s)$ for the lanthanides (see p. 103). They are 20 kcal mole^{-1} for europium and 10 kcal mole^{-1} for ytterbium. The figures in Table XIX then allow us to calculate ΔH^0_{atm} values of 22 and 26 kcal mole^{-1} for tri-*f* europium and ytterbium, respectively. These values raise the europium and ytterbium points in the $-\Delta H^0_{atm}$ plot in Fig. 17 and greatly improve the parallelism; at the same time, they show that the common argument that the low heats of sublimation of europium and ytterbium are due to divalency needs qualification. If they were trivalent they would be even more volatile. They are divalent because the promotion energy $4f^{n+1}6s^2 \rightarrow 4f^n5d^16s^2$ required to reach the trivalent state is larger than for the other lanthanide elements.

3. *Quantitative Estimation of Redox Stability*

The thermodynamic approach described in Sections V,A,1 and 2 can be used to obtain quantitative estimates for the stabilities of both known and unknown di-*f* species. It is only necessary to assume that, provided there is no change in the number of *f* electrons during the condensation process, the lattice energies or solvation energies of the particular set of lanthanide compounds or ions are a smooth function of ionic radii which themselves vary nearly smoothly with atomic number. Known heats or free energies of formation including those of barium and strontium species are used to establish the lattice energy or solvation energy variation across the series, unknown values are interpolated from the plot, and these are then combined with values of ΔH^0_{atm}, I_1, and I_2' to obtain the unknown values of ΔH_f^0 or ΔG_f^0 for the di-*f* species. The method has been applied to the dichlorides (*291*) and to the dipositive aqueous ions (*292*). The values of $E^0[M^{3+}/M^{2+}]'$ and of ΔG^0 for

$$MCl_2(s') = \tfrac{1}{3}M(s) + \tfrac{2}{3}MCl_3(s) \qquad (15)$$

TABLE XX

THERMODYNAMIC PROPERTIES OF LANTHANIDE REDOX PROCESSES

M	ΔG^0[Eq. (15)][a] (kcal mole^{-1})	$E^0[M^{3+}/M^{2+}]'$ (V)	$E^0[M^{3+}/M^{2+}]$ (V)
La	(−73)	(−5.8)	(−3.8)
Ce	(−33)	(−4.2)	(−3.5)
Pr	(−6)	(−3.0)	(−3.0)
Nd	(0 ± 4)	(−2.8)	(−2.8)
Pm	(7)	(−2.5)	(−2.5)
Sm	32 ± 5	−1.50 ± 0.2	−1.50 ± 0.2
Eu	48 ± 3	−0.35 ± 0.03	−0.35 ± 0.03
Gd	(−50)	(−4.9)	(−3.6)
Tb	(−17)	(−3.5)	(−3.5)
Dy	(6)	(−2.6)	(−2.6)
Ho	(1)	(−2.9)	(−2.9)
Er	(−6)	(−3.0)	(−3.0)
Tm	(15)	(−2.1)	(−2.1)
Yb	38 ± 5	−1.10 ± 0.1	−1.10 ± 0.1

[a] Estimated values are in parentheses. Values of ΔG^0[Eq. (15)] in Johnson (*291*) have been adjusted to fit values of ΔH^0_{atm} in Table XIX, and the value of $\Delta H_f{}^0(EuCl_2, s)$ in Morss and Haug (*407*).

which were thus obtained are recorded in Table XX. As before, the primes emphasize that the estimates are appropriate for dipositive ions with $[Xe]4f^{n+1}$ configurations. Like the experimental observations reviewed in Section III,A,2, the values imply that at 298.15 K, compounds $LaCl_2$, $CeCl_2$, $PrCl_2$, $GdCl_2$, $TbCl_2$, and $ErCl_2$ are unstable with respect to disproportionation, and that the stability of the dichlorides decreases from dysprosium to erbium. Compound $PmCl_2$ is likely to be stable. A recent determination of $\Delta H_f{}^0(MCl_2, s)$ for $NdCl_2$ and $TmCl_2$ by (*408*) gave values in close agreement with estimates obtained earlier by this method (*291*). In the case of the aqueous system, the estimated values for all ions other than Sm^{2+}, Eu^{2+}, and Yb^{2+} are consistent with the powerful reducing properties described in Section III,A,3,b and III,C. In Fig. 17, we plot the estimated variation of ΔG^0 for reaction (15) and

$$M^{2+}(aq') + H^+(aq) = M^{3+}(aq) + \tfrac{1}{2}H_2(g) \qquad (17)$$

beneath the variation in I_3'. The parallelism, which was referred to in a qualitative way on pp. 91 and 89, is now quantitatively apparent.

An important problem that not only affects the values in Table XX but also makes a valuable link with the question of the relative

stabilities of the saltlike and metallic forms of compounds, such as MI_2, is the extent to which the values in Table XX are affected when the ground-state configuration of the dipositive ion is not $[Xe]4f^{n+1}$. As we saw on p. 87, for the gaseous ions, lanthanum and gadolinium that have $[Xe]5d^1$ and $[Xe]4f^75d^1$ configurations represent the sum total of such cases, but, in condensed phases, the number of exceptions will be increased because the 5*d* orbitals are destabilized by ligand field effects to a lesser extent than the 4*f*. To estimate any stabilization of the dipositive ions that might be achieved by the adoption of $4f^n5d^1$ configurations, the procedure used by McClure and Kiss (*354*) and by others (*425*, *426*) can be used. Reasonable values for ligand field stabilization energies are estimated and added to the stabilization of the lowest level of the $[Xe]4f^n5d^1$ configuration with respect to the lowest level of the $[Xe]4f^{n+1}$ configuration in the gaseous ions. In the case of the $M^{2+}(aq)$ ions this method suggests that only cerium joins lanthanum and gadolinium in adopting an $[Xe]4f^n5d^1$ configuration and that, through the adoption of such configurations, the E^0 values for lanthanum, cerium, and gadolinium given in column 3 of Table XX are raised by 2.0, 0.7, and 1.3 V, respectively, to the values shown in column 4. All other values remain the same. A very similar distribution of configurations is found in fluoride host lattices (*354*).

A correction procedure of this type could also be applied to the ΔG^0 values for the chloride disproportionation; however, in neither the chloride nor the aqueous systems are the chemical implications of the figures affected.

4. *Distribution of Insulating and Metallic States*

In the previous section, we noted that in condensed phases, ligand field effects can shift the distribution of M^{2+} ground-state configurations slightly from $4f^{n+1}$ toward $4f^n5d^1$. A much more marked shift away from $[Xe]4f^{n+1}$ occurs when an outer orbital such as 5*d* or 6*s* can participate in a conduction band; in such cases, 1 electron per lanthanide atom is delocalized throughout the condensed phase, and a compound with metallic properties results. In the discussion that follows, the outer orbital is assumed to be 5*d*, but the arguments apply equally well if it is taken to be 6*s* or a constant or uniformly varying mixture of 5*d* and 6*s*.

In the metallic phase just described, the 5*d* electrons are bonding, and when they are added to the 2 electrons per lanthanide which, with an ionic model, are assigned to the anion, the total number of bonding electrons per lanthanide becomes 3. The compounds are tri-*f*, as are the metallic dihydrides, $M^{3+}(e^-)(H^-)_2$, or sulfides, $M^{3+}(e^-)S^{2-}$.

In a series of compounds in which the nature of the anion and/or the M—M distance sometimes permits such delocalization, whether or not a particular element forms a saline di-*f* or metallic tri-*f* compound depends on the standard free-energy change of processes such as

$$MH_2(\text{saltlike}) \longrightarrow MH_2(\text{metallic}) \tag{18}$$

which, on an ionic formulation, can be written as

$$M^{2+}[4f^{n+1}](H^-)_2 \longrightarrow M^{3+}[4f^n](e^-)(H^-)_2$$

A possible response to the problem of the variations in ΔG^0 is to argue that, during this process, the number of 4*f* electrons is reduced by 1 and that, consequently, the variations in ΔG^0 will be very similar to those in I_3'. Thus, the probability of a di-*f* saltlike compound being stable with respect to the tri-*f* metallic phase follows I_3' and is greatest at europium, ytterbium, and samarium. This agrees extremely well with the facts: in the sulfide, selenide, and telluride series MX, as shown in Section III,B, the samarium, europium, and ytterbium compounds are insulators or semiconductors, whereas the rest, apart from TmTe, are metallic; in the MB_6 and MH_2 series, the europium and ytterbium compounds are semiconductors and the rest are metallic; and in the MC_2 carbide series, all the compounds seem to be metallic apart from EuC_2.

The correlation of ΔG^0 with I_3' may be stated in a different way by using the thermodynamic cycle shown in Fig. 19. From this cycle,

$$\Delta G^0 = I_3' + U_2 - M - T\Delta S^0 + (11/2)RT \tag{19}$$

Terms U_2, $T\Delta S^0$ and $(11/2)RT$ should be constant or vary nearly smoothly across the series. Quantity M is the standard enthalpy

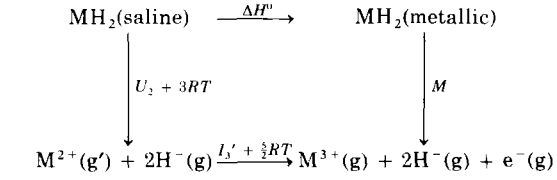

FIG. 19. Thermodynamic cycle for conversion of saline lanthanide dihydrides to a metallic state.

change at 298.15 K for the process,

$$M^{3+}(e^-)(H^-)_2(s) \longrightarrow M^{3+}(g) + 2H^-(g) + e^-(g)$$

This should also vary smoothly across the series because, as noted on p. 91, there is relatively weak coupling between outer electrons, such as those in the conduction band, and the $4f^n$ shell. Thus, the energy of the electrons in the conduction band should vary smoothly with increasing nuclear charge. It follows that, in the context of Eq. (19), all the dominant irregularities in ΔG^0 should be caused by those in I_3'.

In the absence of experimental data, the relative stabilities of di-f and tri-f states in various environments may now be crudely but, in a qualitative sense, successfully represented by Fig. 20. In Fig. 20,

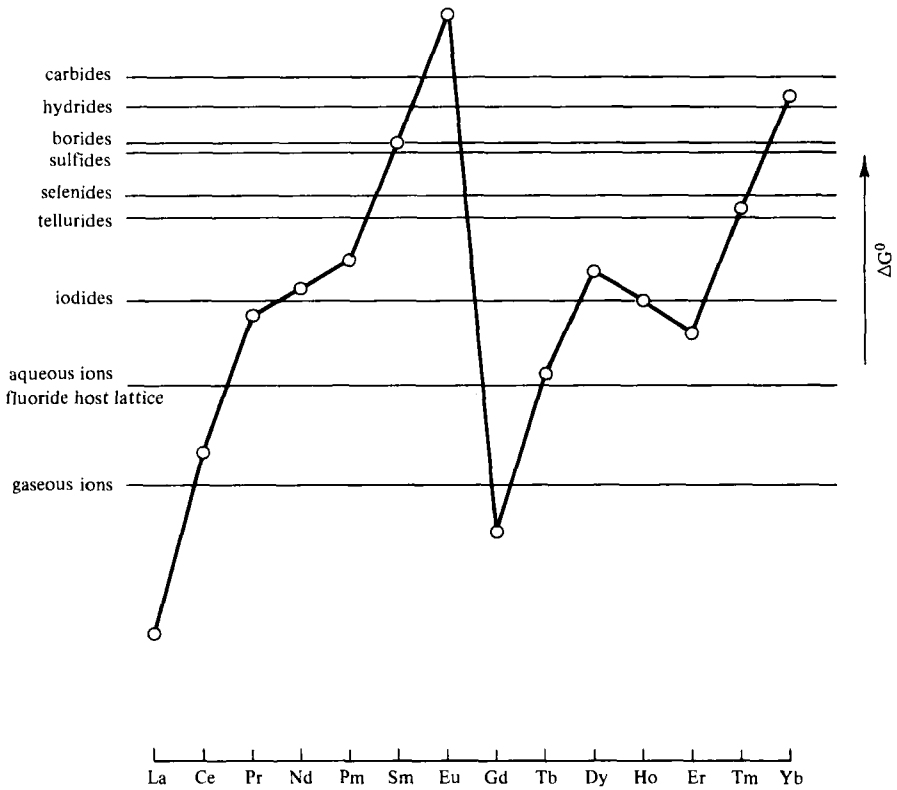

FIG. 20. Zero lines for the estimated variation in ΔG^0 for conversion of various divalent saline lanthanide compounds to the trivalent metallic form.

a single ΔG^0 variation, based on the values of ΔG^0 for the reaction

$$M^{2+}(aq') + H^+(aq) = M^{3+}(aq) + \tfrac{1}{2}H_2(g)$$

calculated from Table XX, is coupled with a series of horizontal zero lines, each of which is peculiar to a particular environment. The ΔG^0 plot represents the standard free-energy change of a process which, in each environment, involves the loss of an electron from a $4f$ shell with the configuration $4f^{n+1}$, and its transfer to an outer $5d$ orbital that can vary from nonbonding, as in the dipositive gaseous ions, to very strongly bonding as in metallic diiodides, chalcogenides, or dihydrides. Intermediate situations are represented by the aqueous ions and by dipositive ions in fluoride host lattices. The zero lines define the demarkation between elements for which conversion is thermodynamically favorable (these lie below the line) and those for which it is thermodynamically unfavorable (these lie above the line). In spite of gross assumptions, such as the use of a common ΔG^0 variation, Fig. 20 can be made to represent the distribution between the two electronically distinct situations in each series of lanthanide species. For example, for the gaseous ions, only the lanthanum and gadolinium points lie below the zero line, so these are the only M^{2+} ions with $[Xe]4f^n5d^1$ configurations; with the carbides, MC_2, all points except that for EuC_2 lie below the line, so all but one of the carbides can be labeled tri-*f*, and, as the $5d$ electron is strongly bonding in a conduction band, they can be written $M^{3+}(e^-)C_2^{2-}$.

We close this consideration of the relative stabilities of saltlike di-*f* insulators and tri-*f* metallic conductors by showing how crude diagrams such as those in Fig. 20 might be further refined. This can be done by examining the very varied properties and stabilities of the diiodides (*293*). Previously, we made the following observations (p. 22) regarding the fourteen elements from lanthanum to ytterbium inclusive: the first three form metallic diiodides; the next four, which include promethium, probably form saline di-*f* diiodides; gadolinium diiodide is metallic; terbium forms no diiodide at all; dysprosium yields a di-*f* diiodide; no lower iodides have been made for holmium and erbium; and the series is completed with saline di-*f* diiodides for thulium and ytterbium.

We first consider the disproportionation of *saline* dihalides

$$3M^{2+}(I^-)_2(s) \longrightarrow M(s) + 2MI_3(s) \qquad (20)$$

No thermodynamic data are available for this reaction, but we estimate that the values of ΔG^0 exceed the figure for the corresponding chloride

system in Table XX by roughly 4 kcal mole^{-1}. This increment was obtained by comparing the standard enthalpies of the reactions

$$3EuI_2 \longrightarrow Eu + 2EuI_3$$

and

$$3EuCl_2 \longrightarrow Eu + 2EuCl_3$$

The difference between the heats of formation of $EuCl_3$ and EuI_3 was estimated from the average difference in the heats of solution of the lanthanide trichlorides and triiodides quoted by Hohmann and Bommer (*74*, *241*) and from the difference in the standard enthalpies of formation of aqueous chloride and iodide ions (*559*). The difference between the heats of formation of $EuCl_2$ and EuI_2 was assumed to be the same as for the corresponding strontium compounds (*442*), a relationship justified by the similarity in the lattice energies of corresponding europium and strontium compounds and in the radii of Sr^{2+} and Eu^{2+}. The plot of ΔG^0 [reaction (20)] obtained in this way is shown in Fig. 21; it shows an I_3-like variation because the outer-electron configurations in the triiodide and solid metal are $4f^n$ and (generally) $4f^n5d^16s^2$, respectively, compared with $4f^{n+1}$ in the saline diiodides, so that there is a decrease of one $4f$ electron per metal atom. By contrast, ΔG^0 for the process

$$3M^{3+}(e^-)(I^-)_2(s) \longrightarrow M(s) + 2MI_3(s) \qquad (21)$$

should vary nearly smoothly across the series because in nearly all cases, the $4f$ electron population is $4f^n$ and the number of $4f$ electrons is conserved during the reaction. The exceptions are at europium and ytterbium where the formation of 2-electron metals (see pp. 91 and 92) lowers ΔG^0 [reaction (21)] by about 20 and 10 kcal mole^{-1} below the smoothly varying function. The location of ΔG^0 [reaction (21)] is fixed fairly precisely by the position of ΔG^0 [reaction (20)], and the qualitative observations of Section III,A,3,d.

The occurrence of metallic diiodides in the early part of the series, and the absence of diiodides for metals such as terbium, holmium, and erbium in the second-half, suggest that the stability of the metallic diiodides with respect to Eq. (21) decreases across the series. The overall slope of ΔG^0 [reaction (21)] should thus be negative. Its position can be fixed more precisely by the assumption that at gadolinium, where the metallic diiodide melts very incongruently (*387*), the value should be close to zero, and by the requirement that the variation should pierce the narrow space between ΔG^0 [reaction (20)] and the

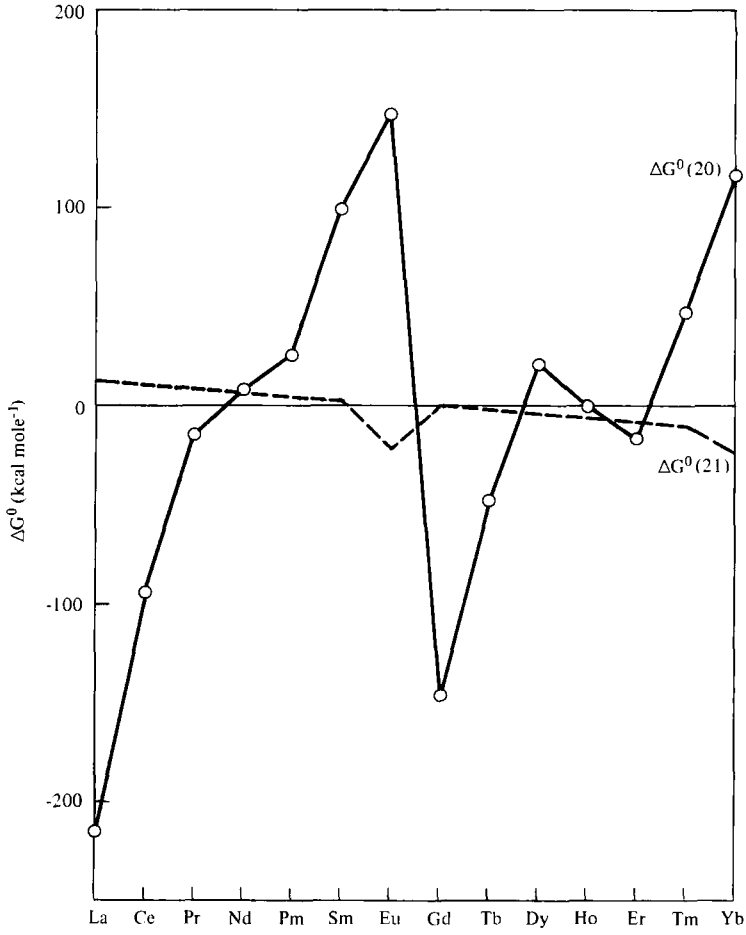

FIG. 21. Rough estimated variations in the standard free energy change for reactions (20) and (21), the disproportionations of diiodides.

zero line at neodymium where a saline diiodide is formed. These conditions generate the form of ΔG^0 [reaction (21)], shown in Fig. 21.

It can be seen in Fig. 21 that the diiodides display a most interesting, even distribution between saltlike and metallic compounds. The lanthanum, cerium, and praseodymium compounds are metallic and the transition to saltlike compounds occurs between praseodymium and neodymium. The saltlike diiodide increases rapidly in stability from neodymium to europium, but ΔG^0 [reaction (20)] falls steeply to well below the zero line after the half-filled shell, and $Gd^{3+}(e^-)(I^-)_2$

seems to be just stable at this point. The overall negative slope of ΔG^0 [reaction (21)] is consistent with the observation that LaI_2, CeI_2, PrI_2, and GdI_2 show increasingly incongruent melting points, but as the melts contain some free electrons, this is not necessarily directly related to the disproportionation equilibrium. It is also consistent with the observation that metallic diiodides are not formed beyond gadolinium. Indeed, beyond gadolinium even saline compounds are only stable where the ΔG^0 [Eq. (20)] plot breaks back above the zero line, at dysprosium, thulium, and ytterbium. If Fig. 21 is an accurate assessment of the situation, there is a good chance that NdI_2 undergoes an insulator–metal transition at accessible pressures. However, as the saline and metallic states appear not to be isostructural (*125*) the transition, unlike those described in Section III,B,4, should occur with a change in structure.

5. *Relative Stabilities of Tetrapositive and Tripositive Oxidation States*

This topic may be dealt with very briefly by noting that if suitable thermodynamic cycles are drawn around reactions of the type,

$$MF_4 \longrightarrow MF_3 + \tfrac{1}{2}F_2$$

$$M^{4+}(aq) + \tfrac{1}{2}H_2(g) \longrightarrow M^{3+}(aq) + H^+(aq)$$

the smooth variations in lattice energies and hydration energies across the lanthanide series mean that the variations in ΔG^0 are determined almost entirely by $-I_4$ (*290*). Term I_4 is the ionization energy for

$$M^{3+}(g) \longrightarrow M^{4+}(g) + e^-(g)$$

This process is of the type $[Xe]4f^n \rightarrow [Xe]4f^{n-1}$ for all the lanthanide metals, so that the variations in I_4 from cerium to lutetium should bear a close qualitative resemblance to those in I_3' from lanthanum to ytterbium. This expectation is perfectly borne out by values obtained by spectroscopic interpolation (*517, 544*); a set of these values is plotted in Fig. 22. As ΔG^0 is expected to correlate with $-I_4$, the stability of the tetrapositive state should vary in the sequence

$$Ce > Pr > Nd > Pm > Sm > Eu > Gd \ll Tb > Dy > Ho \sim Er \sim Tm > Yb > Lu$$

This complete series successfully accommodates the fragments obtained from an examination of existing tetrapositive compounds (quoted on p. 80).

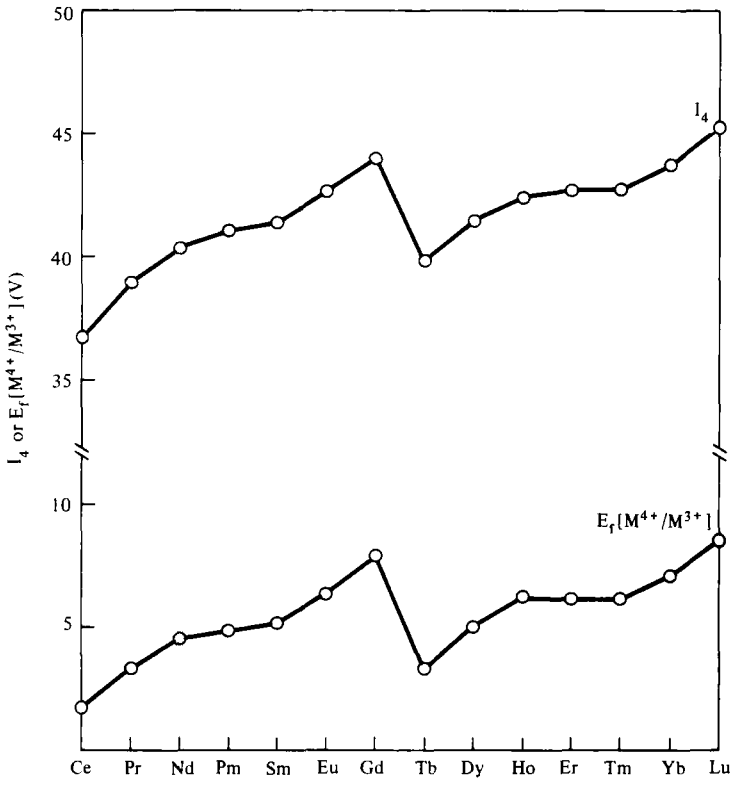

FIG. 22. Estimated values of the fourth ionization energies (*517*) and the formal potentials of the couples M^{4+}/M^{3+} (*426*) obtained by spectroscopic interpolation.

The values of I_4 suggest that in the region of the quarter- and three-quarter-shells, the stability of the tetrapositive state varies less with atomic number. This means that in these regions, the sequence of ΔG^0 values may be critically dependent on the attenuation of $-I_4$ through the intrusion of the lattice energy terms. By themselves, the latter tend to make the tetrapositive states of later elements in the series relatively more stable than those of earlier ones. This, combined with the greater break of the three-quarter-shell effect suggests that, although in the first half of the series the stability order for the +4 state may be Nd > Pm > Sm, in the second, it may be Ho < Er < Tm. This means that attempts to make Cs_3PmF_7 and Cs_3TmF_7 might be worthwhile, in spite of the lack of success with Cs_3HoF_7. Medium-temperature fluorination of Cs_3TmCl_6 and $Cs_3Tm(SO_4)_2$ causes yellowing of the

starting material and very slight oxidation (*23*), but further investigation is needed before this change can be attributed with confidence to the formation of thulium(IV).

6. *Summary*

The arguments in Sections V,A,1–5 may be summarized by saying that the energies of particular lanthanide processes in which the number of f electrons decreases by 1, vary in a quite characteristic way that is typified by the plot of I_3' in Fig. 17. The variation displays an overall increase across the series, but there is a very large downward break at the half-filled shell, and a much smaller downward break at the three-quarter-filled shell that also appears at the quarter-filled shell in an attenuated form. These irregularities are caused by discontinuities in the changes in the repulsion energy between the $4f$ electrons when an f electron is lost from a series of analogous lanthanide species. The very general occurrence of this variation has been demonstrated by showing that it is clearly recognizable in the variations across the series, of the energies of processes as diverse as the following:

$$MCl_2 + \tfrac{1}{2}Cl_2 \longrightarrow MCl_3$$

$$M^{2+}(g) \longrightarrow M^{3+}(g) + e^-(g)$$

$$M^{2+}(aq) + H^+(aq) \longrightarrow M^{3+}(aq) + \tfrac{1}{2}H_2(g)$$

$$M^{3+}(g) \longrightarrow M^{4+}(g) + e^-(g)$$

$$\tfrac{1}{2}M_2O_3 + \tfrac{1}{2}O_2 \longrightarrow MO_2$$

$$M(g) \longrightarrow M(s)$$

$$MH_2(\text{saline}) \longrightarrow MH_2(\text{metallic})$$

$$MS(\text{saline}) \longrightarrow MS(\text{metallic})$$

$$MCl_2 \longrightarrow \tfrac{1}{3}M + \tfrac{2}{3}MCl_3$$

$$M^{2+}[4f^{n+1}](g) \longrightarrow M^{2+}[4f^n5d^1](g)$$

Where the energies of such processes show some departure from this characteristic variation, then, first, it is usually not large and, second, it can be attributed to the fact that, in the case of one or two elements, the process does not involve the decrease of one in the number of $4f$ electrons. Thus, as Fig. 17 shows, the energy of the process,

$$M(g) \longrightarrow M(s)$$

the condensation of gaseous metal atoms, shows small departures at lanthanum, cerium, europium, gadolinium and ytterbium. In all these cases, however, this is attributable to the occurrence of condensation processes in which the number of $4f$ electrons is conserved.

The very general occurrence of the variation is due to two factors. First, the $4f$ electrons in ions or compounds are part of the core, so that they are little affected by any ligand field that is present, and, second, the coupling, between the $4f$ electrons and any other electrons is very small by comparison with the strong coupling that exists between the $4f$ electrons themselves.

The irregular change typified by I_3' is quite unlike the relatively smooth variation observed in the energies of reactions traditionally associated with the chemistry of the lanthanides. In processes of this type, such as the crystallization of a series of isomorphous salts or the elution of cations from an ion exchange resin, the number of $4f$ electrons is conserved.

To emphasize this point, we plot in Fig. 23, the standard enthalpy changes for three very different types of reaction of the lanthanide elements or their ions. The lower plot shows the enthalpy of complexing of the aqueous tripositive ions with $EDTA^{4-}$ (*366*). In this reaction, it is uniformly true that the number of $4f$ electrons is conserved, and, with the scale used in the Fig. 23, the plot appears to be a nearly smooth curve.

The upper plot shows the standard enthalpy of formation of the trichlorides (*291*, *407*). Here the variation is nearly smooth except at europium and ytterbium. These two exceptions exist because, in the formation reactions for europium and ytterbium trichlorides, the $4f$ electrons are not conserved; europium and ytterbium are 2-electron metals and the f-electron population decreases by 1 when their trichlorides are formed. Indeed, the displacements of about 20 and 9 kcal $mole^{-1}$, respectively, for the europium and ytterbium points provide estimates of the extent to which europium and ytterbium metals are stable with respect to their more volatile trivalent allotropes (compare p. 92).

Finally, the central plot shows estimated and experimental values (*291*, *407*, *408*) for ΔH_f^0 of di-f dichlorides. In the case of all metals except barium, europium, and ytterbium, the metallic state is tri-f, and the plot shows a large irregular variation that is largely characteristic of a process in which the number of f electrons changes by 1. For the elements lanthanum–ytterbium, the irregularities in $-\Delta H_f^0$ resemble those in I_3' and dwarf those in the other plots. However, the formation reaction for barium, europium, and ytterbium dichlorides is one in

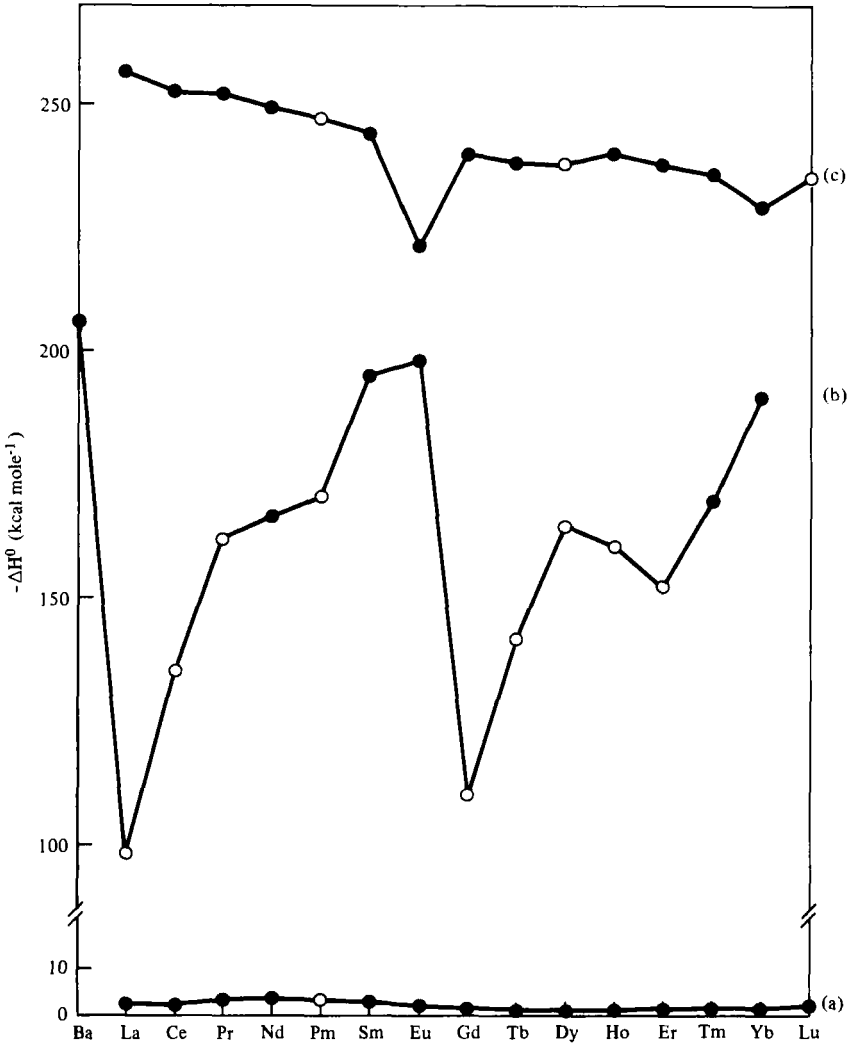

FIG. 23. Values of $-\Delta H^0$ for the following reactions: (a) complexing of $M^{3+}(aq)$ by $EDTA^{4-}(aq)$; (b) $M(s) + Cl_2(g) = MCl_2(s')$; and (c) $M(s) + \frac{3}{2}Cl_2(g) = MCl_3(s)$. Experimental values are represented by filled circles, and estimated values by open circles.

which the *f*-electron population is conserved, and these three points alone display the slight, nearly smooth variation usually associated with a process of this type.

We have used the phrase "nearly smooth" in describing the variation in energy across the series of a particular process in which the *f* elec-

trons are conserved. Deviations from a smooth variation might be expected because of differences in structure and metal coordination number for analogous lanthanide compounds. However, such deviations seem to be very small; thus three different oxide structures occur among the oxides M_2O_3, but the variation in ΔH_f^0 is nearly smooth except, as expected, at europium and ytterbium (*289*). Even when there are no structural variations within the reactants or within the products of a particular reaction, deviation from a smooth variation has been detected in some cases; the points lie on a curve that is broken by cusps at the quarter-, half- and three-quarter-filled shell. In the theory of many-electron atoms, this *tetrad effect* (*298, 423, 446*) is caused by small changes in the Racah parameters when the ligands surrounding the metal change during the reaction. The half-filled shell effect, which is greatest, is caused by changes in E^1, and the quarter- and three-quarter-shell effects by changes in E^3. Here we merely note that it seems that these effects, and those caused by structural variations, do little to diminish the justice of the description nearly smooth, producing discontinuities of the order of 3 kcal $mole^{-1}$ or less. These irregularities are very small compared with those in the energy variation for reactions in which the number of 4*f* electrons changes.

It seems, therefore, that if the change in the 4*f*-electron population during a reaction can be determined, then the type of energy variation across the series can be identified; conversely, in some cases, the energy variation can be used to identify the electronic change. For example, the values of $-D$(M—X), where X is a particular Group VI element (O, S, Se), M is a lanthanide element, and D(M—X) is the dissociation energy of the diatomic molecule, have been determined quite recently (*11, 61, 500*). They show to a large extent the characteristic energy variation of a process in which the number of 4*f* electrons decreases by 1. This is also true of values of $-D$(M—M) (*329*). For the most part, therefore, the 4*f*-electron population in the diatomic molecules must be the one less than that in the gaseous metal atoms, which are usually [Xe]$4f^n6s^2$. This suggests that, in gaseous diatomic molecules, there are in most instances 3 outer electrons per metal atom and that in such instances the molecules are tri-*f* systems.

B. Spectroscopic Correlation

The method of analysis by thermodynamic cycles, described in the preceding sections, is admirably suited to the *interpretation* of the problem of redox stability within the lanthanide series; it can also be

adapted, in some cases, to provide quantitative estimates of the stability of unknown oxidation states. On the other hand, although the direct correlation of suitably chosen spectroscopic transition energies with redox stabilities has so far only been used to estimate the redox potentials $E^0[M^{3+}/M^{2+}]$ and $E^0[M^{4+}/M^{3+}]$ in the lanthanide series, it has provided values of the same quantities in the actinide series where the lack of auxiliary thermodynamic data precludes operation of the thermodynamic method, and it could probably supply estimates of the analogous quantities for solid-state systems. The application of the method to a wide range of problems in lanthanide and actinide chemistry has been reviewed by Nugent (*422*).

The method of spectroscopic correlation has its origin in a paper published by Jørgensen in 1962 (*299*). He recorded the absorption spectra of the tribromides of neodymium, samarium, europium, thulium, and ytterbium in ethanol and assigned certain bands to transitions from molecular orbitals centered mainly on the ligands, to the $4f$ shell of the metal. The theoretical aspect of the work may be explained by referring to the expressions for the ionization energies in Table XVIII. The energy of the molecular orbital on the ligand varies nearly smoothly with nuclear charge, and as usual, the coupling between the $4f$ core and the electrons on the ligand may be regarded as weak. This means that the energy of the transition in which the $4f$ shell acquires an electron from the ligand should follow expressions similar to those implied for $-I$ by Table XVIII, except that a linear function, $a + b(n - 1)$, should be superimposed. Such expressions should take the form

$$A + B(n - 1) + CE^1 + DE^3$$

where n, E^1, and E^3 have the same meaning as in Table XVIII, but, for any given value of n, the coefficients C and D have minus the tabulated values.

The formulas of Table XVIII give the energy difference between the centers of gravity of the ground-state multiplets of the f^n and f^{n-1} configurations, but for quantitative work, it is advisable to make allowances for the fairly small effects of spin-orbit coupling. This allowance was included in Jørgensen's treatment. By using experimental values of E^1, E^3, and spin-orbit coupling constants, it is possible to equate the observed energies of the charge-transfer bands to the appropriate expression, to obtain empirical values of A and B by optimizing the fit, and to predict positions of the bands in ethanolic solutions of other tribromides. In Jørgensen's treatment, the terms in the formulas for the various configurations were grouped differently, and E^1 was regarded as a third constant to be empirically determined. Apart from

this, his procedure was essentially as described, and did achieve a good fit. In the same paper, he assigned bands in the spectra of $CeBr_3$, $PrBr_3$, and $TbBr_3$ in ethanol to $4f \rightarrow 5d$ transitions. Weak $4f - 5d$ coupling suggests that these should also follow the expressions for $I(f^n \rightarrow f^{n-1})$ with the addition of a linear term $a + b(n - 1)$; the fitting procedure was repeated for these transitions.

Now, the relationship between electron-transfer band energies in metal complexes formed with a particular ligand and the analogous redox potential has been recognized for some time; Dainton (*133*, *134*) plotted $E^0[M^{3+}/M^{2+}]$ for the first-row transition metals against the energy of the band edge of the metal–ligand transition in $M^{2+}(aq)$ and obtained a straight line of nearly unit slope. Barnes and Day (*49*) established a similar relationship between the ligand– metal charge-transfer bands in some samarium(III), europium(III), and ytterbium(III) complexes, and the experimental values of $E^0[M^{3+}/M^{2+}]$. By observing the charge-transfer band in thulium(III) complexes, they estimated $E^0[Tm^{3+}/Tm^{2+}] = -2.5$ V from their unit slope correlation. This procedure was repeated by others (*424*) who obtained -2.2 V. Similarly, Nugent *et al.* (*425*) assumed that, as in the actinide series, a unit slope correlation existed between the formal potentials $E_f[M^{4+}/M^{3+}]$ and the energies of the first $4f \rightarrow 5d$ band of the trichlorides or tribromides of cerium, praseodymium, and terbium in ethanol. By drawing such lines through the single points provided by the experimental value $E_f[Ce^{4+}/Ce^{3+}] = 1.74$ V, they obtained

$$E_f[Pr^{4+}/Pr^{3+}] = 3.2 \text{ V} \quad \text{and} \quad E_f[Tb^{4+}/Tb^{3+}] = 3.1 \text{ V}$$

However, only a limited number of estimates can be obtained in this way, because in many instances, experimental observation of the electron transfer or $4f \rightarrow 5d$ bands is prevented by UV cutoff.

This difficulty can be circumvented by assuming a linear correlation between the band energies and the redox potentials, and then fitting the experimental redox potentials directly to the kind of expression used by Jørgensen for the band energies.

Values of $E_f[M^{4+}/M^{3+}]$ for all the lanthanide elements were obtained in this way (*425*); figures of $E_f[Ce^{4+}/Ce^{3+}] = 1.74$ V,

$$E_f[Pr^{4+}/Pr^{3+}] = 3.2 \text{ V}, \quad \text{and} \quad E_f[Tb^{4+}/Tb^{3+}] = 3.1 \text{ V}$$

were used for the fitting process together with experimental values of E^1, of E^3, and of spin-orbit coupling constants for the tripositive aqueous ions. This allowed estimation of the empirical constants equivalent to A and B in the formulas given earlier in this section and subsequent calculation of unknown values of $E_f[M^{4+}/M^{3+}]$.

Further refinements in fitting procedures have been made. Vander Sluis and Nugent (*545*) fitted the energy differences between the lowest levels of the $4f^{n-1}5d^16s^2$ and $4f^n6s^2$ configurations for the gaseous lanthanide atoms to an expression of the type

$$E = A + B(n - 1) + CE^1 + DE^3 + F\zeta \qquad (22)$$

where coefficients C and D have the values given in Table XVIII, and $F\zeta$ accounts for the spin-orbit coupling contribution. With ten experimental values available they used *four* empirical constants in the fitting procedure; in addition to A and B, constant E^1 was written as a linear function of $(n - 1), p + q(n - 1)$, and E^3 was taken to be $E^1/10$ according to the hydrogenic ratio. This avoided possible errors in experimental values of E^1 and E^3 which, in previous publications (*425*, *427*), had been taken from compilations for aqueous ions. Only spin-orbit coupling constants, ζ, then needed to be taken from aqueous ion data, coefficients F being calculated from the quantum numbers J, L, and S. Nugent *et al.* (*426*) then showed that only a change in A and B was needed to make the expressions developed by Vander Sluis and Nugent for the $4f^n6s^2 \rightarrow 4f^{n-1}5d^16s^2$ energies in the atoms yield the experimental values of $E^0[M^{3+}/M^{2+}]$ for samarium, europium, and ytterbium. This was also true for the values of $E_f[M^{4+}/M^{3+}]$ for cerium, praseodymium, and terbium. Thus estimates of $E^0[M^{3+}/M^{2+}]$ and $E_f[M^{4+}/M^{3+}]$ were obtained for all the lanthanide elements. The values of $E^0[M^{3+}/M^{2+}]$ are recorded in Table XXI; corrections for the anomalous ground states of $La^{2+}(aq)$, $Ce^{2+}(aq)$, and $Gd^{2+}(aq)$ were made by a procedure very similar to that described on p. 94. The values of $E_f[M^{4+}/M^{3+}]$ are plotted in Fig. 22, and they supersede earlier estimates (*425*), which are believed to be less accurate. The

TABLE XXI

VALUES OF $E^0[M^{3+}/M^{2+}]$ ESTIMATED BY SPECTROSCOPIC CORRELATION

M	$E^0[M^{3+}/M^{2+}](V)^a$	M	$E^0[M^{3+}/M^{2+}](V)^a$
La	(−3.1)	Gd	(−3.9)
Ce	(−3.2)	Tb	(−3.7)
Pr	(−2.7)	Dy	(−2.6)
Nd	(−2.6)	Ho	(−2.9)
Pm	(−2.6)	Er	(−3.1)
Sm	−1.55	Tm	(−2.3)
Eu	−0.35	Yb	−1.15

[a] Estimated values are in parentheses.

variations revealed by Table XXI and Fig. 22 are in the former case mainly characteristic, and in the latter case entirely characteristic of an $f^n \rightarrow f^{n-1}$ process.

A number of assumptions are involved in the fitting procedures just described and these must largely be justified by the success of the method. Most obvious is the assumption that the variation in redox potential is accurately followed by the expressions of the type given in Eq. (22). Such expressions, like the formulas in Table XVIII, are derived by assuming that E^0, E^1, and E^3 have the same values for both oxidation states involved in the transformation, and these values are transferred from redox system to redox system without taking account of possible changes. More general assumptions implicit in the correlation of spectroscopic transition energies and redox stabilities have been cited by Jørgensen (*297*). It is, therefore, gratifying to find that the values of $E^0[M^{3+}/M^{2+}]$ obtained in this way agree well with the values that were estimated by thermodynamic methods and are recorded in Table XX. The differences between the two sets of figures are greatest at elements where the redox potentials are most removed in energy from the empirically fitted points at samarium, europium, and ytterbium. Again, the spectroscopic correlation method has recently been used to obtain values of I_3 (*544*). The estimates agree closely with those obtained by thermodynamic cycles, as Table XVII shows.

Finally, whatever method is used to estimate redox potentials, it is important that the experimental values used in the fitting operation should be accurate. This is most suspect in the calculation of $E_f[M^{4+}/M^{3+}]$. In the calculation of the values plotted in Fig. 22, figures for cerium, praseodymium, and terbium were used, but an adequate experimental value is available only for cerium; the two other values were obtained from spectroscopic measurements as described on p. 107. For this reason, the figures plotted in Fig. 22 are probably less reliable than those given in Table XXI. In the actinide series, however, there are a much larger number of experimental values of $E_f[M^{4+}/M^{3+}]$, and estimated values obtained by spectroscopic correlation procedures (*426*) are correspondingly more reliable.

VI. Extension to Other Systems

A. Actinide Series

It is natural to ask if the principles of redox stability for the lanthanide series can be applied to other long series in the periodic system. In this section, we show how they can be easily transferred to the

actinides. This study involves a brief review of recent research on the dipositive and tetrapositive oxidation states of the actinides.

The first dipositive actinide ion to be identified in aqueous solution was that of mendeleevium (*262*). It was found that zinc, Cr^{2+}(aq), and Eu^{2+}(aq) reduced Md^{3+} to Md^{2+}. There is slight disagreement as to the degree of reduction of Md^{3+} by V^{2+}(aq) (*262*, *370*, *372*), but it seems clear that $E^0[Md^{3+}/Md^{2+}]$ is only slightly more positive than $E^0[V^{3+}/V^{2+}]$ and this implies that the potential is about -0.15 V. As mendeleevium is the analog of thulium, it was not surprising that nobelium, the analog of ytterbium, was subsequently found to form a very stable dipositive oxidation state. Indeed, in tracer studies it was found that ^{255}No behaved like an alkaline earth element rather than a rare earth metal (*496*). This was corrected by addition of a sufficiently strong oxidizing agent: No^{2+} was oxidized to No^{3+} in acid solution by cerium(IV), bromate, and periodate, but not by thallium(III), nitrate, or iodate. This suggests that $E^0[No^{3+}/No^{2+}]$ is about 1.4 V, and that, in aqueous solution, No^{3+} is a slightly stronger oxidizing agent than dichromate.

The stability of other dipositive states in aqueous solution is less firmly established. Maly (*369*, *371*) showed that, like samarium, europium, and ytterbium, the elements californium, einsteinium, and fermium were more readily extracted from sodium acetate solution by sodium amalgam than other elements that are known to form only tripositive aqueous ions. This suggested that the three actinides might form dipositive oxidation states, that of fermium, the most readily extracted element, being the most stable with respect to oxidation. However, reports that Cf^{3+} could be reduced to Cf^{2+} by Eu^{2+} (*118*) were shown to be erroneous (*189*).

Estimation of $E^0[M^{3+}/M^{2+}]$ by exploiting the correlation between redox potential and the energy of the ligand-to-metal charge-transfer band for the tribromides in ethanol gave values for californium and einsteinium in the region of -1.6 to -1.9 V (*424*). Further experimental work suggested that Cf^{2+}(aq) was too powerful a reducing agent to exist in aqueous solution (*132*), a conclusion consistent with values of $E^0[Cf^{3+}/Cf^{2+}]$ of about -1.5 V estimated from the similarity of the M(III)—M(II) half-wave potential for samarium and californium in acetonitrile (*190*), and from the partial reduction and cocrystallization of californium with $SmCl_2$ following reduction of the trichlorides in aqueous ethanol with magnesium (*398*, *400*). This last method suggested a very similar value for $E^0[Es^{3+}/Es^{2+}]$ (*398*, *400*), and a value for $E^0[Fm^{3+}/Fm^{2+}]$ (*399*) of about -1.0 V in agreement with Maly's work on amalgam extraction which was cited above. The

most recent estimates of $E^0[M^{3+}/M^{2+}]$ were obtained by the spectroscopic correlation method described in Section V,B (*426*) and are plotted in Fig. 24. The values for californium, einsteinium, and fermium are -1.6, -1.3, and -1.1 V, respectively. These figures are in reasonably good agreement with the more experimentally based work already described.

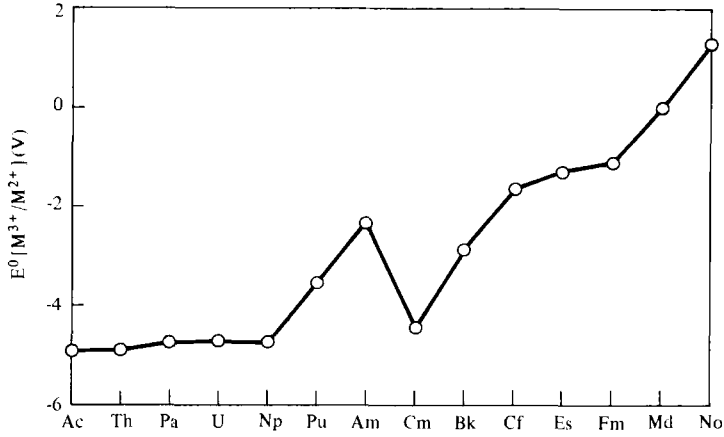

FIG. 24. Estimated values of $E^0[M^{3+}/M^{2+}]$ for the actinide elements obtained by spectroscopic correlations (*426*).

The similarities in the stabilities of californium(II) and samarium(II) in aqueous solution also extends to the solid state. Here it seems that californium(II) is slightly more difficult to prepare than samarium(II). Thus it was not possible to obtain $CfCl_2$ by hydrogen reduction of the trichloride, but an amber-colored dibromide with the tetragonal $SrBr_2$ structure ($c_0 = 7.109$, $a_0 = 11.500$) is formed when the tribromide is heated in hydrogen at 650°C (*449*). As expected from the E^0 value of -1.6 V, the dibromide reduces water forming green californium(III). Partial decomposition of CfI_3 to CfI_2 occurs when it is heated either alone or in hydrogen above 550°C (*263*).

Solid dihalides of the elements from einsteinium to nobelium have not yet been obtained, although they should certainly be capable of existence. Attempts to reduce Es_2O_3 in hydrogen were inconclusive because the α-radiation of ^{253}Es destroyed the crystal structure (*263*), but in view of the existence of only EuO and YbO in the lanthanide series, the preparation of dihalides is a surer route to dipositive einsteinium. The only other actinide known to form dipositive di-*f* compounds is americium, whose dipositive ion has the half-filled shell

configuration [Rn]$5f^7$. The estimated value of $E^0[Am^{3+}/Am^{2+}]$ in Fig. 24 is -2.3 V. Thus, the dipositive ion should reduce water violently, but if americium is heated with mercuric chloride, bromide, or iodide, black dihalides that are isostructural with their europium analogs are obtained (*54*, *55*). The cell parameters are given in Table XXII; comparison with Tables V–VII suggests that the ionic radius of Am^{2+} is slightly greater than that of Eu^{2+}. The [Rn]$5f^7$ configuration of the Am^{2+} ion has been verified for AmI_2 by showing that the molar susceptibility is close to that of Cm^{3+}, and very much greater than that for Am^{3+} (*55*). The melting point of the compound is about 700°C, a value similar to the melting points of the saline lanthanide dihalides, and the compound reduces water violently.

TABLE XXII

CRYSTALLOGRAPHIC DATA FOR AMERICIUM DIHALIDES

Compound	Structure	a (Å)	b (Å)	c (Å)	β (°)
$AmCl_2$	Orthorhombic $PbCl_2$	8.963	7.573	4.532	—
$AmBr_2$	Tetragonal $SrBr_2$	11.592	—	7.121	—
AmI_2	Monoclinic EuI_2	7.677	8.311	7.925	98.46

The estimated variation of $E^0[M^{3+}/M^{2+}]$ in Fig. 24 clearly establishes the relationship to the corresponding lanthanide system. Very approximate estimates of the relative stabilities of the [Rn]$5f^{n+1}$ and [Rn]$5f^n6d^1$ configurations suggested (*426*) that the ground states of the ions Ac^{2+}(aq), Th^{2+}(aq), Pa^{2+}(aq), U^{2+}(aq), and Np^{2+}(aq) would be based on [Rn]$5f^n6d^1$ configurations. Therefore, for the first five elements, we have the typical smooth and gentle energy variation of a process in which f electrons are conserved; thereafter, the characteristic variation for a process in which the f electrons decrease by 1 is observed. The chief difference from the lanthanide case is that the half-filled and three-quarter-filled shell effects are much less, and the superimposed overall increase is greater. These results can be attributed to reduced values of the interelectronic repulsion and, therefore, of E^0, E^1, and E^3, for the more spatially extended $5f$ electrons. One result of this is that in the actinide series, the situation is much closer to that for the first-transition series in which the stability of the dipositive state approaches a steady increase across the series. This stability reaches a maximum at zinc or nobelium, whereas, for the lanthanides, the values of E^1 and the resultant setback in I_3' at the half-filled shell are so great that the stability of Eu^{2+}(aq) is never exceeded in the second half of the series.

Similar comments apply to the estimated values of $E_f[M^{4+}/M^{3+}]$, which are plotted in Fig. 25. Experimental values for uranium, neptunium, and plutonium have been known for some time (*312*, *340*), and both direct potentiometric measurements (*513*) and measurements of the small difference between the potential of Ce(IV)/Ce(III) and Bk(IV)/Bk(III) electrodes under identical conditions (*570*) suggest that $E_f[Bk^{4+}/Bk^{3+}] = 1.54$ V in M HNO_3, and about 1.6 V in M $HClO_4$. Direct measurement of the potential of the couple Am(IV)–Am(III) in concentrated H_3PO_4(*512*, *584*), followed by a correction of 0.56 V equal to the difference between the formal potentials for Bk(IV)/Bk(III) in 10M H_3PO_4 and M $HClO_4$ (*512*), suggests that in M $HClO_4$, the $E_f[Am^{4+}/Am^{3+}] = 2.3$ V.

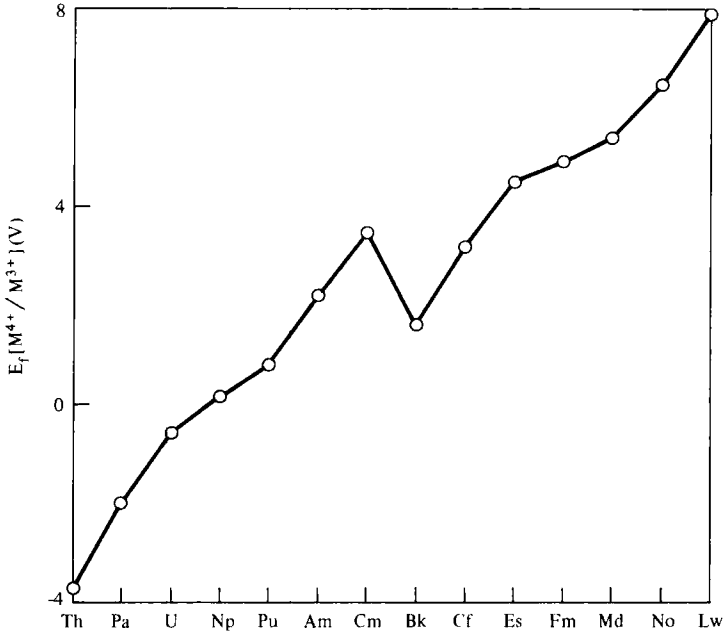

FIG. 25. Estimated and experimental values for the formal potentials of the M^{4+}/M^{3+} couples in the actinide series [see Nugent *et al.* (*426*)].

The other potentials in Fig. 25 were estimated by the fitting procedure described in Section V,B (*426*). It can be seen that unlike in the lanthanide series, there is a fairly steady decrease in the stability of the tetrapositive oxidation state across the series because the setback at the half-filled shell is relatively small and the superimposed overall increase is greater.

Here, we do not review the chemistry of the tetrapositive oxidation state in detail; we merely note that solid dioxides and tetrafluorides have for some time been known for the first seven elements from thorium to curium (*21, 86*), that BkO_2 (*450*) and BkF_4 (*24*) are now well-characterized, and that recently compounds CfO_2 and CfF_4 have been prepared (*56, 220*). It is clear that the californium compounds are the least stable with respect to the tripositive state, a result that is not quite consistent with the estimates for curium and californium in Fig. 25. Thus, unlike the other oxides, CfO_2 could not be made by ignition of Cf_2O_3 in air; pressures of oxygen of about 100 atm at a temperature of 300°C were used, decomposition of the dioxide being noticeable at about 400°C. The green tetrafluoride was made by the fluorination of Cf_2O_3, $CfCl_3$, or CfF_3 and, like the other actinide tetrafluorides, had the monoclinic UF_4 structure. In both the dioxide (*56*) and tetrafluoride (*220, 314*) series, an almost regular decrease in cell parameters across the series is observed, a phenomenon that matches the lanthanide contraction and indicates an absence of strong ligand field effects.

There is every sign, therefore, that when it becomes possible to examine the problem of the relative stabilities of the di- and tripositive and of the tri- and tetrapositive oxidation states of the actinides by means of the kind of thermodynamic cycle shown in Fig. 16, then, in the case of $5f^n$ configurations, it will be found that the lattice energies or hydration energies vary nearly smoothly with atomic number and that the variations in stability are determined by the appropriate $5f^{n+1} \rightarrow 5f^n$ ionization energy whose general variations resemble those contained in the $E_f[M^{4+}/M^{3+}]$ plot in Fig. 25.

B. First-Transition Series

The simplicity implicit in the last paragraph of the preceding section is lost when we turn to the outer transition series, where the *d* orbitals are relatively exposed and more strongly influenced by ligand fields. Under these circumstances, lattice energies and hydration energies no longer change smoothly with atomic number, but show irregular variations whose presence is explained in terms of ligand field stabilization energies. Consequently, although, in the first-transition series, reactions

$$MCl_2(s) + \tfrac{1}{2}Cl_2(g) \longrightarrow MCl_3(s) \tag{23}$$

$$M^{2+}(aq) + H^+(aq) \longrightarrow M^{3+}(aq) + \tfrac{1}{2}H_2(g) \tag{24}$$

are $3d^{n+1} \rightarrow 3d^n$ processes and the changes in ΔG^0 are almost entirely

determined by those in I_3 (*288*, *417*), the I_3 variation is apparent in the ΔG^0 variation only in a strongly attenuated form. This is clear from Fig. 26, where a plot of I_3 and of estimated and experimental values of ΔG^0 for the two reactions are shown side by side. This difference from the two inner-transition series is widened by the realization that chloride and water are weak field ligands. On turning to a strong field ligand, such as cyanide, we find that the relative stabilities of the M(II)–cyanide and M(III)–cyanide complexes in the first-transition series no longer show the influence of I_3 even in an attenuated form because the variations in the metal–ligand interaction

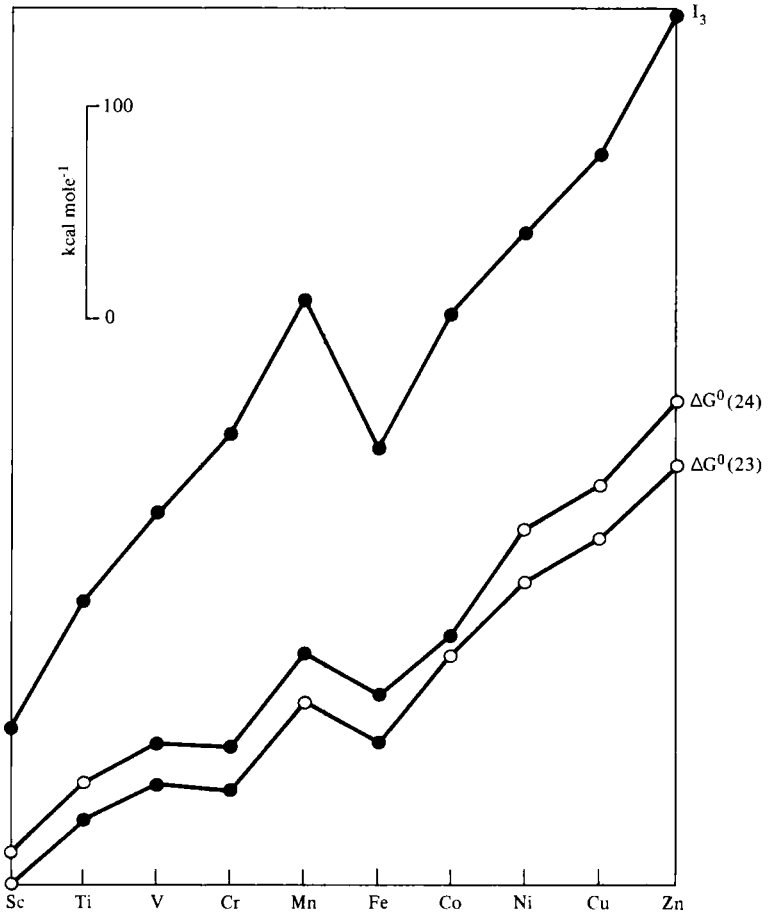

FIG. 26. Variations in ΔG^0 for reactions (23) and (24) and in the third ionization energy for the first-row transition metals. Experimental values are marked by filled circles, and estimated values by open circles.

energies, caused by the very strong ligand fields, are so large (*109*). As noted on p. 89, it is for this reason that general statements about variations in the stabilities of oxidation states from metal to metal are much less reliable for the outer- than for the inner-transition series.

VII. Conclusion

The classical view of the chemistry of the lanthanide elements was that they were alike, and this view was prompted by the difficulties of the separation problem and by rationalization of the chemical similarities (*73*) in terms of electronic configuration. This view is approximately correct for reactions in which the number of *f* electrons is conserved—reactions such as the complexing or crystallizing processes of the tripositive oxidation state, which were of major importance in classical separation methods. The energies of such reactions vary nearly smoothly across the series, any irregularities are comparatively small, although the total variation is in some cases quite large.

The classical view is, however, quite inappropriate for reactions in which there is a change in the number of *f* electrons. In these cases, there are marked irregularities in the energies of the reactions as we move across the lanthanide series, irregularities that are caused by discontinuities in the changes in interelectronic repulsion energy when an electron is lost or gained by the 4*f* shell. Many cases of this second type of reaction are now known, and a number of them are listed on p. 102. However, the best known and most accessible are to be found in the study of the stabilities of the dipositive and tetrapositive oxidation states with respect to the tripositive state.

Aknowledgments

Once again I must thank Dr. P. G. Nelson for the many pleasant hours that we have spent, both in and out of doors, discussing the chemistry of the inner-transition elements. He made invaluable comments on the manuscript, and much of the argument in Section V,A was originally developed in collaboration with him. I, of course, take full responsibility for this published version. This also seems the appropriate point to thank Professor S. F. Kettle and his colleagues at the School of Chemical Sciences, University of East Anglia, for their kind hospitality during a spell of study leave in which much of this article was written.

References

1. Achard, J. C., *C. R. Hebd. Seances Acad. Sci.* **250**, 3025 (1960).
2. Achard, J. C., and Albert, L., *C. R. Hebd. Seances Acad. Sci.* **262**, 1066 (1966).
3. Adin, A., and Sykes, A. G., *J. Chem. Soc. A* p. 1230 (1966).

4. Adin, A., and Sykes, A. G., *J. Chem. Soc. A* p. 354 (1968).
5. Afanas'ev, Y. A., Khanaev, E. I., and Andrushchenko, O. V., *Radiokhimiya* **14**, 654 (1972).
6. Ahn, K. Y., *J. Appl. Phys.* **43**, 231 (1972).
7. Ahn, K. Y., Tu, K. N., and Reuter, W., *J. Appl. Phys.* **42**, 1769 (1971).
8. Alascio, B., and Lopez, A., *Solid State Commun.* **14**, 321 (1974).
9. Allard, G., *Bull. Soc. Chim. Fr.* **51**, 1213 (1932).
10. Allen, G. C., Wood, M. B., and Dyke J. M., *J. Inorg. Nucl. Chem.* **35**, 2311 (1973).
11. Ames, L. L., Walsh, P. N., and White, D., *J. Phys. Chem.* **71**, 2707 (1967).
12. Anderson, J. S., and Bagshaw, A. N., *Rev. Chim. Miner.* **9**, 115 (1972).
13. Anderson, J. S., Clark, N. J., and McColm, I. J., *J. Inorg. Nucl. Chem.* **30**, 105 (1968).
14. Andersson, S., Collén, B., Kuylenstierna, U., and Magneli, A., *Acta Chem. Scand.* **11**, 1641, (1957).
15. Andrieux, L., *Ann. Chim.* **12**, 423 (1929).
15a. Aono, M., Kawai, S., Kono, S., Okusawa, M., Sagawa, T., and Takehena, Y., *Solid State Commun.* **16**, 13 (1975).
16. Apers, D. J., De Block, R., and Capron, P. C., *J. Inorg. Nucl. Chem.* **36**, 1441 (1974).
17. Archer, R. D., and Mitchell, W. N., *Inorg. Synth.* **10**, 77 (1967).
18. Asker, W. J., and Wylie, A. W., *Aust. J. Chem.* **18**, 959 (1965).
19. Asprey, L. B., *in* "Rare Earth Research" (E. V. Kleber, ed.), Vol. 1, p.58. Macmillan, New York, 1961.
20. Asprey, L. B., Coleman, J. S., and Reisfeld, M. J., *Adv. Chem. Ser.* **71**, 122 (1967).
21. Asprey, L. B., and Cunningham, B. B., *Prog. Inorg. Chem.* **2**, 267 (1960).
22. Asprey, L. B., Ellinger, F. H., and Staritsky, E., *in* "Rare Earth Research" (K. S. Vorres, ed.), Vol. 2, p. 11. Gordon & Breach, New York, 1964
23. Asprey, L. B., Johnson, D. A., and Nelson, P. G., unpublished observations.
24. Asprey, L. B., and Keenan, T. K., *Inorg. Nucl. Chem. Lett.* **4**, 537 (1968).
25. Asprey, L. B., and Keenan, T. K., *J. Inorg. Nucl. Chem.* **16**, 260 (1961).
26. Asprey, L. B., and Kruse, F. H., *J. Inorg. Nucl. Chem.* **13**, 32 (1960).
27. Atoji, M., *J. Chem. Phys.* **35**, 1950 (1961).
28. Atoji, M., *J. Chem. Phys.* **52**, 6431 (1970).
29. Atoji, M., *J. Chem. Phys.* **57**, 2410 (1972).
30. Atoji, M., and Flowers, R. H., *J. Chem. Phys.* **52**, 6430 (1970).
31. Atoji, M., Gschneidner, K., Daane, A. H., Rundle, R. E., and Spedding, F. H., *J. Am. Chem. Soc.* **80**, 1804 (1958).
32. Atoji, M., and Medrud, R. C., *J. Chem. Phys.* **31**, 332 (1959)
33. Azzoni, C. B., Del Nero, G. L., Lanzi, G., and Cola, M., *Lett. Nuovo Cimento* **4**, 959 (1970).
33a. Bachmann, R., Lee, K. N., Geballe, T. H., and Menth, A., *J. Appl. Phys.* **41**, 1431 (1970)
34. Baenziger, N. C., Eick, H. A., Schuldt, H. S., and Eyring, L., *J. Am. Chem. Soc.* **83**, 2219 (1961).
35. Baernighausen, H., *J. Prakt. Chem.* **14**, 313 (1961).
36. Baernighausen, H., *J. Prakt. Chem.* **34**, 1 (1966).
37. Baernighausen, H., *Rev. Chim. Miner.* **10**, 77 (1973).
38. Baernighausen, H., *Z. Anorg. Allg. Chem.* **342**, 233 (1966).
39. Baernighausen, H., *Z. Anorg. Allg. Chem.* **374**, 201 (1970).
40. Baernighausen, H., and Brauer, G., *Acta Crystallogr.* **15**, 1059 (1962).
41. Baernighausen, H., Patow, H., and Beck, H. P., *Z. Anorg. Allg. Chem.* **403**, 45 (1974).
42. Baernighausen, H., and Rietschel, E. Th., *Z. Anorg. Allg. Chem.* **354**, 23 (1967)
43. Baernighausen, H., and Schultz, N., *Acta Crystallogr., Sect. B* **25**, 1104 (1969).

44. Baernighausen, H., and Warkentin, E., *Rev. Chim. Miner.* **10**, 141 (1973).
45. Baker, F. B., and Holley, C. E., *J. Chem. Eng. Data* **13**, 405 (1968).
46. Baker, F. B., Huber, E. J., Holley, C. E., and Krikorian, N. H., *J. Chem. Thermodyn.* **3**, 77 (1971).
47. Ball, R. W., and Yntema, L. F., *J. Am. Chem. Soc.* **52**, 4264 (1930).
48. Banks, E., La Placa, S. J., Kunnmann, W., Corliss, L. M., and Hastings, J. M., *Acta Crystallogr., Sect. B* **28**, 3429 (1972).
49. Barnes, J. C., and Day, P., *J. Chem. Soc.* p. 3886 (1964).
50. Bartram, S. F., *Inorg. Chem.* **5**, 749 (1966).
51. Basset, H., *Chem. News* **65**, 3 (1892).
52. Batsonova, L. R., Zakharev, Y. V., and Opalovskii, A. A., *Zh. Neorg. Khim.* **18**, 905 (1973).
53. Baxter, G. P., and Tuemmler, F. D., *J. Am. Chem. Soc.* **60**, 602 (1938)
54. Baybarz, R. D., *J. Inorg. Nucl. Chem.* **35**, 483 (1973).
55. Baybarz, R. D., Asprey, L. B., Strouse, C. E., and Fukushima, E., *J. Inorg. Nucl. Chem.* **34**, 3427 (1972).
56. Baybarz, R. D., Haire, R. G., and Fayey, J. A., *J. Inorg. Nucl. Chem.* **34**, 557 (1972).
57. Beck, G., and Nowacki, W., *Naturwissenschaften* **26**, 495 (1938).
58. Beck, H. P., and Baernighausen, H., *Z. Anorg. Allg. Chem.* **386**, 221 (1971).
59. Bedford, R. G., and Catalano, E., *J. Solid State Chem.* **3**, 112 (1971).
60. Bent, M. F., Cook, D. D., and Persson, B. I., *Phys. Rev. C* **3**, 1419 (1971).
61. Bergman, C., Coppens, P., Drowart, J., and Smoes, S., *Trans. Faraday Soc.* **66**, 800 (1970).
62. Bergsma, J., and Loopstra, B.O., *Acta Crystallogr.* **15**, 92 (1962).
63. Berkooz, O., Malamud, M., and Shtrikman, S., *Solid State Commun.* **6**, 185 (1968).
64. Bevan, D. J. M., *J. Inorg. Nucl. Chem.* 1, 49 (1955).
65. Biedermann, G., and Silber, H. R., *Acta Chem. Scand.* **27**, 3761, (1973).
66. Biefeld, R. M., and Eick, H. A., *J. Chem. Phys.* **63**, 1190 (1975).
67. Bloch, D., and Georges, R., *Phys. Rev. Lett.* **20**, 1240 (1968).
68. Blokhin, S. M., Vainshtein, E. E., and Bertenev, V. M., *Fiz. Tverd. Tela. (Leningrad)* **7**, 3558 (1965).
69. Blum, P., and Bertaut, F., *Acta Crystallogr.* **7**, 81 (1954).
70. Bode, H., and Voss, E., *Z. Anorg. Allg. Chem.* **290**, 1 (1957).
71. Bogdanovich, N. G., Pechurova, N. I., Spitsyn, V. I., and Martynenko, L. I., *Zh. Neorg. Khim.* **15**, 2145 (1970).
72. Bohr, N., *Nature (London)* **107**, 104 (1921).
73. Bohr, N., "The Theory of Atomic Spectra and Atomic Constitution," p. 110. Cambridge Univ. Press, London and New York, 1922.
74. Bommer, H., and Hohmann, E., *Z. Anorg. Allg. Chem.* **248**, 373 (1941).
75. Bos, W. G., *Acc. Chem. Res.* **5**, 342 (1972).
76. Boyd, E. L., *Phys. Rev.* **145**, 174 (1966).
77. Brauer, G., *Prog. Sci. Technol. Rare Earths* **1**, 152. (1964).
78. Brauer, G., *Prog. Sci. Technol. Rare Earths* **2**, 312. (1966).
79. Brauer, G., *Prog. Sci. Technol. Rare Earths* **3**, 434. (1968).
80. Brauer, G., Barnighausen, H., and Schultz, N., *Z. Anorg. Allg. Chem.* **356**, 46 (1967).
81. Brauer, G., and Mueller, R., *Z. Naturforsch.* **10b**, 178 (1955).
82. Brauer, G., Mueller, R., and Rapp, K. H., *Z. Anorg. Allg. Chem.* **280**, 40 (1955).
83. Brauer, G., and Pfieffer, B., *J. Less-Common Met.* **5**, 171 (1963).
84. Brewer, L., *in* "The Chemistry and Metallurgy of Miscellaneous Materials; Thermodynamics" (L. L. Quill, ed.), Nat. Nucl. Energy Ser., Division IV, Vol. 19B, p. 124. McGraw-Hill, New York, 1950.

85. Brinton, P. M., and Pagel, H. A., *J. Am. Chem. Soc.* **45**, 1460 (1923)
86. Brown, D., "Halides of the Lanthanides and Actinides." Wiley (Interscience), New York, 1968.
87. Brown, J. P., Cohen, R. L., and West, K. W., *Chem. Phys. Lett.* **20**, 271 (1973).
88. Bucher, E., Andres, K., di Salvo, F. J., Maita, J. P., Gossard, A. C., Cooper, A. S., and Hull, G. W., *Phys. Rev. B* **11**, 500 (1975).
89. Bucher, E., and Maines, R. G., *Solid State Commun.* **11**, 1441 (1972).
90. Bucher, E., Narayanamurti, V., and Jayaraman, A., *J. Appl. Phys.* **42**, 1741 (1971).
91. Burgess, J., Hague, D. N., Kemmit, R. D. W., and McAuley, A., "Inorganic Reaction Mechanisms," Vol. 1, p. 12. Chem. Soc., London, 1971.
92. Burgess, J., Hague, D. N., Kemmit, R. D. W., and McAuley, A., "Inorganic Reaction Mechanisms," Vol. 2, pp. 23-25. Chem. Soc., London, 1972.
93. Burnham, D. A., and Eyring, L., *J. Phys. Chem.* **72**, 4415 (1968).
94. Burnham, D. A., Eyring, L., and Kordis, J., *J. Phys. Chem.* **72**, 4424 (1968).
95. Bury, C. R., *J. Am. Chem. Soc.* **43**, 1602 (1921).
96. Busch, G., *J. Appl. Phys.* **38**, 1386 (1967).
97. Busch, G., Junod, P., Morris, R., Musheim, J., and Stutius, W., *Phys. Lett.* **11**, 9 (1964).
98. Butement, F. D. S., *Trans. Faraday Soc.* **44**, 617 (1948).
99. Calderazzo, F., Pappalardo, R., and Losi, S., *J. Inorg. Nucl. Chem.* **28**, 987 (1966).
100. Campagna, M., Bucher, E., Wertheim, G. K., Buchanan, D. N. E., and Longinotti, L. D., *Phys. Rev. Lett.* **32**, 885 (1974).
101. Campagna, M., Bucher, E., Wertheim, G. K., and Longinotti, L. D., *Phys. Rev. Lett.* **33**, 165 (1974).
102. Candlin, J. P., Halpern, J., and Trimm, D. L., *J. Am. Chem. Soc.* **86**, 1019 (1964).
103. Canterford, J. H., and Colton, R., "Halides of the Second and Third Row Transition Metals," p. 127. Wiley (Interscience) New York, 1968.
104. Carlyle, D. W., and Espenson, J. H., *J. Am. Chem. Soc.* **90**, 2273 (1968).
105. Caro, P. E., *Proc. Mater. Res. Symp. 5th, Nat. Bur. Std. Spec. Pub. 364*, pp. 367–383 (1972).
106. Caro, P. E., and Corbett, J. D., *J. Less-Common Met.* **18**, 1 (1969).
107. Catalano, E., Bedford, R. G., Silveira, V. G., and Wickman, H. H., *J. Phys. Chem. Solids* **30**, 1613 (1969).
108. Caterall, R., and Symons, M. C. R., *J. Chem. Soc.* p. 3763 (1965).
109. Chadwick, B. M., and Sharpe, A. G., *Adv. Inorg. Chem. Radiochem.* **8**, 83 (1966).
110. Chandrashekhar, G. V., Mehrotra, P. N., Subba Rao, G. V., Subbarao, E. C., and Rao, C. N. R., *Trans. Faraday Soc.* **63**, 1295 (1967).
111. Charap, S. H., and Boyd, E. L., *Phys. Rev.* **133**, A811 (1964).
112. Chase, W. S., *J. Am. Chem. Soc.* **39**, 1576 (1917).
113. Chaterjee, A., Singh, A. K., and Jayaraman, A., *Phys. Rev. B* **6**, 2285 (1972).
114. Chia-Ling Chien and Greedan, J. E., *Phys. Lett. A* **36**, 197 (1971).
115. Christensen, R. J., Espenson, J. H., and Butcher, A. B., *Inorg. Chem.* **12**, 564 (1973).
116. Clifford, A. F., *in* "Rare Earth Research" (K. S. Vorres, ed.), Vol. 2, p. 45. Gordon & Breach, New York, 1964.
117. Clifford, A. F., and Beachell, H. C., *J. Am. Chem. Soc.* **70**, 2730 (1948).
118. Cohen, L. H., Aten, A. H. W., and Kooi, J., *Inorg. Nucl. Chem. Lett.* **4**, 249 (1968).
119. Cohen, R. L., Eibschutz, M., and West, K. W., *Phys. Rev. Lett.* **24**, 383 (1970).
120. Cohen, R. L., Eibschutz, M., West, K. W., and Buehler, E., *J. Appl. Phys.* **41**, 898 (1970).
121. Colquhoun, I., Greenwood, N. N., McColm, I. J., and Turner, G. E., *J. Chem. Soc., Dalton Trans.* p. 1337 (1972).

122. Cooley, R. A., and Yost, D. M., *Inorg. Synth.* **2**, 69 (1946).
123. Corbett, J. D., Personal communication, 1974.
124. Corbett, J. D., *Rev. Chim. Miner.* **10**, 239 (1973).
125. Corbett, J. D., Druding, L. F., Burkhard, W. J., and Lindahl, C. B., *Discuss. Faraday Soc.* **32**, 79 (1962).
126. Corbett, J. D., Johnson, D. A., McCollum, B. C., and Schraeder, E., unpublished observations, 1969.
127. Corbett, J. D., and McCollum, B. C., *Inorg. Chem.* **5**, 938 (1966).
128. Corbett, J. D., Pollard, D. L., and Mee, J. E., *Inorg. Chem.* **5**, 761 (1966).
129. Corbett, J. D., Sallach, R. A., and Lokken, D. A., *Adv. Chem. Ser.* **71**, 56 (1967).
130. Cotti, P., and Munz, P., *Phys. Kondens. Mater.* **17**, 307 (1974).
130a. Coulson. C. A., *Chem. Br.* **10**, 16 (1974)
131. Cunningham, B. B., Feay, D. C., and Rollier, M. A., *J. Am. Chem. Soc.* **76**, 3361 (1954).
132. Cunningham, B. B., Morss, L. R., and Parson, T. C., Annu. Rep. UCRL-19530, p. 276. UCRL Nuclear Chemistry, 1970.
133. Dainton, F. S., and James, D. G. L., *J. Chim. Phys.* **48**, 17 (1951).
134. Dainton, F. S., *J. Chem. Soc.* p. 1533 (1952).
135. Dekock, C. W., and Radtke, D. D., *J. Inorg. Nucl. Chem.* **32**, 3687 (1970).
136. Dekock, C. W., Welsey, R. D., and Radtke, D. D., *High Temp. Sci.* **4**, 41 (1972).
137. Dekock, R. L., and Weltner, W., *J. Phys, Chem.* **75**, 514 (1971)
138. De Pous, O., and Achard, J. C., *Bull. Soc. Chim. Fr.* p. 3417 (1970).
139. Didchenko, R., and Gortsema, F. P., *J. Phys. Chem. Solids* **24**, 863 (1963).
140. Didchenko, R., and Litz, L. M., *J. Electrochem. Soc.* **109**, 247 (1962).
141. Dimmock, J. O., *IBM J. Res. Dev.* **14**, 301 (1970).
142. Dockal, E. R., and Gould, E. S., *J. Am. Chem. Soc.* **94**, 6673 (1972).
143. Döll, W., and Klemm, W., *Z. Anorg. Allg. Chem.* **241**, 239 (1939).
144. Döll, W., and Klemm, W., *Z. Anorg. Allg. Chem.* **241**, 242 (1939).
145. Domange, L., Flahaut, J., and Guittard, M., *C. R. Hebd. Seances Acad. Sci.* **249**, 679 (1959).
146. Domange, L., Flahaut, J., Guittard, M., and Loriers, J., *C. R. Hebd. Seances Acad. Sci.* **247**, 1614 (1958).
147. Douglas, D. L., and Yost, D. M., *J. Chem. Phys.* **17**, 1345 (1949).
148. Douglas, D. L., and Yost, D. M., *J. Chem. Phys.* **18**, 1687 (1950).
149. Doyle, J., and Sykes, A. G., *J. Chem. Soc. A* p. 2836 (1968).
150. Druding, L. F., and Corbett, J. D., *J. Am. Chem. Soc.* **81**, 5512 (1959).
151. Druding, L. F., and Corbett, J. D., *J. Am. Chem. Soc.* **83**, 2462 (1961).
152. Druding, L. F., Corbett, J. D., and Ramsey, B. N., *Inorg. Chem.* **2**, 869 (1963).
153. Dworkin, A. S., and Bredig, M. A., *J. Phys. Chem.* **75**, 2340 (1971).
154. Dyke, J. M., and Hush, N. S., *J. Electroanal. Chem.* **36**, 337 (1972).
155. Eastman, D. E., Holtzberg, F., and Methfessel, S., *Phys. Rev. Lett.* **23**, 226 (1969).
155a. Eastman, E. D., Brewer, L., Bromley, L. A., Gilles, P. W., and Lofgren, N. L., *J. Am. Chem. Soc.* **72**, 2248 (1950).
156. Eick, H. A., Baenziger, N. C., and Eyring, L., *J. Am. Chem. Soc.* **78**, 5147 (1956).
157. Eick, H. A., and Gilles, P. W., *J. Am. Chem. Soc.* **81**, 5030 (1959).
158. Ekstrom, A., and Johnson, D. A., *J. Inorg. Nucl. Chem.* **36**, 2557 (1974).
159. Eschenfelder, A. H., *J. Appl. Phys.* **41**, 1372 (1970).
160. Espenson, J. H., and Christensen, R. J., *J. Am. Chem. Soc.* **91**, 7311 (1969).
161. Étourneau, J., Mercurio, J., Naslain, R., and Hagenmuller, P., *J. Solid State Chem.* **2**, 332 (1970).
162. Evans, D. F., Fazakerly, G. V., and Phillips, R. F., *J. Chem. Soc. A* p.1931 (1971).

163. Evans, R. C., "An Introduction to Crystal Chemistry," 2nd ed., Cambridge Univ. Press, London and New York, 1966.
164. Eyring, L., and Holmberg, E., *Adv. Chem. Ser.* **39**, 46 (1963).
165. Eyring, L., Lohr, H. R., and Cunningham, B. B., *J. Am. Chem. Soc.* **74**, 1186 (1952).
166. Faircloth, R. L., Flowers, R. H., and Pummery, F. C. W., *J. Inorg. Nucl. Chem.* **30**, 499 (1968).
167. Faktor, M. M., and Hanks, R., *J. Inorg. Nucl. Chem.* **31**, 1649 (1969).
168. Fan, G. Y., and Greiner, J. H., *J. Appl. Phys.* **39**, 1216 (1968).
169. Fan, G. Y., and Greiner, J. H., *J. Appl. Phys.* **41**, 1401 (1970).
170. Farragi, M., and Feder, A., *Inorg. Chem.* **12**, 236 (1973).
171. Farragi, M., and Feder, A., *J. Chem. Phys.* **56**, 3294 (1972).
172. Farragi, M., and Tendler, Y., *J. Chem. Phys.* **56**, 3287 (1972).
172a. Feistel, G. R., and Mathai, T. P., *J. Am. Chem. Soc.* **90**, 2988 (1968).
173. Felmlee, T. L., and Eyring, L., *Inorg. Chem.* 7, 660 (1968).
174. Ferguson, R. E., Guth, E. D., and Eyring, L., *J. Am. Chem. Soc.* **76**, 3890 (1954).
175. Ferguson, R. E., Guth, E. D., and Eyring, L., *J. Am. Chem. Soc.* **76**, 3892 (1954).
176. Fischel, N. A., and Eick, H. A., *J. Inorg. Nucl. Chem.* **33**, 1198 (1971).
177. Fischel, N. A., Haschke, J. M., and Eick, H. A., *Inorg. Chem.* **9**, 413 (1970).
178. Fischer, P., Haelg, W., Von Wartenburg, W., Schwob, P., and Vogt, O., *Phys. Kondens. Mater.* **9**, 249 (1969).
179. Fischer, E. O., and Fischer, H., *Angew. Chem.* **76**, 52 (1964).
180. Fischer, E. O., and Fischer, H., *J. Organomet. Chem.* **3**, 181 (1965).
181. Fisk, Z., *Phys. Lett. A* **34**, 261 (1971).
182. Fitzgibbon, G. C., and Holley, C. E., *J. Chem. Eng. Data* **13**, 63 (1968).
183. Flahaut, J., *Inorg. Chem. Ser. One* **10**, 189–241 (1972).
184. Flauhaut, J., *Prog. Sci. Technol. Rare Earths* **3**, 209–283 (1968).
185. Flahaut, J., and Laruelle, P., *Prog. Sci. Technol. Rare Earths* **3**, 149–208 (1968).
186. Fong, F. K., *Prog. Solid State Chem.* **3**, 135 (1967).
187. Fred, M., *Adv. Chem. Ser.* **71**, 188 (1967).
188. Freehouf, J. L., Eastman, D. E., Grobman, W. D., Holtzberg, F., and Torrance, J. B., *Phys. Rev. Lett.* **33**, 161 (1974).
189. Fried, S., and Cohen, D., *Inorg. Nucl. Chem. Lett.* **4**, 611 (1968).
190. Friedman, H. A. Stokely, J. R., and Barbarz, R. D., *Inorg. Nucl. Chem. Lett.* 8, 433 (1972).
191. Frisbee, R. H., and Senozan, N. M., *J. Chem. Phys.* **57**, 1248 (1972).
192. Ganopol'skii, V. I., Barkovskii, V. F., and Ipatova, N. P., *Zh. Prikl. Spektrosk.* **5**, 805 (1966).
193. Garton, G., and Hukin, D. A., *in* "Rare Earth Research" (K. Vorres, ed.) Vol. 2, p.3. Gordon & Breach, New York, 1964.
194. Gasgnier, M., Ghys, J., Schiffmacher, G., La Blanchetais, C. H., Caro, P. E., Boulesteix, C., Loier, C., and Pardo, B., *J. Less-Common Met.* **34**, 131 (1974).
195. Geballe, T. H., Matthias, B. T., Andres, K., Maita, J. P., Cooper, A. S., and Corenzwit, E., *Science* **160**, 1443 (1968).
196. Gebelt, R. E., and Eick, H. A., *Inorg. Chem.* **3**, 335 (1964).
197. Gebelt, R. E., and Eick, H. A., *J. Chem. Phys.* **44**, 2872 (1966).
198. Goodenough, J. B., "Magnetism and the Chemical Bond," p. 149. Wiley (Interscience), New York, 1963.
199. Gorter, E. W., *J. Appl. Phys.* **34**, 1253 (1963).
200. Greedan, J. E., *J. Cryst. Growth* **6**, 119 (1970).
201. Greedan, J. E., *J. Phys. Chem. Solids* **32**, 819 (1971).
202. Greedan, J. E., McCarthy, G. J., and Sipe, C., *Inorg. Chem.* **14**, 775 (1975).

203. Greiner, J. D., Smith, J. F., Corbett, J. D., and Jelinek, F. J., *J. Inorg. Nucl. Chem.* **28**, 971 (1966).
204. Greiner, J. H., and Fan, G. J., *Appl. Phys. Lett.* **9**, 27 (1966).
205. Griffith, J. S., *J. Inorg. Nucl. Chem.* **3**, 15 (1956).
206. Griffith, J. S., "The Theory of Transition Metal Ions," pp. 99–101. Cambridge Univ. Press, London and New York, 1961.
207. Groll, G., *Phys. Lett. A* **32**, 99 (1970).
208. Gruen, D. M., Koehler, W. C., and Katz, J. J., *J. Am. Chem. Soc.* **73**, 1475 (1951).
209. Gschneidner, K. G., "Rare Earth Alloys." Van Nostrand-Reinhold, Princeton, New Jersey, 1961.
210. Guerci, C. F., Moruzzi, V. L., and Teaney, D. T., *Bull. Am. Phys. Soc.* **9**, 225 (1964).
211. Guerci, C. F., and Shafer, M. W., *J. Appl. Phys.* **37**, 1406 (1966).
212. Guittard, M., and Benacerraf, A., *C. R. Hebd. Seances Acad. Sci.* **248**, 2589 (1959).
213. Guntherodt, G., and Wachter, P., *Surf. Sci.* **37**, 288 (1973).
214. Guth, E. D., and Eyring, L., *J. Am. Chem. Soc.* **76**, 5242 (1954).
215. Guth, E. D., Holden, J. R., Baenziger, N. C., and Eyring, L., *J. Am. Chem. Soc.* **76**, 5239 (1954).
216. Haas, C., *Crit. Rev. Solid State Sci.* **1**, 47 (1970).
217. Hacker, H., Shimada, Y., and Chung, K. S., *Phys. Status Solidi A* **4**, 459 (1971).
218. Hadenfeldt, C., Jacobs, H., and Juza, R., *Z. Anorg. Allg. Chem.* **379**, 144 (1970).
219. Hadenfeldt, C., and Juza, R., *Naturwissenschaften* **56**, 282 (1969).
220. Haire, R. G., and Asprey, L. B., *Inorg. Nucl. Chem. Lett.* **9**, 869 (1973).
221. Hampson, G. C., and Pauling, L., *J. Am. Chem. Soc.* **60**, 2702 (1938).
222. Hardcastle, K. I., and Warf, J. C., *Inorg. Chem.* **5**, 1728 (1966).
223. Hariharan, A. V., and Eick, H. A., *High Temp. Sci.* **4**, 91 (1972).
224. Hariharan, A. V., and Eick, H. A., *High Temp. Sci.* **4**, 379 (1972).
225. Hariharan, A. V., Fishel, N. A., and Eick, H. A., *High Temp. Sci.* **4**, 405 (1972).
226. Haschke, J. M., and Clark, R. M., *High Temp. Sci.* **4**, 386 (1972).
227. Haschke, J. M., and Eick, H. A., *J. Am. Chem. Soc.* **92**, 1526 (1970).
228. Haschke, J. M., and Eick, H. A., *J. Inorg. Nucl. Chem.* **32**, 2153 (1970).
229. Haschke, J. M., and Eick, H. A., *J. Phys. Chem.* **72**, 1697 (1968).
230. Haschke, J. M., and Eick, H. A., *J. Phys. Chem.* **72**, 4235, (1968).
231. Haschke, J. M., and Eyring, L., *Inorg. Chem.* **10**, 2267 (1971).
232. Hass, Y., Stein, G., and Tenne, R., *Isr. J. Chem.* **10**, 529 (1972).
233. Hastie, J. W., Hauge, R. H., and Margrave, J. L., *High Temp. Sci.* **3**, 56 (1971).
234. Haug, H. O., and Haussmann, K., *Nucl. Sci. Abstr.* **25**, 31889 (1971).
235. Hayes, R. G., and Thomas, J. L., *J. Am. Chem. Soc.* **91**, 6876 (1969).
236. Heckman, R. C., Rep. SC-RR-69-571 (USAEC), Sandia Corp. Albuquerque, New Mexico, 1969.
237. Henderson, A. J., Brown, G. R., Reed, T. B., and Meyer, H., *J. Appl. Phys.* **41**, 946 (1970).
238. Hirst, L. L., *J. Phys. Chem. Solids* **35**, 1285 (1974).
239. Hirst, L. L., *Phys. Kondens. Mater.* **11**, 255 (1970).
240. Hoefdraad, H. E., *J. Inorg. Nucl. Chem.* **37**, 1917 (1975).
241. Hohmann, E., and Bommer, H., *Z. Anorg. Allg. Chem.* **248**, 383 (1941).
242. Holleck, L., and Noddack, W., *Angew. Chem.* **50**, 819 (1937).
243. Holley, C. E., Huber, E. J., and Baker, F. B., *Prog. Sci. Technol. Rare Earths* **3**, 343 (1968).
244. Holmes, L., and Schieber, M., *J. Appl. Phys.* **37**, 968 (1966).
245. Holmes, L., and Schieber, M., *Phys. Rev.* **167**, 449 (1968).
246. Holtzberg, F., and Methfessel, S. I., Fr. Patent, 1,437,063 (1966).

247. Holtzberg, F., and Torrance, J. B., *AIP Conf. Proc.* **5**, 860 (1971).
248. Honig, J. M., Cella, A. A., and Cornwell, J. C., *in* "Rare Earth Research" (K. S. Vorres, ed.), Vol. 2, p.555. Gordon & Breach, New York, 1964.
249. Hoppe, R., *Bull. Soc. Chim. Fr.* p. 1115 (1965).
250. Hoppe, R., and Lidecke, W., *Naturwissenschaften* **49**, 255 (1962).
251. Hoppe, R., and Liebe, W., *Z. Anorg. Allg. Chem.* **313**, 221 (1961).
252. Hoppe, R., and Rödder, K. M., *Z. Anorg. Allg. Chem.* **312**, 277 (1961).
253. Hoppe, R., and Rödder, K. M., *Z. Anorg. Allg. Chem.* **313**, 154 (1961).
254. Hoppe, R., and Seeger, K., *Naturwissenschaften* **55**, 297 (1968).
255. Hoskins, B. F., and Martin, R. L., *J. Chem. Soc., Dalton Trans.* 576 (1975).
256. Howell, J. K., and Pytlewski, L. L., *Inorg. Nucl. Chem. Lett.* **6**, 681 (1970).
257. Howell, J. K., and Pytlewski, L. L., *J. Less-Common Met.* **18**, 437 (1969).
258. Howell, J. K., and Pytlewski, L. L., *J. Less-Common Met.* **19**, 399 (1969).
259. Huber, E. J., and Holley, C. E., *J. Chem. Thermodyn.* **1**, 307 (1969)
260. Huber, E. J., and Holley, C. E., *J. Chem. Thermodyn.* **2**, 896 (1970).
261. Huffner, S., Kienle, P., Quitman, D., and Brix, P., *Z. Phys.* **187**, 67 (1965).
262. Hulet, E. K., Lougheed, R. W., Brady, J. D., Stone, R. E., and Coops, M. S., *Science* **158**, 486 (1967).
263. Hulet, E. K., Wild, J. F., Lougheed, R. W., and Hayes, W. N., Rep. UCRL-738-43 Univ. of California Lawrence Radiation Lab, 1972.
264. Hulliger, F., *Solid State Commun.* 8, 1477 (1970).
265. Hurst, H. J., and Taylor, J. C., *Acta Crystallogr., Sect. B* **26**, 417 (1970).
266. Hurst, H. J., and Taylor, J. C., *Acta Crystallogr., Sect. B* **26**, 2136 (1970).
267. Hurych, Z., Wang, C. C., and Wood, C., *Phys. Lett.* A **34**, 291 (1971).
268. Hyde, B. G., Bevan, D. J. M., and Eyring, L., *Philos. Trans. R. Soc. London, A Ser.* **259**, 583 (1966).
269. Hyde, B. G., and Eyring, L., *in* "Rare Earth Research" (L. Eyring, ed.), Vol. 3, p. 623. Gordon & Breach, New York, 1965.
270. Hyde, B. G., Garver, E. E., Kuntz, U. E., and Eyring, L., *J. Phys. Chem.* **69**, 1667 (1965).
271. Iandelli, A., *in* "Rare Earth Research" (E. V. Kleber, ed.), Vol. 1, p. 135. Macmillan, New York, 1961.
272. Jacobson, A., Tofield, B. C., and Fender, B. E. F., *Acta Crystallogr., Sect. B* **28**, 956 (1972).
273. Jantsch, G., *Naturwissenschaften* **18**, 155 (1930).
274. Jantsch, G., Alber, H., and Grubitsch, H., *Monatsch. Chem.* **53–4**, 305 (1929).
275. Jantsch, G., and Klemm, W., *Z. Anorg. Allg. Chem.* **216**, 80 (1933).
276. Jantsch, G., and Klemm, W., *Z. Anorg. Allg. Chem.* **216**, 82 (1933).
277. Jantsch, G., Rüping, H., and Kunze, W., *Z. Anorg. Allg. Chem.* **161**, 210 (1927).
278. Jantsch, G., and Skalla, N., *Z. Anorg. Allg. Chem.* **193**, 391 (1930).
279. Jantsch, G., Skalla, N., and Grubitsch, H., *Z. Anorg. Allg. Chem.* **212**, 65 (1933).
280. Jantsch, G., Skalla, N., and Grubitsch, H., *Z. Anorg. Allg. Chem.* **216**, 75 (1933).
281. Jantsch, G., Skalla, N., and Jawurek, H., *Z. Anorg. Allg. Chem.* **201**, 207 (1932).
282. Jayaraman, A., *Phys. Rev. Lett.* **29**, 1674 (1972).
283. Jayaraman, A., Dernier, P., and Longinotti, L. D., *Phys. Rev. B* **11**, 2783 (1975).
284. Jayaraman, A., Narayanamurti, V., Bucher, E., and Maines, R. G., *Phys. Rev. Lett.* **25**, 368 (1970).
285. Jayaraman, A., Narayanamurti, V., Bucher, E., and Maines, R. G. *Phys. Rev. Lett.* **25**, 1430 (1970).
286. Jayaraman, A., Singh, A. K., Chaterjee, A., and Usha Devi, S., *Phys. Rev. B* **9**, 2513 (1974).

287. Jensen, N. L., and Hoffman, C. J., *in* "Rare Earth Research" (L. Eyring, ed.), Vol. 3, p. 485. Gordon & Breach, New York, 1965.
288. Johnson, D. A., "Some Thermodynamic Aspects of Inorganic Chemistry," Chapter 6. Cambridge Univ. Press, London and New York, 1968.
289. Johnson, D. A., *J. Chem. Soc. A* p. 1525 (1969).
290. Johnson, D. A., *J. Chem. Soc. A* p. 1529 (1969).
291. Johnson, D. A., *J. Chem. Soc. A* p. 2578 (1969).
292. Johnson, D. A., *J. Chem. Soc., Dalton Trans.* p. 1671 (1974).
293. Johnson, D. A., and Corbett, J. D., *Colloq. Inte. CNRS* **180**, 429 (1970).
294. Johnson, K. E., McKenzie, J. R., and Sandoe, J. N., *J. Chem. Soc. A* p. 2644 (1968).
295. Johnson, K. E., and Sandoe, J. N., *J. Chem. Soc. A* p. 1694 (1969).
296. Johnson, K. E., and Sandoe, J. N., *Mol. Phys.* **14**, 595 (1968).
297. Jørgensen, C. K., *in* "Halogen Chemistry" (V. Guttman, ed.), Vol. 1, pp. 329–330. Academic Press, New York, 1967.
298. Jørgensen, C. K., *J. Inorg. Nucl. Chem.* **32**, 3127 (1970).
299. Jørgensen, C. K., *Mol. Phys.* **5**, 271 (1962); **7**, 17 (1963) for errata.
300. Jørgensen, C. K., "Orbitals in Atoms and Molecules," pp. 148–150. Academic Press, New York, 1962.
301. Jørgensen, C. K., *Struc. Bonding (Berlin)* **13**, 223 (1973).
302. Juza, R., and Hadenfeldt, C., *Naturwissenschaften* **55**, 229 (1968).
303. Kaiser, E. W., Falconer, W. E., and Klemperer, W., *J. Chem. Phys.* **56**, 5392 (1972).
304. Kaiser, E. W., Sunder, W. A., and Falconer, W. E., *J. Less-Common Met.* **27**, 383 (1972).
305. Kajita, K., and Masumi, T., *Appl. Phys. Lett.* **21**, 332 (1972).
306. Kaldis, W., and Verrault, R., *J. Less-Common Met.* **20**, 177 (1970).
307. Kaldis, E., and Wachter, P., *Solid State Commun.* **11**, 907 (1972).
308. Kapfenberger, W., *Z. Anorg. Allg. Chem.* **238**, 273 (1938).
309. Kapfhammer, W., Maurer, W., Wagner, F. E., and Kienle, P., *Z. Naturforsch. A* **26**, 357 (1971).
310. Kapustiniskii, A. F., *Q. Rev. Chem. Soc.* **10**, 283 (1956).
311. Kasuya, T., *Prog. Theor. Phys.* **16**, 45 (1956).
312. Katz, J. J., and Seaborg, G. T., "The Chemistry of the Actinide Elements," p. 419. Methuen, London, 1957.
313. Kaufman, M., Muenter, J., and Klemperer, W., *J. Chem. Phys.* **47**, 3365 (1967).
314. Keenan, T. K., and Asprey, L. B., *Inorg. Chem.* **8**, 235 (1969).
314a. Kenshea, F. J., and Cubiciotti, D., *J. Chem. Eng. Data* **6**, 507 (1961).
315. Kern, S., *J. Chem. Phys.* **40**, 208 (1964).
316. Kirk, J. L., Vedam, K., Narayanamurti, V., Jayaraman, A., and Bucher, E., *Phys. Rev. B* **6**, 3023 (1972).
317. Kirshenbaum, A. D., and Cahill, J. A., *J. Inorg. Nucl. Chem.* **14**, 148 (1960).
318. Klemm, W., *Z. Anorg. Allg. Chem.* **184**, 345 (1929).
319. Klemm, W., *Z. Anorg. Allg. Chem.* **187**, 29 (1930).
320. Klemm, W., *Z. Anorg. Allg. Chem.* **209**, 321 (1932).
321. Klemm, W., and Döll, W., *Z. Anorg. Allg. Chem.* **241**, 233 (1939).
322. Klemm, W., and Henkel, P., *Z. Anorg. Allg. Chem.* **220**, 180 (1934).
323. Klemm, W., and Rockstroh, J., *Z. Anorg. Allg. Chem.* **176**, 181 (1928).
324. Klemm, W., and Schuth, W., *Z. Anorg. Allg. Chem.* **184**, 352 (1929).
325. Klemm, W., and Senff, H., *Z. Anorg. Allg. Chem.* **241**, 259 (1939).
326. Klemm, W., and Senff, H., *Z. Anorg. Allg. Chem.* **242**, 92 (1939).
327. Kokoszka, G. F., and Mammano, N. J., *J. Solid State Chem.* **1**, 227 (1969).
328. Komaru, T., Hihara, T., and Koi, Y., *J. Phys. Soc. Jpn.* **31**, 1391 (1971).

329. Kordis, J., and Gingerich, K. A., *J. Phys. Chem.* **77**, 700 (1973).
330. Kornblit, A., Ahlers, G., and Buehler, E., *Phys. Lett. A* **43**, 531 (1973).
331. Korst, W. L., and Warf, J. C., *Acta Crystallogr.* **9**, 452 (1956).
332. Korst, W. L., and Warf, J. C., *Inorg. Chem.* **5**, 1719 (1966).
333. Kumar, J., and Srivastava, O. N., *Jpn. J. Appl. Phys.* **11**, 118 (1972).
334. Kunz, A. H., *J. Am. Chem. Soc.* **53**, 98 (1931).
335. Kuznia, C., and Kneer, G., *Phys. Lett. A* **27**, 664 (1968).
336. La Blanchetais, C. H., *J. Rech. CNRS* **29**, 103 (1954).
337. Laitinen, H. A., *J. Am. Chem. Soc.* **64**, 1133 (1942).
338. Laitinen, H. A. and Taebel, W. A., *Ind. Eng. Chem. Anal. Ed.* **13**, 825 (1941).
339. Lang, G., *Z. Anorg. Allg. Chem.* **348**, 246 (1966).
340. Latimer, W. M., "The Oxidation States of the Elements and their Potentials in Aqueous Solution," 2nd ed., p. 42. Prentice-Hall, New York, 1952.
341. Lee, K., Muir, H., and Catalano, E., *J. Phys. Chem. Solids* **26**, 523 (1965).
342. Libowitz, G. G., *Ber. Bunsenges. Phys. Chem.* **76**, 837 (1972).
343. Libowitz, G. G., *Inorg. Chem. Ser. One*, **10**, 79 (1972).
344. Llinares, C., Monteil, E., Bordure, G., and Paparoditis, C., *Solid State Commun.* **13**, 205 (1973).
345. Lochner, U., and Corbett, J. D., *Inorg. Chem.* **14**, 426 (1975).
346. Logfren, K.-E., Tuomi, T., and Stubb, T., *Solid State Commun.* **14**, 1285 (1974).
347. Lokken, D. A., and Corbett, J. D., *J. Am. Chem. Soc.* **92**, 1799 (1970).
348. Lokken, D. A., and Corbett, J. D., *Inorg. Chem.* **12**, 556 (1973).
349. Longuet-Higgins, H. C., and Roberts, M. de V., *Proc. R. Soc. London* **224**, 336 (1954).
350. McCarthy, G. J., and Greedan, J. E., *Inorg. Chem.* **14**, 772 (1975).
351. McCarthy, G. J., and White, W. B., *J. Less-Common Met.* **22**, 409 (1970).
352. MacChesney, J. B., Williams, H. J., Sherwood, R. C., and Potter, J. F., *J. Chem. Phys.* **41**, 3177 (1964).
353. MacChesney, J. B., Williams, H. J., Sherwood, R. C., and Potter, J. F., *J. Chem. Phys.* **44**, 596 (1966).
354. McClure, D. S., and Kiss, Z., *J. Chem. Phys.* **39**, 3251, (1963).
355. McClure, J. W., *J. Phys. Chem. Solids* **24**, 871 (1963).
356. McColm, I. J., and Thompson, S., *J. Inorg. Nucl. Chem.* **34**, 3801 (1972).
357. McCoy, H. N., *J. Am. Chem. Soc.* **58**, 1577 (1936).
358. McCoy, H. N., *J. Am. Chem. Soc.* **59**, 1131 (1937).
359. McCoy, H. N., *J. Am. Chem. Soc.* **61**, 2455 (1939).
360. McCullough, J. D., *J. Am. Chem. Soc.* **72**, 1386 (1950).
361. McGuire, T. R., Argyle, B. E., Shafer, M. W., and Smart, J. S., *Appl. Phys. Lett.* **1**, 18 (1962).
362. McGuire, T. R., Argyle, B. E., Shafer, M. W., and Smart, J. S., *J. Appl. Phys.* **34**, 1345 (1963).
363. McGuire, T. R., Holtzberg, F., and Joenk, R. J., *J. Phys. Chem. Solids* **29**, 410 (1968).
364. McGuire, T. R., and Shafer, M. W., *J. Appl. Phys.* **35**, 984 (1964).
365. McGuire, T. R., Torrance, J. B., and Shafer, M. W., *AIP Conf. Proc.* **10**, 1289 (1973).
366. Mackey, J. L., Powell, J. E., and Spedding, F. H., *J. Am. Chem. Soc.* **84**, 2047 (1962).
367. McMasters, O. D., Gschneidner, K. A., Kaldis, E., and Sampietro, G., *J. Chem. Thermodyn.* **6**, 845 (1974).
368. Magnéli, A., *Acta Crystallogr.* **6**, 495 (1953).
369. Malý, J., *Inorg. Nucl. Chem. Lett.* **3**, 373 (1967).

370. Malý, J., *J. Inorg. Nucl. Chem.* **31**, 741 (1969).
371. Malý, J., *J. Inorg. Nucl. Chem.* **31**, 1007 (1969).
372. Malý, J., and Cunningham, B. B., *Inorg. Nucl. Chem. Lett.* **3**, 445 (1967).
373. Maple, M. B., and Wohlleben, D., *Phys. Rev. Lett.* **27**, 511 (1971).
374. Marsh, J. K., *J. Chem. Soc.* p. 398 (1942).
375. Marsh, J. K., *J. Chem. Soc.* p. 531 (1943).
376. Marsh, J. K., *J. Chem. Soc.* p. 20 (1946).
377. Martin, R. L., *J. Chem. Soc., Dalton Trans.* p. 1335 (1974).
378. Martin, R. L., *Nature (London)* **165**, 202 (1950).
379. Masset, F., *Phys. Rev. B* **3**, 2364 (1971).
380. Masset, F., and Callaway, J., *Phys. Rev. B* **2**, 3657 (1970).
381. Matignon, C. A., and Cazes, E., *Ann. Chim. Phys.* [8] **8**, 417 (1906).
382. Matignon, C. A., and Cazes, E., *C. R. Hebd. Seances Acad. Sci.* **142**, 83 (1906).
383. Matthias, B. T., *Phys. Lett. A* **27**, 511 (1968).
384. Matthias, B. T., Bozorth, R. M., and Van Vleck, J. H., *Phys. Rev. Lett.* **7**, 160 (1961).
385. Matthias, B. T., Geballe, T. H., Andres, K., Corenznit, E., Hull, G. W., and Maita, J. P., *Science* **159**, 530 (1968).
386. Mayer, I., Fischbein, E., and Cohen, S., *J. Solid State Chem.* **14**, 307 (1975).
387. Mee, J. E., and Corbett, J. D., *Inorg. Chem.* **4**, 88 (1965).
388. Meier, D. J., and Garner, C. S., *J. Phys. Chem.* **56**, 853 (1952).
388a. Mellors, G. W., and Senderoff, S., *J. Phys. Chem.* **63**, 1110 (1959).
389. Menth, A., Buehler, E., and Geballe, T. H., *Phys. Rev. Lett.* **22**, 295 (1969).
390. Messer, C. E., Cho, T. Y., and Gibb, T. R. G., *J. Less-Common Met.* **12**, 411 (1967).
391. Messer, C. E., Eastman, J. C., and Mers, R. G., *Inorg. Chem.* **3**, 776 (1964).
392. Messer, C. E., and Granoukos, P. C., *J. Less-Common Met.* **15**, 377 (1968).
393. Messer, C. E., and Hardcastle, K., *Inorg. Chem.* **3**, 1327 (1964).
394. Messer, C. E., and Levy, I. S., *Inorg. Chem.* **4**, 543 (1965).
395. Methfessel, S., *Z. Angew. Phys.* **18**, 414 (1965).
396. Methfessel, S., and Mattis, D. C., *in* "Encyclopaedia of Physics" (S. Flugge, ed.), Vol. 18, p. 511. Springer-Verlag, Berlin and, New York, 1968.
397. Mikheev, N. B., D'yachkova, R. A., Telegina, L. I., and Rosenkevich, N. A., *Zh. Neorg. Khim.* **17**, 2052 (1972).
398. Mikheev, N. B., and Rumer, I. A., *Radiokhimiya* **14**, 492 (1972).
399. Mikheev, N. B., Spitsyn, V. I., Kamenskaya, A. N., Gvozdev, B. A., Druin, V. A., Rumer, I. A., Dyachkova, R. A., Rosenkevitch, N. A., and Auerman, L. N., *Inorg. Nucl. Chem. Lett.* **8**, 929 (1972).
400. Mikheev, N. B., Spitsyn, V. I., Kamenskaya, A. N., Rosenkevich, N. A., Rumer, I. A., and Auerman, L. N., *Inorg. Nucl. Chem. Lett.* **8**, 869 (1972).
401. Mikler, J., and Auer-Welsbach, H., *Monatsch. Chem.* **96**, 2018 (1965).
402. Mioduski, T., and Siekierski, S., *J. Inorg. Nucl. Chem.* **37**, 1647 (1975).
403. Moeller, T., *in* "Comprehensive Inorganic Chemistry," Vol. 4, pp. 28–36. Pergamon, Oxford, 1973.
404. Moeller, T., and Fogel, N., *J. Am. Chem. Soc.* **73**, 4481 (1951).
405. Mordovin, O. A., and Timofeeva, E. N., *Zh. Neorg. Khim.* **13**, 3155 (1968).
406. Morss, L. R., *J. Phys. Chem.* **75**, 392 (1971).
407. Morss, L. R., and Haug, H. O., *J. Chem. Thermodyn.* **5**, 513 (1973).
408. Morss, L. R., and McCue, M. C., *Inorg. Chem.* **14**, 1624 (1975).
409. Moruzzi, V. L., and Teaney, D. T., *Solid State Commun.* **1**, 127 (1963).
410. Mueller, W. M., Blackledge, J. P., and Libowitz, G. G., *in* "Metal Hydrides" (W. M. Mueller, ed.), Chapter 9. Academic Press, New York, 1968.
411. Murphy, E., and Toogood, G. E., *Inorg. Nucl. Chem. Lett.* **7**, 755 (1971).

412. Mustachi, A., *J. Phys. Chem. Solids* **35**, 1447 (1974).
413. Myasoedov, B. F., Lebeder, I. A., Mikhailov, V. M., and Frenkel, V. Y., *Radiochem. Radioanal. Lett.* **17**, 359 (1974).
414. Nagai, S., Shinmei, M., and Yokokawa, T., *J. Inorg. Nucl. Chem.* **36**, 1904 (1974).
415. Narayanamurti, V., Jayaraman, A., and Bucher, E., *Phys. Rev. B* **9**, 2521 (1974).
416. Nelson, P. G., Ph.D. Thesis, Cambridge University (1962).
417. Nelson, P. G., and Sharpe, A. G., *J. Chem. Soc. A* p. 501 (1966).
418. Nereson, N. G., Olsen, G. E., and Arnold, G. P., *Phys. Rev.* **127**, 2101 (1962).
419. Nickerson, C. J., White, R. M., Lee, K. N., Bachmann, R., Geballe, T. H., and Hull, G. W., *Phys. Rev. B* **3**, 2030 (1971).
420. Nihara, K., *Bull. Chem. Soc. Jpn.* **44**, 963 (1971).
421. Noyes, A. A., and Garner, C. S., *J. Am. Chem. Soc.* **58**, 1265 (1936).
422. Nugent, L. J., *Inorg. Chem. Ser. Two*, **7**, 195 (1975).
423. Nugent, L. J., *J. Inorg. Nucl. Chem.* **32**, 3485 (1970).
424. Nugent, L. J., Baybarz, R. D., and Burnett, J. L., *J. Phys. Chem.* **73**, 1177 (1969).
425. Nugent, L. J., Baybarz, R. D., Burnett, J. L., and Ryan, J. L., *J. Inorg. Nucl. Chem.* **33**, 2503 (1971).
426. Nugent, L. J., Baybarz, R. D., Burnett, J. L., and Ryan, J. L., *J. Phys. Chem.* **77**, 1528 (1973).
427. Nugent, L. J., and Vander Sluis, K. L., *J. Opt. Soc. Am.* **61**, 1112 (1971).
428. Oesterreicher, H., Mammano, N., and Sienko, M. J., *J. Solid State Chem.* **1**, 10 (1969).
429. Oliver, M. R., Dimmock, J. O., McWhorter, A. L., and Reed, T. B., *Phys. Rev. B* **5**, 1078 (1972).
430. Oliveira, N. F., Foner, S., Shapira, Y., and Reed, T. B., *Phys. Rev. B* **5**, 2634 (1972).
431. Paderno, Y. B., Pokrzynnicki, S., and Stalinski, B., *Phys. Status Solidi* **24**, K73 (1967).
432. Paderno, Y. B., and Samsonov, G. V., *Dokl. Akad. Nauk SSSR* **137**, 646 (1960).
433. Pagel, H. A., and Brinton, P. H. M., *J. Am. Chem. Soc.* **51**, 42 (1929).
434. Pajakoff, S., *Monatsch. Chem.* **94**, 482 (1963).
435. Pajakoff, S., *Monatsch. Chem.* **94**, 527 (1963).
436. Pajakoff, S., *Monatsch. Chem.* **97**, 733 (1966).
437. Pajakoff, S., *Monatsch. Chem.* **99**, 484 (1968).
438. Paletta, E., and Hoppe, R., *Naturwissenschaften* **53**, 611 (1966).
439. Parker, F. T., and Kaplan, M., *Chem. Phys. Lett.* **23**, 437 (1973).
440. Parker, F. T., and Kaplan, M., *Chem. Phys. Lett.* **24**, 280 (1974).
441. Parker, F. T., and Kaplan, M., *Phys. Rev. B* 8, 4318 (1973).
442. Parker, V. B., Wagman, D. D., and Evans, W. H., *Natl. Bur. Stand. (U.S.), Tech. Note* **270–6** (1971).
443. Pauling, L., *J. Am. Chem. Soc.* **59**, 1132 (1937).
444. Pearce, D. W., *Chem. Rev.* **16**, 121 (1935).
445. Penney, T., Shafer, M. W., and Torrance, J. B., *Phys. Rev. B* **5**, 3669 (1972).
446. Peppard, D. F., Bloomquist, C. A. A., Horowitz, E. P., Lewey, S., and Mason, G. W., *J. Inorg. Nucl. Chem.* **32**, 339 (1970).
447. Perros, T. P., Munson, T. R., and Naeser, C. R., *J. Chem. Educ.* **30**, 402 (1953).
448. Perros, T. P., and Naeser, C. R., *J. Am. Chem. Soc.* **74**, 3694 (1952).
449. Peterson, J. R., and Baybarz, R. D., *Inorg. Nucl. Chem. Lett.* **8**, 423 (1972).
450. Peterson, J. R., and Cunningham, B. B., *Inorg. Nucl. Chem. Lett.* **3**, 327 (1967).
451. Petzel, T., *Inorg. Nucl. Chem. Lett.* **10**, 119 (1974).
452. Petzel, T., and Greis, O., *Z. Anorg. Allg. Chem.* **388**, 137 (1972).
453. Petzel, T., and Greis, O., *Z. Anorg. Allg. Chem.* **396**, 95 (1973).

454. Phillips, C. G. S., and Williams, R. J. P., "Inorganic Chemistry" Vol. 2, Chapter 21. Oxford Univ. Press, London and New York, 1966.
455. Pickart, S. J., and Alperin, H. A., *J. Phys. Chem. Solids* **29**, 414 (1968).
455a. Picon, M., Domange, L., Flahaut, J., Guittard, M., and Patrie, M., *Bull. Soc. Chim. Fr.* p. 221 (1960).
456. Picon, M., and Patrie, M., *C. R. Hebd. Seances Acad. Sci., Ser. C* **242**, 1321 (1956).
457. Pink, H., *Z. Anorg. Allg. Chem.* **353**, 247 (1967).
458. Pink, H., *Z. Anorg. Allg. Chem.* **364**, 248 (1969).
459. Polyachenok, O. G., and Novikov, G. I., *Zh. Neorg. Khim.* **8**, 2818 (1963).
460. Popov, A. I., and Glockler, G., *J. Am. Chem. Soc.* **71**, 4114 (1949).
461. Popov, A. I., and Glockler, G., *J. Am. Chem. Soc.* **74**, 1357 (1952).
462. Popov, A. I., and Wendlandt, W. W., *Proc. Iowa Acad. Sci.* **60**, 300 (1953).
463. Post, B, *in* "Boron, Metallo-Boron Compounds and Boranes" (R. M. Adams, ed.), p. 301. Wiley (Interscience), New York, 1964.
464. Prandtl, W., and Kogl, H., *Z. Anorg. Allg. Chem.* **172**, 265 (1928).
465. Prandtl, W., and Rieder, G., *Z. Anorg. Allg. Chem.* **238**, 225 (1938).
466. Propst, R. C., *J. Inorg. Nucl. Chem.* **36**, 1085 (1974).
467. Quezal-Ambrunaz, S., and Bertaut, E. F., *Solid State Commun.* **11**, 605 (1972).
468. Rabideau, S., *J. Chem. Phys.* **19**, 874 (1951).
469. Racah, G., *Phys. Rev.* **76**, 1352 (1949).
470. Rau, R. C., *Acta Crystallogr.* **20**, 716 (1966).
471. Reid, F. J., Matson, L. K., Miller, J. F., and Himes, R. C., *J. Phys. Chem. Solids* **25**, 969 (1964).
472. Rietschel, E. T., and Baernighausen, H., *Z. Anorg. Allg. Chem.* **368**, 62 (1969).
473. Rodder, K. M., Ph.D. Thesis, Westfalischen, Wilhelms-Universität, Munster, 1963.
474. Rooymans, C. J. M., *Ber. Bunsenges. Phys. Chem.* **70**, 1036 (1966).
475. Rossmanith, K., and Muckenhubar, E., *Monatsch. Chem.* **92**, 600 (1961).
476. Roughan, P. E., and Daane, A. H., Unpublished work cited in ref. 106.
477. Ruderman, M. A., and Kittel, C., *Phys. Rev.* **96**, 99 (1954).
478. Salamon, M., *Solid State Commun.* **13**, 1741 (1973).
479. Sallach, R. A., and Corbett, J. D., *Inorg. Chem.* **2**, 457 (1963).
480. Sallach, R. A., and Corbett, J. D., *Inorg. Chem.* **3**, 993 (1964).
481. Salot, S., and Warf, J. C., *J. Am. Chem. Soc.* **90**, 1932 (1968).
482. Samsonov, G. V., Sorin, L. A., Vlasova, M. V., Shcherbina, V. I., *Dokl. Akad. Nauk SSSR* **178**, 1346 (1968).
483. Sastry, R. L. N., Mehrotra, P. N., and Rao, C. N. R., *J. Inorg. Nucl. Chem.* **28**, 2167 (1966).
484. Sawyer, J. O., Hyde, B. G., and Eyring, L., *Bull. Soc. Chim. Fr.* p. 1190 (1965).
485. Schwab, G. M., and Bohla, F., *Z. Naturforsch. Teil A* **23**, 1555 (1968).
486. Seifert, K., *Fortschr. Mineral.* **45**, 214 (1967).
487. Selwood, P. W., *J. Am. Chem. Soc.* **56**, 2392 (1934).
488. Selwood, P. W., "Magnetochemistry," 2nd ed., pp. 154–157. Wiley (Interscience), New York, 1956.
489. Shafer, M. W., *J. Appl. Phys.* **36**, 1145 (1965).
490. Shafer, M. W., *Mater. Res. Bull.* **7**, 603 (1972).
491. Shafer, M. W., Torrance, J. B., and Penney, T., *J. Phys. Chem. Solids* **33**, 2251 (1972).
492. Shannon, J. R., and Sienko, M. J., *Inorg. Chem.* **11**, 904 (1972).
493. Shapira, Y., and Reed, T. B., *Phys. Rev. B* **5**, 4877 (1972).
494. Sherrill, M. S., King, C. B., and Spooner, R. C., *J. Am. Chem. Soc.* **65**, 170 (1943).
495. Shull, C. G., Strauser, W. A., and Wollan, E. O., *Phys. Rev.* **83**, 333 (1951).

496. Silva, R. J., Sikkeland, T., Nurmia, M., Ghiorso, A., and Hulet, E. K., *J. Inorg. Nucl. Chem.* **31**, 3405 (1969).
497. Simon, W., and Eyring, L., *J. Am. Chem. Soc.* **76**, 5872 (1954).
498. Slaugh, L., *Inorg. Chem.* **6**, 851 (1967).
499. Smeggil, J. G., and Eick, H. A., *Inorg. Chem.* **10**, 1458 (1971).
500. Smoes, S., Coppens, P., Bergman, C., and Drowart, J., *Trans. Faraday Soc.* **65**, 682 (1969).
501. Smith, G. F., and Getz, C. A., *Ind. Eng. Chem. Anal. Ed.* **10**, 191 (1938).
502. Soriano, J., Givon, M., and Shamir, J., *Inorg. Nucl. Chem. Lett.* **2**, 13 (1966).
503. Soriano, J., and Marcus, Y., *Inorg. Chem.* **3**, 901 (1964).
504. Speca, A. N., and Pytlewski, L. L., *J. Less-Common Met.* **22**, 459 (1970).
505. Spedding, F. H., and Daane, A. H., *Metall. Rev.* **5**, 297 (1960).
506. Spedding, F. H., and Daane, A. H., *Trans. Am. Inst. Min., Metall. Pet. Eng.* **212**, 379 (1958).
507. Spedding, F. H., Gschneidner, K., and Daane, A. H., *J. Am. Chem. Soc.* **80**, 4499 (1958).
508. Spitsyn, V. I., Kiselev, Y. M., and Martynenko, L. I., *Zh. Neorg. Khim.* **18**, 1125 (1973).
509. Stalinski, B., *J. Chem. Thermodyn.* **5**, 1 (1973).
510. Staveley, L. A. K., Markham, D. R., and Jones, M. R., *J. Inorg. Nucl. Chem.* **30**, 231 (1968).
511. Stezkowskii, J. J., and Eick, H. A., *Inorg. Chem.* **9**, 1102 (1970).
512. Stokely, J. R., and Baybarz, R. D., Work cited in ref. 425.
513. Stokely, J. R., Baybarz, R. D., and Peterson, J. R., *J. Inorg. Nucl. Chem.* **34**, 392 (1972).
514. Stubblefield, C. T., Eick, H. A., and Eyring, L., *J. Am. Chem. Soc.* **78**, 3018 (1956).
515. Stubblefield, C. T., and Eyring, L., *J. Am. Chem. Soc.* **77**, 3004 (1955).
516. Sugar, J., and Kaufman, V., *J. Opt. Soc. Am.* **55**, 1283 (1965).
517. Sugar, J., and Reader, J., *J. Chem. Phys.* **59**, 2083 (1973).
518. Sugar, J., and Reader, J., *J. Opt. Soc. Am.* **55**, 1286 (1965).
519. Suits, J. C., Argyle, B. E., and Freiser, M. J., *J. Appl. Phys.* **37**, 1391 (1966).
520. Suits, J. C., and Lee, K., *J. Appl. Phys.* **42**, 3258 (1971).
521. Suryanarayanan, R., Ferre, J., and Briat, B., *Phys. Rev. B* **9**, 554 (1974).
522. Sutin, N., *Annu. Rev. Phys. Chem.* **17**, 150 (1966).
523. Swendsen, R. H., *Phys. Rev. B* **5**, 116 (1972).
524. Tanguy, B., Portier, J., Vlasse, M., and Pouchard, M., *Bull. Soc. Chim. Fr.* **3**, 946 (1972).
525. Templeton, D. H., and Dauben, C. H., *J. Am. Chem. Soc.* **76**, 5237 (1954).
526. Thompson, D. S., Hazen, E. E., and Waugh, J. S., *J. Chem. Phys.* **44**, 2954 (1966).
527. Thompson, D. S., Schaefer, D. W., and Waugh, J. S., *Inorg. Chem.* **5**, 325 (1966).
528. Thompson, D. S., Stone, M. J., and Waugh, J. S., *J. Phys. Chem.* **70**, 934 (1966).
529. Thompson, W. A., Penney, T., Kirkpatrick, S., and Holtzberg, F., *Phys. Rev. Lett.* **29**, 779 (1972).
530. Thomsen, J., *Z. Anorg. Allg. Chem.* **9**, 190 (1895).
531. Timnick, A., and Glockler, G., *J. Am. Chem. Soc.* **70**, 1347 (1948).
532. Torrance, J. B., Shafer, M. W., and McGuire, T. R., *Bull. Am. Phys. Soc.* **17**, 315 (1972).
533. Torrance, J. B., Shafer, M. W., and McGuire, T. R., *Phys. Rev. Lett.* **29**, 1168 (1972).
534. Triplett, B. B., Nixon, N. S., Boolchard, P., Hanna, S. S., and Bucher, E., *J. Phys. (Paris) Colloq.* (6) 653 (1974).
535. Urbain, G., and Bourion, F., *C. R. Hebd. Seances Acad. Sci.* **153**, 1155 (1911).

536. Urbain, G., and Jantsch, G., *C. R. Hebd. Seances Acad. Sci.* **146**, 127 (1908).
537. Vagina, N.S., *Zh. Prikl. Khim.* **43**, 47 (1970).
538. Vainshtein, E. E., Blokhin, S. M., and Paderno, Y. B., *Fiz. Tverd. Tela (Leningrad)* **6**, 2909 (1964).
539. Van Houten, S., *Phys. Lett.* **2**, 215 (1962).
540. Van Vleck, J. H., "The Theory of Electric and Magnetic Susceptibilities," Oxford Univ. Press, London and New York, 1932.
541. Van Vleck, J. H., and Frank, A., *Phys. Rev.* **34**, 1494 (1929).
542. Van Vleck, J. H., and Frank, A., *Phys. Rev.* **34**, 1625 (1929).
543. Van Vugt, N., Wigmans T., and Blasse, G., *J. Inorg. Nucl. Chem.* **35**, 2601 (1973).
544. Vander Sluis, K. L., and Nugent, L. J., *J. Chem. Phys.* **60**, 1927 (1974).
545. Vander Sluis, K. L., and Nugent, L. J., *Phys. Rev. A* **6**, 86 (1972).
546. Varga, L. P., and Asprey, L. B., *J. Chem. Phys.* **48**, 139 (1968).
547. Varga, L. P., and Asprey, L. B., *J. Chem. Phys.* **49**, 4674 (1968).
548. Vickery, R. C., and Ruben, A., *J. Chem. Soc.* 510 (1959).
549. Vickery, R. C., Sedlacek, R., and Ruben, A., *J. Chem. Soc.* p. 498 (1959).
550. Vickery, R. C., Sedlacek, R., and Ruben, A., *J. Chem. Soc.* p. 503 (1959).
551. Vickery, R. C., Sedlacek, R., and Ruben, A., *J. Chem. Soc.* p. 505 (1959).
552. Von Dreele, R. B., Eyring, L., Bowman, A. L., and Yarnell, J. L. *Acta Crystallogr., Sect. B* **31**, 971 (1975).
553. Von Scheele, C., *Z. Anorg. Allg. Chem.* **17**, 310 (1898).
554. Von Stackelberg, M., *Z. Electrochem.* **37**, 542 (1931).
555. Von Stackelberg, M., and Neumann, F., *Z. Phys. Chem. B* **19**, 314 (1932).
556. Von Wartenberg, H., *Z. Anorg. Allg. Chem.* **244**, 337 (1940).
557. Von Welsbach, A., *Monatsch. Chem.* **6**, 477 (1885).
558. Wadsley, A. D., *Adv. Chem. Ser.* **39**, 33 (1963).
559. Wagman, D. D., Evans, W. H., Halow, I., Parker, V. B., Bailey, S. M., and Schummn, R. H., *Natl. Bur. Stand. (U.S.) Tech. Note* **270–3**, (1968).
560. Wallace, W. E., *Ber. Bunsenges. Phys. Chem.* **76**, 832 (1972).
561. Wallace, W. E., Kubota, Y., and Zanowick, R. L., *Adv. Chem. Ser.* **39**, 122 (1963).
562. Wang, P. J., and Drickhamer, H., *J. Chem. Phys.* **58**, 4444 (1973).
563. Warf, J. C., and Gutmann, V., *J. Inorg. Nucl. Chem.* **33**, 1583 (1971).
564. Warf, J. C., and Hardcastle, K. I., *Inorg. Chem.* **5**, 1736 (1966).
565. Warf, J. C., and Hardcastle, K. I., *J. Am. Chem. Soc.* **83**, 2206 (1961).
566. Warf, J. C., and Korst, W. L., *J. Phys. Chem.* **60**, 1590 (1956).
567. Warf, J. C., Korst, W. L., and Hardcastle, K. I., *Inorg. Chem.* **5**, 1726 (1966).
568. Waring, R. K., *J. Appl. Phys.* **42**, 1763 (1971).
569. Watt, G. W., and Gillow, E. W., *J. Am. Chem. Soc.* **91**, 775 (1969).
570. Weaver, B., and Stevenson, J. N., *J. Inorg. Nucl. Chem.* **33**, 1877 (1971).
571. Wells, A. F., "Structural Inorganic Chemistry," 3rd ed., Oxford Univ. Press, London and New York, 1962.
572. Werner, A., *Ber.* **38**, 914 (1905).
573. Westrum, E. F., and Beale, A. F., *J. Phys. Chem.* **65**, 353 (1961).
573a. Wharton, L., Berg, R. A., and Klemperer, W., *J. Chem. Phys.* **39**, 2023 (1963).
574. White, H. W., McCollum, D. C., and Callaway, J., *Phys. Lett. A* **25**, 388 (1967).
575. Wickman, H. H., and Catalano, E., *J. Appl. Phys.* **39**, 1248 (1968).
576. Wilbert, Y., Duquesnoy, A., and Marion, F., *C. R. Hebd. Seances Acad. Sci. Ser. C* **271**, 1080 (1970).
577. Wild, R. L., and Archer, R. D., *Bull. Am. Phys. Soc.* **7**, 440 (1962).
578. Will, G., Pickart, S. J., Alperin, H. A., and Nathans, R., *J. Phys. Chem. Solids* **24**, 1679 (1963).

579. Wong, C. C., and Wood, C., *Phys. Lett. A* **34**, 125 (1971).
580. Wood, V. E., *Phys. Lett. A* **37**, 357 (1971).
581. Wybourne, B. G., *J. Opt. Soc. Am.* **55**, 928 (1965).
582. Wyckoff, R. W. G., "Crystal Structures," 2nd ed., Vols. 1–3. Wiley (Interscience), New York, 1963–1965.
583. Yanase, A., and Kasuya, T., *J. Phys. Soc. Jpn.* **25**, 1025 (1968).
584. Yanir, E., Givon, M., and Marcus, Y., *Inorg. Nucl. Chem. Lett.* **6**, 415 (1970).
584a. Yntema, L. F., *J. Am. Chem. Soc.* **52**, 2782 (1930).
585. Yosida, K., *Phys. Rev.* **106**, 893 (1957).
586. Zachariasen, W. H., *Acta Crystallogr.* **1**, 265 (1948).
587. Zachariasen, W. H., *Acta Crystallogr.* **2**, 388 (1949).
588. Zachariasen, W. H., *Acta Crystallogr.* **7**, 792 (1954).
589. Zanowick, R. L., and Wallace, W. E., *Phys. Rev.* **126**, 537 (1962).
590. Zhuze, V. P., Golubkov, A. V., Goncharova, E. V., Komarova, T. I., and Sergeeva, V. M., *Fiz. Tverd. Tela (Leningrad)* **6**, 268 (1964).
591. Zhuze, V. P., Goncharova, E. V., Kartenko, N. F., Komarova, T. I., Parfeneva, L. S., Sergeeva, V. M., and Smirnov, I. A., *Phys. Status Solidi A* **18**, 63 (1973).
592. Zintl, E., and Morawietz, W., *Z. Anorg. Allg. Chem.* **245**, 26 (1940).
593. Zwickel, A., and Taube, H., *J. Am. Chem. Soc.* **83**, 793 (1961).

Appendix

This appendix mentions some of the work published since the review was completed. The only references that are included are those relevant to the general theoretical ideas emphasized in the main text.

Dr. L. R. Morss very kindly sent me a preprint of his detailed review of lanthanide thermochemistry (*5*). This includes his as yet unpublished experimental values of ΔH_f^0 ($SmCl_2$, s) and ΔH_f^0($DyCl_2$, s). These values agree closely with those plotted in Fig. 23, and they lead to values of ΔG^0 (Eq. 15) in substantial agreement with the estimates in Table XX.

As suggested on p. 4, $NdBr_2$ is readily obtained by reproportionation. The compound is leaf-green and has the $PbCl_2$ structure. Its magnetic properties (*4*) resemble those described for other neodymium dihalides.

Evidence relevant to the stability sequences advanced in the main text includes the observation that PrF_4 loses fluorine at temperatures as low as 90°C (*3*), and the fact that unlike BkF_4, CfF_4 loses fluorine at room temperature (*2*).

Haschke (*1*) has obtained the cell parameters of the strontium dibromide form of $SmBr_2$. He found $a_0 = 11.588$, $c_0 = 7.100$ Å. He also obtained evidence for a homologous series of intermediate phases, Sm_nX_{2n+1}, between $SmBr_2$ and $SmBr_3$ analogous to the praseodymium oxide system. A coherent structural interpretation of the stoichiometries described in Section III,A,3,e may therefore be possible.

Finally, the range of metal–metal bonded compounds has been substantially widened by the preparation of Tb_2Cl_3 which is isostructural with Gd_2Cl_3, and of GdCl, TbCl, ErCl, and LuCl. The monochlorides were obtained by heating the trichlorides with the metals at 800°C, and contain sheets of metal octahedra sharing edges with halogen atoms above and below the sheets. Magnetic measurements should show if they are tri-*f* compounds which may be crudely formulated as $M^{3+}(2e^-)Cl^-$. If this is the case, their standard free energies of disproportionation into the metal and trichloride should vary smoothly across the series. It may then be possible to prepare them for all lanthanide elements, except where the stability of the di-*f* state intrudes strongly. It is noteworthy that they have so far been prepared for elements where the tri-*f* state is particularly stable with respect to the di-*f*.

Appendix References

1. Haschke, J. M., *Inorg. Chem.* **15**, 198 (1976).
2. Haug, H. O., and Baybarz, R. D., *Inorg. Nucl. Chem. Lett.* **11**, 847 (1975).
3. Kiselev, Y. M., Martynenko, L. I., Sevost'yanov, V. G., and Spitsyn, V. I., *Dokl. Akad. Nauk. SSSR* **222**, 356 (1975).
4. Leuken, H., Bronger, W., and Lochner, U., *Rev. Chim. Miner.* **13**, 113 (1976).
5. Morss, L. R., *Chem. Rev.* **76**, 827 (1976).
6. Simon, A., Mattausch, H., and Holzer, N., *Angew. Chem.* **88**, 685 (1976)